

First JSPS-NWO Seminar

Research Network on Learning in Machines

New Perspectives for Future Nanoscale Production

3-7 JULY 2023

TOKYO, JAPAN



Book of Abstracts

The First JSPS-NWO Seminar “*Research Network on Learning in Machines: New Perspectives for Future Nanoscale Production*” is sponsored by



Leontine Aarnoudse¹, Max van Haren¹, Masahiro Mae², Wataru Ohnishi², Tom Oomen^{1,3} and Kentaro Tsuromoto²

¹Leontine Aarnoudse, Max van Haren and Tom Oomen are with the Eindhoven University of Technology, The Netherlands.

²Masahiro Mae, Wataru Ohnishi and Kentaro Tsuromoto are with the University of Tokyo, Japan

³Tom Oomen is with the Delft Center for Systems and Control, Delft University of Technology, The Netherlands.

Welcome message

The purpose of this seminar is to bring together researchers who have the ambition to push the boundaries of manufacturing machines and scientific instruments. The topic is centrally organised around a fundamentally new framework for controlling manufacturing machines and scientific instruments by exploiting and learning from data. This will lead to unparalleled performance for state-of-the-art high-tech systems that are presently still controlled by traditional control philosophies that do not exploit the major opportunities of the abundance of data.

Manufacturing machines and scientific instruments have a key role in our society. Wafer scanner technology is arguably the most important example in this respect, since Integrated Circuits (ICs) have led to ubiquitous computing power, leading to major developments in communication, medical equipment, transportation, etc. In fact, Moore's law dictates a doubling of IC complexity every two years, which is enabled by progress in wafer scanner technology. This wafer scanner technology is developed primarily by industries in The Netherlands and Japan, and it is crucial that this advantage is reinforced.

Positioning systems, or motion systems, are key in wafer scanner technology because they enable accurate positioning of the ICs within manufacturing machines. Future machines must achieve a high accuracy of 0.1 nm to allow for a doubling of IC complexity through miniaturization. At the same time, extreme speeds and accelerations are required to achieve high throughput and hence market viability of the machine and low cost of IC production for the end-user.

Although major achievements have been made to follow Moore's law already for decades, a major breakthrough in the control paradigm is foreseen to be essential to continue the exponential growth of Moore's law. The aim of this seminar is to exploit the huge amount of sensors, actuators, and data in controlling high-tech mechatronic systems, such as wafer scanners, to the limits of performance. Indeed, the working hypothesis of this seminar is that everything in the system's behaviour that can be predicted can also be compensated for. However, this is by no means possible through traditional design philosophies that are still common in the current state-of-the-art systems. The goal is to bring together researchers to develop a new fundamental design framework for learning from data in complex mechatronic systems in view of new generations of future data-intensive mechatronic systems with unparalleled performance.

On a longer horizon, the research will have a major impact on the development of radically new data-intensive mechatronic systems, where the use of data and control will be used to design radically different and lightweight systems. Indeed, a radically new view on mechatronic design, automatic control, and machine learning is foreseen, where new system designs will be combined with spatially distributed actuators that control spatiotemporal deformations, leading to a huge potential in speed and accuracy. These systems will be continuously monitored in real time through data and models, which constitute digital twins, to monitor their performance, identify faults, and use predictive maintenance.

We welcome everyone to the seminar, and look forward to new collaborations.

Finally, we thank JSPS and NWO for the generous support through the Joint Seminars program, enabling the exchange of a large number of early career researchers.

Tom Oomen (NL) and Wataru Ohnishi (JP), General organisers

Leontine Aarnoudse (NL), Max van Haren (NL), Masahiro Mae (JP), Kentaro Tsurumoto (JP), Editors



Part I

Submitted Abstracts

(Machine) learning for feedforward in precision mechatronics

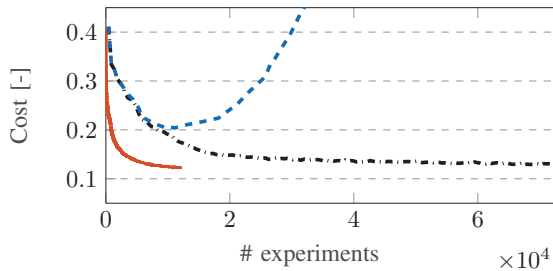
Leontine Aarnoudse¹ and Tom Oomen^{1,2}

I. RESEARCH OVERVIEW

High tracking performance for mechatronic systems requires accurate feedforward control, which can be learned from data through dedicated efficient algorithms. This research is positioned at the intersection of machine learning (neural nets, random learning), controls (feedforward), and precision mechatronics. First, an overview of three different research topics is given, and secondly the topic of nonlinear filters in iterative learning control (ILC) is elaborated upon.

Randomized experiments lead to efficient learning of MIMO feedforward signals [1]

A trick using adjoints allows gradient-based ILC to be run fully model-free, yet this does not extend well to multivariable systems: generating gradients requires $n_i \times n_o$ experiments per iteration and is comparable to tuning by turning one knob at a time. Instead, an unbiased gradient estimate can be generated through one experiment for any MIMO system. All experiments are run simultaneously ('turn all knobs') in randomized directions. These gradient estimates lead to fast convergence of a stochastic gradient descent algorithm (—), which is much more efficient than deterministic approaches (--) that may diverge when data is noisy (- -).



Neural networks for flexible feedforward: cost functions, model structures and training data [2]

Neural networks are promising for flexible feedforward control, but combining them in a harmonious way with state-of-the-art feedback control is subtle and requires care:

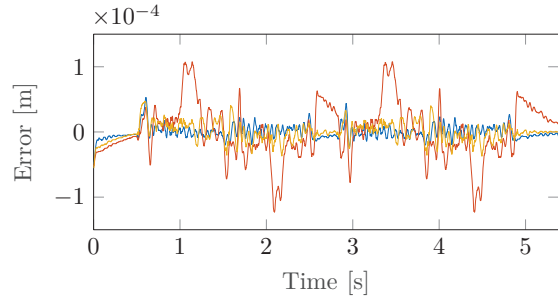
*This work is part of the research programme VIDI with project number 15698, which is (partly) financed by the NWO.

¹The authors are with the Dept. of Mechanical Engineering, Control Systems Technology, Eindhoven University of Technology, Eindhoven, The Netherlands. l.i.m.aarnoudse@tue.nl

²Tom Oomen is also with the Delft Center for Systems and Control, Delft University of Technology, Delft, The Netherlands.

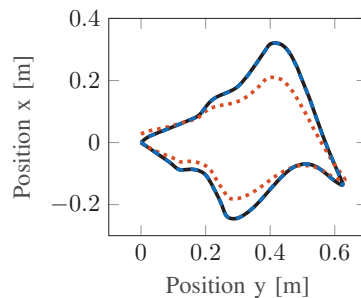
- The cost function used for training should reflect the aim of minimizing the tracking error, as $\|f_{\text{train}} - f_{\text{nn}}\|$, with $e(f_{\text{train}}) = 0$, being small does not necessarily mean that $e(f_{\text{nn}})$ will be small.
- The model structure should allow for non-causal feedforward, as many systems contain delays.
- Training data, consisting of references and feedforward signals, should be generated in closed-loop, for example using ILC, as nonlinearities manifest along trajectories.

The figure compares the performance of f_{train} (—), and non-causal time-delay (—) and recurrent neural networks (—).



Weighting the errors that matter: cross-coupled iterative learning control [3]

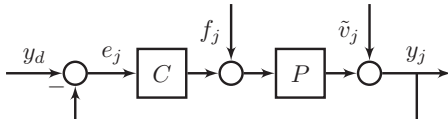
For contour tracking applications, the error in time domain is less important than the deviation from the contour. Cross-coupled ILC can be used to design feedforward signals for these specific cases, by using a cost function that weights this contour error explicitly. The cost function also weights the error tangential to the contour error, to allow for specifying different aims in different parts of the trajectory. For example, one might want to slow down in sharp corners and make up for lost time when moving straight. The figure shows contour tracking (—) with (--) and without (....) cross-coupled ILC.



II. SEMINAR TOPIC - NONLINEAR ITERATIVE LEARNING CONTROL [4]

Iterative learning control (ILC) can attenuate repeating disturbances completely, yet it also amplifies iteration varying disturbances up to a factor two [5]. The aim of this research is to develop a nonlinear ILC framework that achieves fast convergence, robustness, and low converged error values in ILC. To this end, a nonlinear deadzone is added to the learning filter, which differentiates between varying and repeating disturbances based on their amplitude characteristics and applies different learning actions: fast attenuation of repeating disturbances, and slow averaging of varying disturbances.

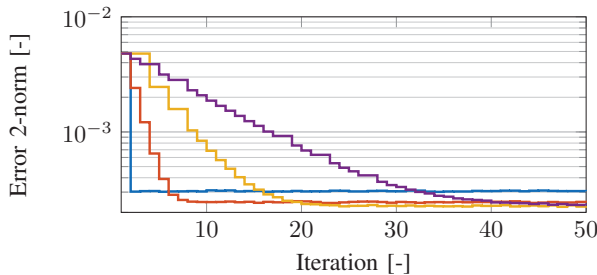
A. Problem formulation



ILC is applied to the SISO LTI system above, according to

$$e_j = S(y_d - \tilde{v}_j) - Jf_j, \quad f_{j+1} = Q(f_j + \alpha Le_j) \quad (1)$$

with $S = (1 + PC)^{-1}$, $J = SP$ and $L \approx J^{-1}$. Robustness filter Q is typically a low-pass filter. The learning gain $\alpha \in (0, 1]$ influences both the number of iterations required to compensate the iteration-invariant disturbance y_d , and the amplification of iteration-varying disturbance v_j , as illustrated for $\alpha = 1$ (blue), 0.5 (red), 0.2 (yellow), and 0.1 (purple). The aim is to achieve both small converged errors and fast convergence.



B. Approach: nonlinear ILC

To achieve both fast convergence and limited amplification of varying disturbances, a deadzone nonlinearity φ is included in the feedforward update, such that

$$f_{j+1} = Q(f_j + \alpha Le_j + L\varphi(e_j)), \quad (2)$$

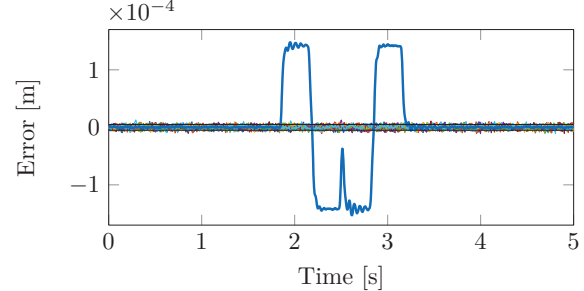
with, for deadzone width δ and gain $\gamma > 0$,

$$\varphi(e_j(k)) = \begin{cases} 0, & \text{if } |e_j(k)| \leq \delta \\ \left(\gamma - \frac{\gamma\delta}{|e_j(k)|}\right)e_j(k), & \text{if } |e_j(k)| > \delta. \end{cases} \quad (3)$$

The deadzone nonlinearity satisfies an incremental sector condition with γ , which enables convergence analysis, leading to the following convergence condition:

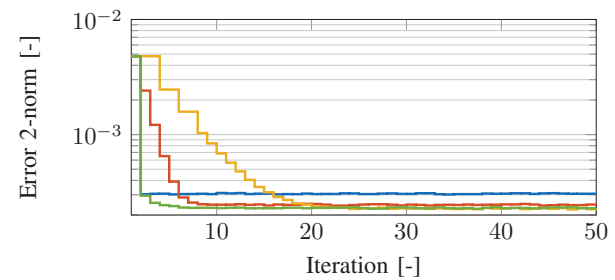
$$\left\| Q \left(1 - \alpha JL - \frac{\gamma}{2} JL \right) \right\|_{\mathcal{L}_{\infty}} + \frac{\gamma}{2} \| Q JL \|_{\mathcal{L}_{\infty}} < 1. \quad (4)$$

Through the deadzone with width δ (—), a high learning gain is applied to the iteration-invariant disturbance (—) and the amplification of iteration-varying disturbances is limited.



C. Conclusions and future work

A nonlinear frequency-domain ILC algorithm (—) is developed that achieves both fast convergence and a small converged error in the presence of iteration-varying disturbances, as compared in simulation to standard ILC with $\alpha = 1$ (—), 0.5 (—), 0.2 (—), and 0.1 (—). Ongoing research is aimed at extending this approach to lifted ILC and repetitive control.



REFERENCES

- [1] L. Aarnoudse and T. Oomen, "Model-Free Learning for Massive MIMO Systems: Stochastic Approximation Adjoint Iterative Learning Control," *IEEE Control Syst. Lett.*, vol. 5, no. 6, pp. 1946–1951, 2021.
- [2] L. Aarnoudse, W. Ohnishi, M. Poot, P. Tacx, N. Strijbosch, and T. Oomen, "Control-relevant neural networks for intelligent motion feedforward," in *2021 IEEE Int. Conf. Mechatronics*, 2021.
- [3] L. Aarnoudse, J. Kon, K. Classens, M. van Meer, M. Poot, P. Tacx, N. Strijbosch, and T. Oomen, "Cross-Coupled Iterative Learning Control for Complex Systems: A Monotonically Convergent and Computationally Efficient Approach," in *Conf. Decis. Control*, Cancún, Mexico, 2022.
- [4] L. Aarnoudse, A. Pavlov, and T. Oomen, "Nonlinear iterative learning control: a frequency-domain approach for fast convergence and high accuracy," in *2023 IFAC World Congr.*, 2023.
- [5] T. Oomen and C. R. Rojas, "Sparse iterative learning control with application to a wafer stage: Achieving performance, resource efficiency, and task flexibility," *Mechatronics*, vol. 47, pp. 134–147, 2017.



Leontine Aarnoudse received the B.Sc degree (2017) and M.Sc degree (cum laude) (2019) in Mechanical Engineering from the Eindhoven University of Technology, Eindhoven, The Netherlands. She is currently pursuing a Ph.D. degree in the Control Systems Technology group within the department of Mechanical Engineering at Eindhoven University of Technology. Her research interests are centered around the development of learning control theory for precision mechatronics.

Study of Current Command Generation Method for Iron Loss Reduction in Permanent Magnet Synchronous Motors

Kaiki Akizuki¹, Toshiyuki Fujita^{1,2}, Sakahisa Nagai^{1,3} and Hiroshi Fujimoto^{1,4}

I. RESEARCH OVERVIEW

Permanent Magnet Synchronous Motors(PMSMs) are widely used for their high efficiency, ease of maintenance, and controllability advantages. Particularly, interior permanent magnet synchronous motors(IPMSMs) are often used for electric vehicles due to its large torque. For further effective utilization of energy, it is necessary to drive PMSMs with high efficiency through control. Analyzing the causes of driving loss and taking measures are important in order to achieve the high efficient motor driving. The loss of PMSM is mainly classified into the copper loss and the iron loss. The copper loss occurs in the motor windings and the iron loss occurs in the electromagnetic steel sheet. Typical examples of high efficient current control are $i_d = 0$ control and maximum torque per ampere (MTPA) control. These methodologies reduce copper loss. However, these are not necessarily the most efficient control methods because they do not take the iron loss into account.

Topic 1 Plant model of IPMSM.

The IPMSM model on dq coordinate system is shown in Fig. 1. The dq axis voltage equation is expressed as follows:

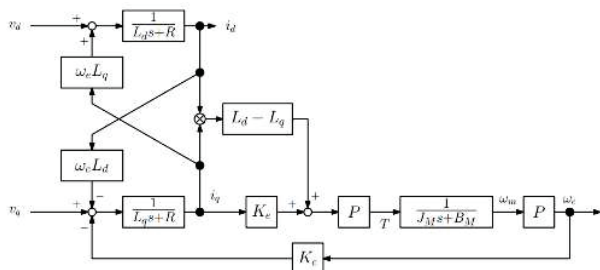


Fig. 1. IPMSM model

$$\begin{bmatrix} v_d \\ v_q \end{bmatrix} = \begin{bmatrix} R + sL_d & -\omega_e L_q \\ \omega_e L_d & R + sL_q \end{bmatrix} \begin{bmatrix} i_d \\ i_q \end{bmatrix} + \begin{bmatrix} 0 \\ \omega_e K_e \end{bmatrix} \quad (1)$$

Since the dq axis current has coupling terms, the decoupling

^{1,2,3,4} The authors are with the University of Tokyo, Japan, corresponding e-mail: akizuki.kaiki22@ae.k.u-tokyo.ac.jp.

control is widely used. In order to eliminate the coupling terms, the dq voltages are calculated as follows:

$$v_d = v'_d - \omega_e L_q i_q \quad (2)$$

$$v_q = v'_q + \omega_e(L_q i_d + K_e) \quad (3)$$

State variables are defined as the dq axis current and inputs are defined as the decoupled dq axis voltage. The IPMSM continuous time equation of state is expressed as follows:

$$\dot{x}(t) = A_c x(t) + B_c u(t), y(t) = C_c x(t) + D_c u(t) \quad (4)$$

where

$$x(t) = \begin{bmatrix} i_d(t) \\ i_q(t) \end{bmatrix}, u(t) = \begin{bmatrix} v'_d(t) \\ v'_q(t) \end{bmatrix} \quad (5)$$

$$A_c = \begin{bmatrix} -\frac{R}{L_d} & 0 \\ 0 & -\frac{R}{L_q} \end{bmatrix}, B_c = \begin{bmatrix} \frac{R}{L_d} & 0 \\ 0 & \frac{R}{L_q} \end{bmatrix}, C_c = \begin{bmatrix} 1 & 0 \\ 0 & 1 \end{bmatrix}, D_c = O$$
(6)

Causes of iron loss[1,2].

The iron loss occurs in the iron core of PMSM and is broadly classified into the hysteresis loss and the eddy current loss. The IPMSM core contains various harmonic components of magnetic flux density, and these components increase the iron loss caused by minor loops of the hysteresis loop. Harmonic currents are one of the factors that increase iron loss. By using Repetitive Perfect Tracking Control(RPTC), harmonic currents are suppressed and iron loss is reduced. RPTC consists of Perfect tracking control(PTC) combined with repetitive control. Iron loss is determined by subtracting output, copper loss, and mechanical loss from input power.

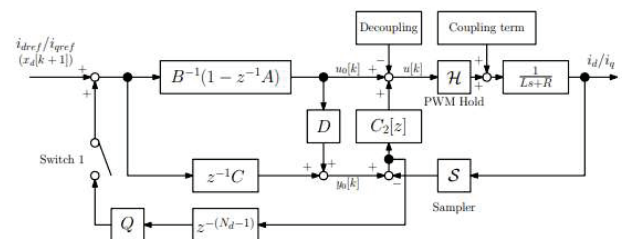


Fig. 2. Block diagram of RPTC

II. SEMINAR TOPIC - Current command generation method

A. Evaluation of iron loss of PI controll and RPTC

The motor bench which I use now can directly measure magnetic field information. On the drive side, a coil for measuring the magnetic field strength and a search coil for measuring the magnetic flux density are located. The electrical signals obtained from the coils are acquired with an oscilloscope, and the data is processed in MATLAB for direct iron loss evaluation.

Fig. 3 shows the dq-axis current results with PI control and with RPTC applied. It was confirmed that the application of RPTC reduced current harmonics compared to PI control. Furthermore, the iron loss evaluation during each current control is shown in Fig. 4 by BH curve. In this case, the iron loss in the teeth was measured, and the area of the BH curve is the iron loss value. Fig. 5 shows that the iron loss was reduced when RPTC was applied compared to the case with PI control.

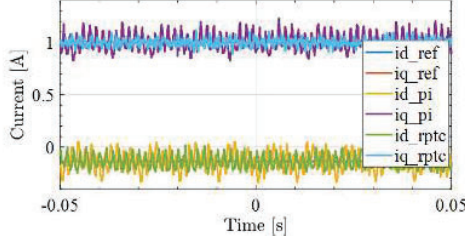


Fig. 3. PI control and RPTC dq-axis currents

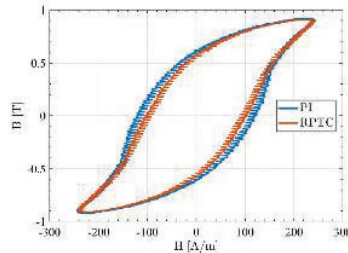


Fig. 4. Iron loss comparison by BH curve(harmonic suppression)

B. Consideration for current harmonic injection

From the results in Figure 4, we considered that the injection of current harmonics may reduce the iron loss in some cases. Fig. 5 shows the current harmonic injection method. This system injects harmonics into the commanded value of 3-phase current. Fig. 6 shows a comparison of iron loss by BH curve when only one of the three phases injects current harmonics and when PI control is used. The results in Fig. 6 experimentally confirm the case where iron loss is reduced even when harmonic currents are injected.

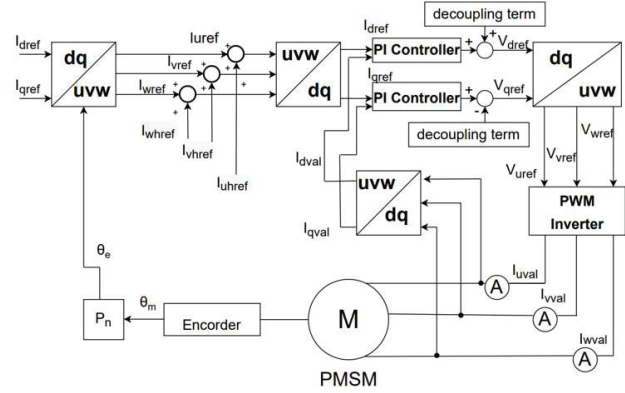


Fig. 5. Harmonic currents injection method

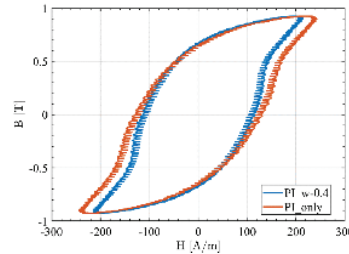


Fig. 6. Iron loss comparison by BH curve(harmonic injection)

III. CONCLUSION

The above results suggest that there is an optimal current command value for the purpose of iron loss reduction. Therefore, we will theoretically consider how to generate the optimum current command value in the future.

REFERENCES

- [1] H. Fujimoto, Y. Hori, and A. Kawamura, "Perfect tracking control based on multirate feedforward control with generalized sampling periods," IEEE Transactions on Industrial Electronics, vol. 48, no. 3, pp. 636–644, 2001.
- [2] Y. Inagaki, M. Mae, O. Shimizu, S. Nagaki, H. Fujimoto, T. Miyajima, Y. Yasuda, A. Yamagiwa, "Effect of Harmonic Current Suppression on Iron Loss of IPMSM Using Repetitive Perfect Tracking Control," IEEJ Journal of Industry Applications, Vol.11, No.2, pp. 317–326, 2022.



Kaiki Akizuki received the B.E degree from the University of Utsunomiya in 2022. He is currently working toward the M.E. degree in Departement of Advanced Energy, Graduate School of Frontier Sciences, the University of Tokyo. His interests are in motor drive systems.

Loop-Shaping Technique for Hard Disk Drive

Takenori Atsumi¹

I. RESEARCH OVERVIEW

The future of the cloud service is dependent on the hard disk drive (HDD) capacity growth because demands for the data capacity in the cloud service are rapidly increasing. To solve this issue, we are going to improve the accuracy of a magnetic-head positioning control system so that size of bits for data stored on a disk decreases. In this paper, we have proposed the control system design method for the quadruple-stage actuator system which is a future technology for HDDs.

Quadruple-stage actuator system in HDD.

Fig. 1 shows the basic schematics of the control system for the quadruple-stage actuator system in the HDDs. The controlled object in this system is the multi-input single-output (MISO) system.

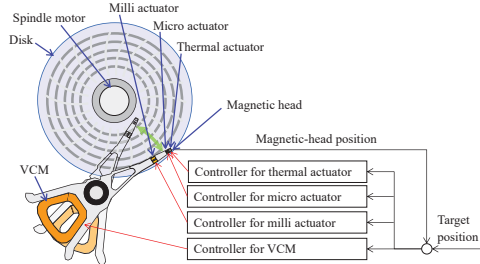


Fig. 1. Magnetic-head positioning system with quadruple-stage actuator system.

Fig. 2 shows the block diagrams of the control system for the quadruple-stage actuator system. Here, C_{VCM} is the feedback controller for the VCM, C_{Mil} is the feedback controller for the milli actuator, C_{Mic} is the feedback controller for the micro actuator, C_{The} is the feedback controller for the thermal actuator, I_p is the interpolator, N_{VCM} is the multi-rate notch filter for the VCM, N_{Mil} is the multi-rate notch filter for the milli actuator, N_{Mic} is the multi-rate notch filter for the micro actuator, \mathcal{H} is the zero-order hold (ZOH), \mathcal{H}_m is the multi-rate ZOH, P_{VCM} is the VCM, P_{Mil} is the milli actuator, P_{Mic} is the micro actuator, P_{The} is the thermal actuator, \mathcal{S} is the sampler, r is the reference, e is the error, y_{Mil} is the output signal from P_{Mil} , y_{Mic} is the output signal from P_{Mic} , y_{The} is the output signal from P_{The} , d is the disturbance, y_c is the actual magnetic-head position, and y_d is the measured magnetic-head position.

¹ Takenori Atsumi is with the Department of Mechanical Engineering, Chiba Institute of Technology, Japan, corresponding e-mail: takenori.atsumi@p.chibakoudai.jp.

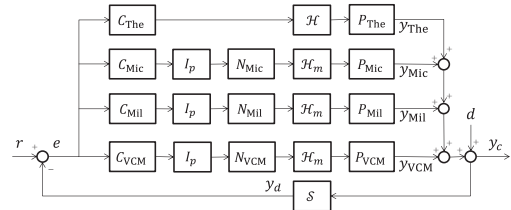


Fig. 2. Block diagram of initial control system.

Rboust Bode plot.

The controller design with the Robust Bode (RBode) plot uses two weighting functions: W_S (for the sensitivity function) and W_T (for the co-sensitivity function). Here, P_r is the real plant, P is the nominal plant, C is the feedback controller, and Δ_m is the multiplicative uncertainty. P_r is given as follows:

$$P_r = P(1 + \Delta_m). \quad (1)$$

The nominal open-loop characteristics L , nominal sensitivity function S , and nominal co-sensitivity function T are given as follows:

$$L = PC, S = \frac{1}{1 + L}, T = \frac{L}{1 + L}. \quad (2)$$

The weighting function W_T specifies the plant uncertainty as follows:

$$|W_T| > |\Delta_m| = \left| \frac{P_r}{P} - 1 \right|. \quad (3)$$

The weighting function W_S specifies the robust performance as follows:

$$|W_S|^{-1} > \left| \frac{1}{1 + P_r C} \right|. \quad (4)$$

If L is stable and S and T satisfy

$$|W_T L| + |W_S S| = \frac{|W_T L| + |W_S|}{|1 + L|} < 1, \quad (5)$$

then the control system achieves (4).

Solving (5) for $|L|$, we have

$$(1 - |W_T|^2)|L|^2 + 2(\cos(\angle L) - |W_T||W_S|)|L| + 1 - |W_S|^2 > 0. \quad (6)$$

Solving (5) for $\cos(\angle L)$, we have

$$\cos(\angle L) > \frac{|W_S|^2 - 1}{2|L|} + |W_T||W_S| + \frac{(|W_T|^2 - 1)|L|}{2}. \quad (7)$$

The RBode plots partition the conventional Bode plots into allowable regions that meet the specific robust performance criterion and forbidden regions that do not meet the criteria (6) and (7).

II. SEMINAR TOPIC - Loop-Shaping Technique for Quadruple-Stage Actuator System in HDD

In the quadruple-stage actuator system, the micro and thermal actuators have narrow ranges of movements. This means that these actuators can NOT work when their movements are over their ranges under a large disturbance. Therefore, we have to design a control system that makes $|y_{\text{Mic}}|$ and $|y_{\text{The}}|$ small even if the control system has a large disturbance.

To solve the above-mentioned problem, we have proposed the control system shown in Fig. 3 for the quadruple-stage actuator system. Here, L_{VCM} is the transfer function from e to y_{VCM} , L_{Mil} is that from e to y_{Mil} , L_{Mic} is that from e to y_{Mic} , and L_{The} is that from e to y_{The} . F_{l1} is the loop-shaping filter for L_{VCM} and L_{Mil} . F_{l2} is the loop-shaping filter for L (the transfer function from e to y_d). In the proposed method, F_{l1} is used to reject the large disturbances, and F_{l2} is used to increase the stability margins of the control system. By using this framework, we can reject the large disturbances without increasing the $|y_{\text{Mic}}|$ or $|y_{\text{The}}|$ because the loop-shaping filters do not increase the gain of L_{Mic} nor L_{The} around the disturbance frequencies.

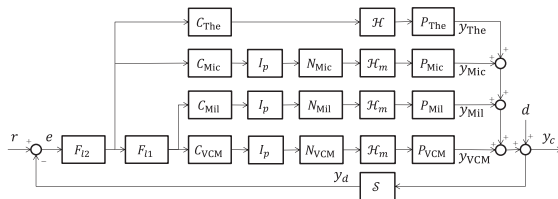


Fig. 3. Block diagram of proposed control system.

Fig. 4 shows the RBode plot with the initial control system. In the RBode plot, we can see the relationship between the open-loop characteristics and the robust performance criteria. The gray area indicates the forbidden regions. When the open-loop characteristic does not overlap the forbidden regions on the RBode plot, the control system meets the robust performance criteria. Therefore, Fig. 4 indicates that we have to increase the gain of the open-loop characteristic from 100 to 400 Hz and decrease the gain around the Nyquist frequency to meet the robust performance criteria.

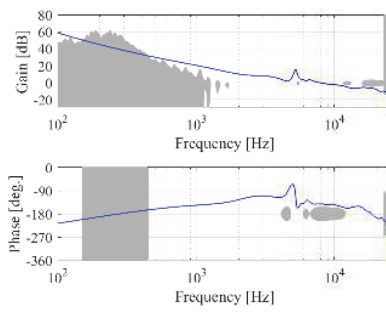


Fig. 4. RBode plot with initial control system.

In order to eliminate overlapping between the forbidden regions and the open-loop characteristics, we designed the loop-shaping filters F_{l1} and F_{l2} . Fig. 5 show the RBode plot with F_{l1} and F_{l2} . This figure indicates that the open-loop characteristics with F_{l1} and F_{l2} meet the robust performance criteria for all frequencies.

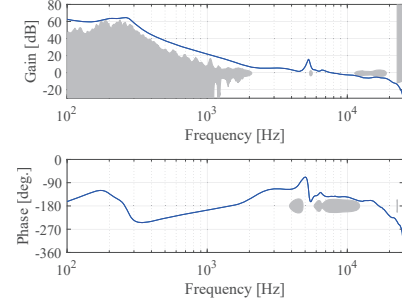


Fig. 5. RBode plot with F_{l1} and F_{l2} .

To evaluate the positioning accuracy of the magnetic-head positioning control system, we have to see the magnetic-head position in the continuous time y_c . Fig. 6 shows the simulation results of y_c . In these figures, (a) shows the results with the initial control system, and (b) shows that with the proposed control system. These results indicate that the proposed method enables us to improve the positioning accuracy by about 78%.

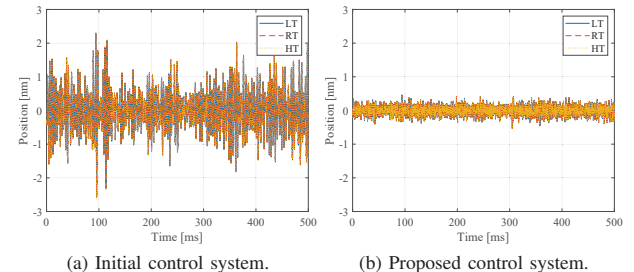


Fig. 6. Simulation results of y_c .

REFERENCES

- [1] T. Atsumi and S. Yabui, "Loop-Shaping Technique for Quadruple-Stage Actuator System in Hard Disk Drive", *The IEEE Transactions on Industry Applications*, (Early access)



Takenori Atsumi (Member, IEEE) received the B.S., M.S., and Ph.D. degrees in mechanical engineering from Chiba University, Chiba, Japan, in 1997, 1999, and 2006, respectively. He started his career with Hitachi, Ltd. Ibaraki, Japan in 1999. From 2009 to 2010, he was a Visiting Fellow in the Data Storage Systems Center (DSSC), Carnegie Mellon University. From 1999 to 2015, he has worked for Hitachi Ltd. and HGST Japan to develop control technologies for hard disk drives. Since 2015, he has been with Department of Mechanical Engineering, Chiba Institute of Technology, Chiba, Japan.

Learning for data-intensive industrial machines

Lennart Blanken^{1,2}, Max van Haren¹, and Tom Oomen^{1,3}

I. RESEARCH OVERVIEW

The productivity and product quality of many manufacturing systems hinge on the performance of mechatronic positioning systems. Examples include large-format printing systems, see Fig. 1a, and the intelligent substrate carrier for industrial printing, see Fig. 1b. To meet future requirements on accuracy, speed, and product dimensions, it is foreseen that a significant increase is required in the complexity of positioning systems. This leads to the manifestation of pronounced disturbances and complex dynamical behavior, including large numbers of dynamic modes, inherently multivariable behavior, and position-dependent behavior, which potentially restrict performance of control systems.



(a) Large-format printing system (b) Intelligent substrate carrier

Fig. 1: Data-intensive mechatronic positioning systems.

A new control design paradigm is foreseen to manage the increasing system complexity. The key observation is that over the operational lifetime of a machine, huge amounts of data becomes available, while this data is often not exploited in control. The aim of this research is to enable radical performance improvements in future positioning systems by improving control systems through learning from data. By exploiting the abundance of data in mechatronic systems, in potential performance can be achieved up to the limit of reproducibility, far beyond what can be achieved with traditional model-based control approaches.

The key challenge in successful application of learning algorithms to industrial machines lies in managing their extreme systems complexity, while guaranteeing fast and safe learning to avoid machine downtime and production losses.

This research is supported by ECSEL 101007311 (IMOCO4.E).

¹ The authors are with the Control Systems Technology research section, Eindhoven University of Technology, the Netherlands, corresponding e-mail: l.l.g.blanken@tue.nl.

² Also with Sioux Technologies, Eindhoven, the Netherlands.

³ Also with the Delft Center for Systems and Control, Delft University of Technology, the Netherlands.

Multivariable learning control designs: balancing modeling effort with performance [1]–[3].

Although learning control is conceptually promising for complex mechatronic systems, it is not often employed in industrial environments due to associated high modeling requirements. To this end, developments have been made for multivariable learning controllers, including Iterative Learning Control (ILC) [1] and Repetitive Control (RC) [2], [3], that explicitly address trade-offs between modeling and performance requirements. This is done by judiciously combining limited parametric model knowledge with the use of non-parametric frequency response function (FRF) models, and the development of various user-friendly design techniques, ranging from decentralized approaches to centralized designs.

Learning for feedforward control: the use of prior knowledge [4]–[7].

To enable extreme performance in the presence of varying tasks, a parametrized feedforward control structure can be adopted whose parameters are to be learned from data. The key difficulty lies in selecting a suitable model structure and order, particularly in view of the extreme system complexity of future industrial machines. A crucial aspect is the use of system knowledge, i.e., prior information, while retaining sufficient freedom to effectively learn from data. In particular, prior knowledge is exploited to

- construct parsimonious parametrizations [4], [6] with beneficial properties for control (non-causality) and optimization (convexity);
- address model order selection for (non-causal) feedforward control in a systematic manner [5]; and
- construct physics-motivated parametrizations for position-dependent feedforward that facilitate engineering interpretation [7].

Identification above the Nyquist frequency [8], [9].

The performance and convergence properties of learning control algorithms heavily rely on the used models. This is especially crucial for learning control since the control action is potentially effective over the entire frequency range up to the Nyquist frequency, and high-frequency dynamics, including intersample behavior, can hence not be ignored. A method is developed for fast and accurate FRF identification up to and beyond the Nyquist frequency of multirate systems [8], [9]. The key aspect is that aliased contributions can be uniquely distinguished and disentangled by exploiting local smoothness of the system response.

II. SEMINAR TOPIC - REPETITIVE CONTROL DESIGN FOR INDUSTRIAL MACHINES

Repetitive control (RC) can significantly improve the control performance of systems that are subject to dominantly periodic disturbances. The control action is periodically updated on the basis of past measurement data in combination with a model of the system to guarantee closed-loop stability, see Fig. 2 for a typical implementation.

The aim of this seminar is to present a tutorial on RC design, that has enabled successful applications in industrial machines.

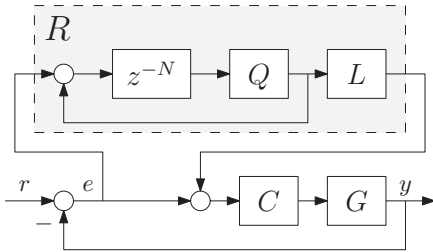


Fig. 2: Add-on repetitive control configuration.

A. Robust Design for Industrial Machines

Robust stability of RC algorithms is crucial to deal with inevitable, and often deliberate, modeling errors. A technical analysis is presented that facilitates robust RC design while taking into account the trade-off between performance and modeling requirements. In particular, a systematic design approach is presented that uses low-order approximate nominal models for control design, and considers the deliberate modeling errors as uncertainty, i.e., through robust stability, which can be directly evaluated using inexpensive nonparametric FRF measurements, see Fig. 3.

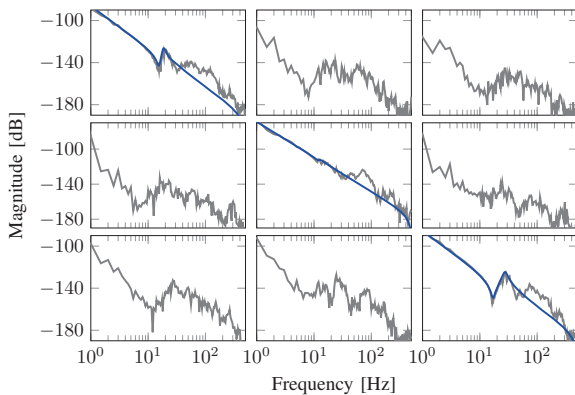


Fig. 3: Models for robust RC design: low-order parametric models (blue) for nominal control design, and non-parametric multivariable FRF measurement (grey) that enables direct evaluation of robust stability.

B. Application to Large-Format Printing System of Fig. 1a

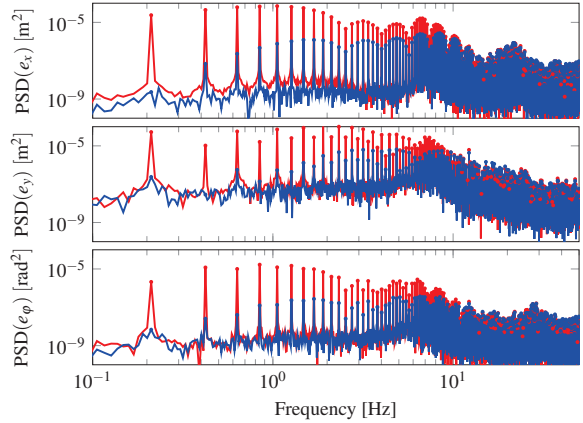


Fig. 4: Power spectral density (PSD) of servo errors before (red) and after RC convergence (blue), visualizing the performance increase.

REFERENCES

- [1] L. Blanken and T. Oomen, "Multivariable iterative learning control design procedures: From decentralized to centralized, illustrated on an industrial printer," *IEEE Transactions on Control Systems Technology*, vol. 28, no. 4, pp. 1534–1541, 2019.
- [2] L. Blanken, S. Koekebakker, and T. Oomen, "Multivariable repetitive control: Decentralized designs with application to continuous media flow printing," *IEEE/ASME Transactions on Mechatronics*, vol. 25, no. 1, pp. 294–304, 2020.
- [3] L. Blanken, P. Bevers, S. Koekebakker, and T. Oomen, "Sequential multi-period repetitive control design with application to industrial wide-format printing," *IEEE/ASME Transactions on Mechatronics*, vol. 25, no. 2, pp. 770–778, 2020.
- [4] L. Blanken, F. Boeren, D. Bruijnen, and T. Oomen, "Batch-to-batch rational feedforward control: from iterative learning to identification approaches, with application to a wafer stage," *IEEE/ASME Transactions on Mechatronics*, vol. 22, no. 2, pp. 826–837, 2017.
- [5] L. Blanken and T. Oomen, "Kernel-based identification of non-causal systems with application to inverse model control," *Automatica*, vol. 114, p. 108830, 2020.
- [6] L. Blanken, S. Koekebakker, and T. Oomen, "Data-driven feedforward tuning using non-causal rational basis functions: With application to an industrial flatbed printer," *Mechatronics*, vol. 71, p. 102424, 2020.
- [7] M. van Haren, L. Blanken, and T. Oomen, "Polynomial Feedforward for Linear Parameter-Varying Systems: a Kernel Regularized Approach," in *22nd World Congress of the International Federation of Automatic Control*, Yokohama, Japan, 2023.
- [8] ———, "Frequency Domain Identification of Multirate Systems: A Lifted Local Polynomial Modeling Approach," in *2022 IEEE 61st Conference on Decision and Control*, Cancun, Mexico, 2022.
- [9] ———, "Beyond Nyquist in Frequency Response Function Identification: Applied to Slow-Sampled Systems," *To appear*, 2023.



Lennart Blanken received the MSc. degree (cum laude) and Ph.D. degree in mechanical engineering from the Eindhoven University of Technology, Eindhoven, the Netherlands. He is currently a System Designer Mechatronics at Sioux Technologies, and a part-time Assistant Professor with the Mechanical Engineering Department, Eindhoven University of Technology. His research interest includes advanced feedforward control, learning control, and their applications to industrial mechatronic systems.

Time Optimal Temperature Control in Semiconductor Vertical Furnace

Christian Milleneuve Budiono¹, Wataru Ohnishi¹, Takafumi Koseki¹,
Akira Hirata², Ryosuke Shibatsuji², Tatsuya Yamaguchi²

I. RESEARCH OVERVIEW

Semiconductor vertical furnace (Fig. 1) is an equipment in the semiconductor manufacturing process used for some front-end processes, such as oxidation and layer deposition. It is classified as batch type, which processes approximately 100 wafers at once. Faster and more precise control of this equipment will contribute to the improvement in the throughput of the semiconductor manufacturing process.

Processes in this furnace use Chemical Vapor Deposition (CVD) method. Gases react with wafers producing layers through chemical reactions. The reactions occur at certain temperatures; thus, temperature rise and fall are common operations. The faster these operations are, the shorter the time consumed for each process. Moreover, the layer thickness is affected by the operating temperature. Even layers on the wafer surface can be achieved by controlling the temperature precisely.

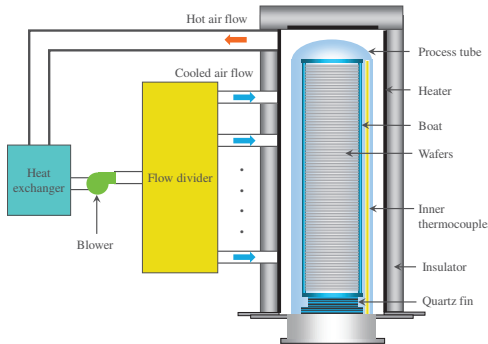


Fig. 1: Semiconductor vertical furnace. [1]

Plant Description [2].

Fig. 2 shows two main problems in the temperature control of semiconductor vertical furnace: temperature dependency [3] and location dependency. As shown in Fig. 3, the equipment can be described as an MIMO plant system with the power of heater and cooler devices as inputs, and the temperatures as outputs.

Moreover, the heater and cooler were integrated using a constant gain to achieve a simple SISO plant [1]. This idea has enabled a more intuitive controller design in frequency domain [1].

¹ The authors are with the Department of Electrical Engineering and Information Systems Graduate School of Engineering, The University of Tokyo, Japan.

² The authors are with the Tokyo Electron Technology Solutions Ltd.

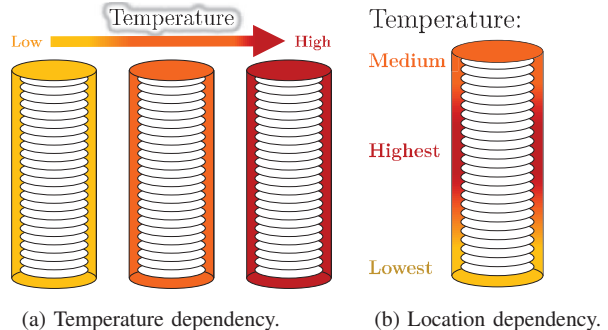


Fig. 2: Two main problems in temperature control of semiconductor vertical furnace. In (a), the plant characteristics change with temperature difference. In (b), the temperature distribution is uneven.

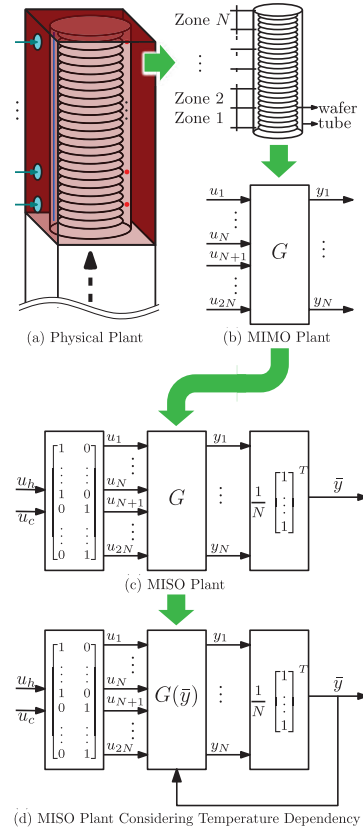


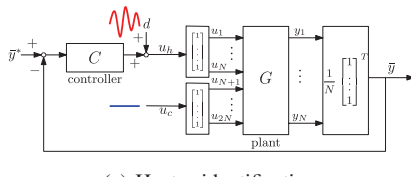
Fig. 3: Semiconductor vertical furnace as target plant. u_h, u_c, \bar{y} are heater power, cooler power, and temperature [2].

II. SEMINAR TOPIC - FAST TEMPERATURE RISE USING TIME OPTIMAL CONTROL

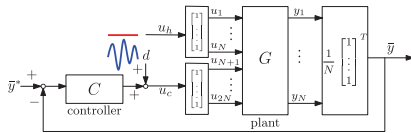
A. Plant System Identification

Due to the temperature dependency property, the system identification was conducted in the closed-loop configuration, as shown in Fig. 4. Each input-to-output frequency response was determined in separate experiments. To prevent any dead zones during the identification of a particular input, a constant value was added to the other input.

Fig. 5 shows the identification results. The plant was generally second-order, with heater-to-temperature response had a higher gain compared to cooler-to-temperature response.



(a) Heater identification.



(b) Cooler identification.

Fig. 4: Closed-loop system identification scheme.

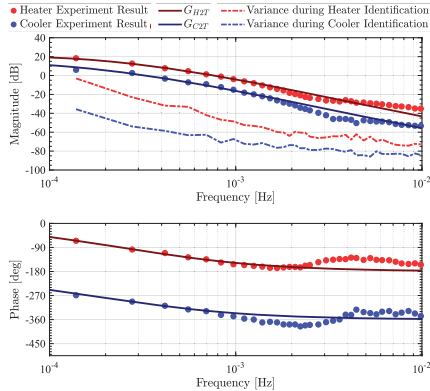


Fig. 5: System identification result.

B. Time Optimal Control Control Algorithm

The time optimal control was proposed to utilize the maximum capacity of the heater and cooler. This can be formulated as an optimization problem determining the heater time t_h and the overall time t_{\max} . In Eq. 1, y represents temperature. y_{aim} is the temperature aim. Also, t, u means time, input power, and subscript h, c means heater, cooler, respectively.

$$\begin{aligned}
 & \min_{t_{\max}} |y(t_{\max}) - y_{\text{aim}}| \\
 \text{subj.to} \quad & y(t_{\max}) < y_{\text{aim}} \\
 & \min_{t_h} \left. \frac{dy}{dt} \right|_{t_{\max}} \\
 \text{subj.to} \quad & t_h + t_c = t_{\max}, 0 < t_h, t_c \leq t_{\max} \\
 & u_h(t) = \begin{cases} 100 & 0 < t \leq t_h \\ 0 & t_h < t \leq t_{\max} \end{cases} \\
 & u_c(t) = \begin{cases} 0 & 0 < t \leq t_h \\ 100 & t_h < t \leq t_{\max} \end{cases} \\
 & y(0) = y_{\text{start}}
 \end{aligned} \tag{1}$$

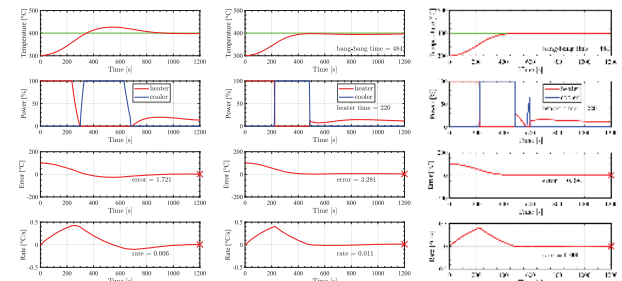


Fig. 6: Simulation results (TO: time optimal, Traj.: target trajectory). (b), (c) has no overshoots. (c) has the least error.

III. CONCLUSION AND FUTURE WORKS

Simulation results show that time optimal control was able to achieve fast temperature rise without overshoots. Further examinations on the constant value effect during system identification, other approaches to achieve fast temperature control, and the solution to the location dependency problem will be done.

REFERENCES

- [1] W. Ohnishi, A. Hirata, R. Shibatsuji, and T. Yamaguchi, "Fast and precise temperature control for a semiconductor vertical furnace via heater-cooler integration," IEEE Trans. Semicond. Manuf., 2023.
- [2] C. M. Budiono, (supervisor: W. Ohnishi, T. Koseki, in Japanese) "Research on fast and high precision temperature control in semiconductor thermal processing system considering temperature dependency," Bachelor thesis, The University of Tokyo, 2023.
- [3] C. M. Budiono, W. Ohnishi, T. Koseki, A. Hirata, R. Shibatsuji, and T. Yamaguchi, "Analysis of temperature dependency in batch type semiconductor vertical furnace through frequency domain closed-loop system identification," The Papers of Technical Meeting on "Mechatronics Control", IEE Japan, MEC-22-038, 2022 (in Japanese).



Christian Milleneuve Budiono received the BEng. in electrical and electronic engineering from The University of Tokyo in 2023. Currently, he is pursuing a master degree at the department of electrical engineering at The University of Tokyo. His research interests are centered around the development of fast and high-precision control on MIMO systems.

Vertical Vibration Suppression Control Using Disturbance Observer for In-wheel Motor EV Considering Under-sprung Motion

Qi Chen¹, Binmin Nguyen¹ Sakahisa Nagai¹ and Hiroshi Fujimoto¹

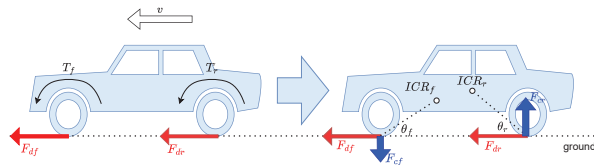
I. RESEARCH OVERVIEW

Riding comfort attracts attention with the development of In-Wheel-Motor EVs. Aiming for vertical vibration suppression and enhancement of robustness against the nominal error, this paper proposes a disturbance observer combined with triple skyhook control. Simulation and experiments are carried out to prove the effectiveness of the proposed method.

Suspension reaction force.

The horizontal driving force generated by torque output of motors or engines can be converted to vertical direction due to the feature of instant rotation motion around a instant center of rotation(ICR). Thus some vertical motion control can be down with torque output control, aka, driving force control. Considering the angle between rotation arm and ground to be θ , the vertical reaction force F_c can be given as following, where F_d represents the driving force:

$$F_c = F_d \tan \theta \quad (1)$$



Quarter Car Vibration Model.

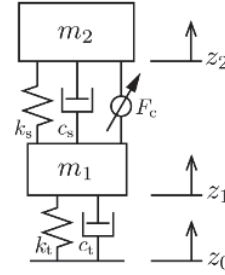
A quarter car model with 1/4 body mass m_2 , a suspension system with damper c_s and sprung k_s , under-sprung mass m_1 and tire characteristics k_t, c_t shown in the graph can be described with following equations, where F_c represents controller input force (here, the suspension reaction force):

$$\begin{cases} m_1 z_1 s^2 = -(c_s s + k_s)(z_1 - z_2) + (c_t s + k_t)(z_0 - z_1) - F_c \\ m_2 z_2 s^2 = (c_s s + k_s)(z_1 - z_2) + F_c \end{cases} \quad (2)$$

And the transfer function of vibration can be given as:

$$z_2 = \frac{c_s s + k_s}{m_2 s^2 + c_s s + k_s} z_1 + \frac{1}{m_2 s^2 + c_s s + k_s} F_c \quad (3)$$

¹ The authors are with the Graduate School of Frontier Sciences The University of Tokyo, Japan, corresponding e-mail: chen-qi4396@g.ecc.u-tokyo.ac.jp.



Triple Skyhook Control.

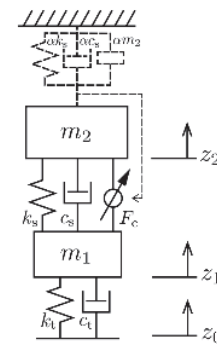
With the transfer function equation(2), [1] proposed a skyhook controller based on the coefficient cancellation as following, where α is a tunable gain:

$$F_c = -\alpha(m_2 s^2 + c_s s + k_s)z_2 \quad (4)$$

With this controller, the vibration of body mass can be suppressed by $\frac{1}{1+\alpha}$ as following:

$$z_2 = \frac{1}{1 + \alpha} \frac{c_s s + k_s}{m_2 s^2 + c_s s + k_s} z_1 \quad (5)$$

Also, a low-pass filter is usually used to deal with high frequency sensor noise and enhance system stability with a cut-off frequency around 10Hz, which is the upper bound of the control target frequency based on human sensitivity.



II. SEMINAR TOPIC - Design of Vertical Vibration Suppression Controller

A. Problem of Conventional Methods

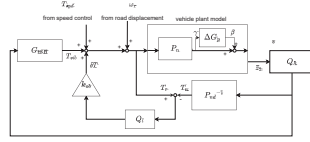


Fig. 1. Controller structure

1) *Offset and Noise of Vibration Sensor:* To make the algorithm practical in real vehicle plant, the feedback sensor noise and offset should be considered. In [1], a low pass filter with cutoff frequency of 10Hz is used to deal with the noise as well as enhance the stability of controller. But considering the double integrator characteristic of equation(4) when using the acceleration feedback, a small offset of the feedback signal may cause a fast diverge of suspension force output. Thus, an 1Hz high pass filter is necessary according to experiments.

2) *Robustness against Model error:* To enhance the robustness of triple skyhook(tSH) control, which is based on the vehicle plant parameter, a disturbance observer based structure [2] is introduced to help reduce the sensitivity toward β to γ shown in fig.1. The sensitivity of both situations can be given as:

$$G_{0tSH} = \frac{G_{tSH}G_{Pn}}{1 + G_{tSH}G_{Pn}} \quad (6)$$

$$G_{0DOB} = \frac{G_{tSH}G_{Pn} - k_{ob}Q}{1 + G_{tSH}G_{Pn}} \quad (7)$$

Thus the sensitivity towards model error δG_p can be reduced with the structure of DOB.

In some previous researches [3], a simple inertial nominal model shown as equation(8) is used to help suppress the vibration.

$$P_{ndc}^{-1} = \frac{T}{\ddot{z}_2} = \frac{r}{\tan\theta}m_2 \quad (8)$$

However, considering the use of high pass filter, this kind of simple model cannot help the vibration suppression performance, which means some improvement need to be done to help achieve a better vibration suppression.

B. Proposal Design of Controller

Aiming on the enhancement of vibration suppression with the use of high pass filter, which mainly influence the low frequency performance, a two-inertial frame structure based nominal model is proposed as following:

$$P_{ndp}^{-1} = \frac{T}{\ddot{z}_2} = \frac{r}{\tan\theta}\left(m_2 + \frac{c_s}{s}\frac{m_1 + m_2}{m_1} + \frac{k_s}{s^2}\frac{m_1 + m_2}{m_1}\right) \quad (9)$$

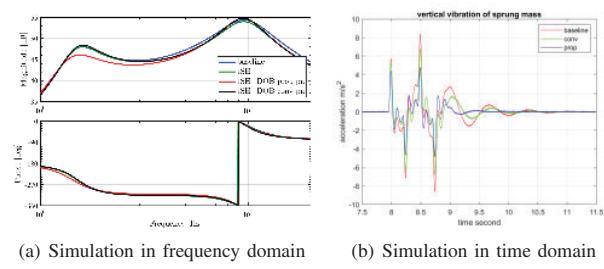
With the characteristic of integrator, the vibration feedback of low frequency is replenished to enhance the suppression performance.

C. Simulation

The simulation result are shown in fig.2 with both frequency and time domain.

Fig.2.1 shows the transfer characteristics from road disturbance input to sprung mass vibration with the using of both low pass filter(10Hz) and high pass filter(1Hz) to deal with sensor noise and offset. As it is shown in the graph, conventional tSH method(green) shows little effect below 3Hz. The proposal tSH+DOB structure with traditional inertia nominal model(black) shows nearly the same performance. And the proposal method with newly designed nominal model(red) has a better performance in low frequency while the same performance to conventional method in high frequency.

Fig.2.2 shows the time domain simulation with the imaginative road disturbance in around 2Hz. Compared to conventional tSH, which has a suppression of 10% peak to peak and 23.5% in RMSE(to the situation without control), the proposal method reduces the peak to peak value about 22% and the RMSE about 40.5%(to the situation without control), which clearly shows the effectiveness of proposal method.



(a) Simulation in frequency domain (b) Simulation in time domain

Fig. 2. Simulation result

REFERENCES

- [1] E. Katsuyama, "Improvement of ride comfort by triple skyhook control," in *9th International Munich Chassis Symposium 2018*. Springer, 2019, pp. 215–234.
- [2] T. Umeno and Y. Hori, "Robust speed control of dc servomotors using modern two degrees-of-freedom controller design," *IEEE Transactions on industrial electronics*, vol. 38, no. 5, pp. 363–368, 1991.
- [3] Y. R.Sato, H.Fujimoto, "Improvement of rough terrain running ability for mobility robot with in-wheel motor," *IEEE International Workshop on Sensing, Actuation, Motion Control, and Optimization*, 2016.



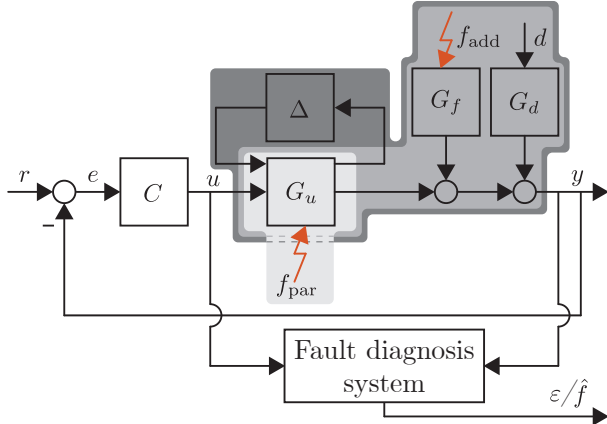
Qi Chen received the Bachelor's degree in automation from the Nanjing University of Aeronautics and Astronautics, China, in 2019. Currently, he is pursuing a Master degree at the department of electrical engineering at the University of Tokyo, Japan.

Fault Diagnosis for Precision Mechatronics

Koen Classens¹, W.P.M.H. (Maurice) Heemels¹ and Tom Oomen^{1,2}

I. RESEARCH OVERVIEW

The economic value of high-tech production equipment is proportional to its productivity. A key enabler for high productivity in manufacturing machines are positioning systems. The accuracy and speed of these positioning systems rely on an excellent and refined mechanical design in conjunction with effective control algorithms. In spite of exceptional mechanical system design and advanced control strategies, high-tech production equipment continues to experience considerable downtime. To minimize this downtime, fault diagnosis systems are essential which facilitate effectively scheduled and targeted maintenance such that productivity is maximized [1]. First, an overview of three different research topics is given, each considering a different model-class, as indicated in the figure below. Secondly, the seminar topic of optimal $\mathcal{H}_-/\mathcal{H}_\infty$ fault diagnosis is examined [2].



Parametric Fault Diagnosis [3].

A key indicator for increased risk for failures is the shifting of resonances. Such change in G_u can be considered as a parametric fault, f_{par} , and is particularly important as it affects closed-loop performance and stability margins. The aim is to track this time-varying behavior online and during normal operation through computationally cheap online algorithms. Algorithms, dedicated for closed-loop mechatronic systems, are developed and its effectiveness is illustrated on an over-actuated and oversensed setup which allows to artificially manipulate its effective resonances.

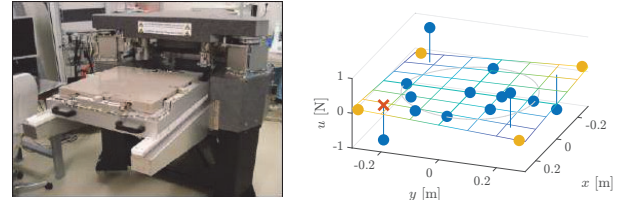
This work is supported by Topconsortia voor Kennis en Innovatie (TKI), and is supported by ASML Research, Veldhoven, The Netherlands.

¹ The authors are with the Dept. of Mechanical Engineering, Control Systems Technology, Eindhoven University of Technology, The Netherlands, corresponding e-mail: k.h.j.classens@tue.nl.

² Tom Oomen is with the Delft Center for Systems and Control, Delft University of Technology, Delft, The Netherlands.

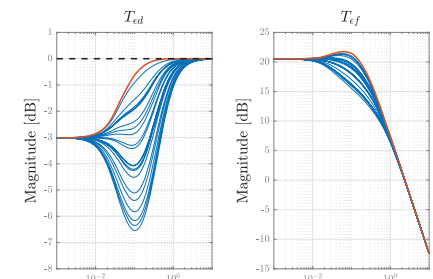
Nullspace-based Fault Detection and Isolation for Large Multivariable Systems [4], [5].

Fault Detection and Isolation (FDI) is the process of detecting faults and pinpointing its origin. It is shown that effective fault diagnosis filters can be synthesized to isolate additive faults, f_{add} , in real-time and optimally attenuate disturbances d . By means of a numerical case study and experimental validation on a next-generation prototype wafer stage, the effectiveness of this algorithm is illustrated. The system guarantees fault detection and isolation of a large number of imposed actuator and sensor faults. To this end, a bank residuals signals, ε , is used.



Robust Fault Diagnosis for Closed-loop Systems [6].

The effect of modeling uncertainties, Δ , is crucial in the model-based FDI concept. To guarantee a specified fault detectability on the true system, this uncertainty should explicitly be taken into account during fault diagnosis filter synthesis. Robust FDI synthesis tools are developed and are based upon fundamental theory of control such as LMI and Riccati-based optimization, and a generalization of the structured singular value, μ_g . This approach gives robust performance guarantees and allows to discriminate between unmodeled system dynamics, disturbances and faulty system behavior.



II. SEMINAR TOPIC - DIRECT SHAPING OF MINIMUM AND MAXIMUM SINGULAR VALUES FOR FAULT DIAGNOSIS

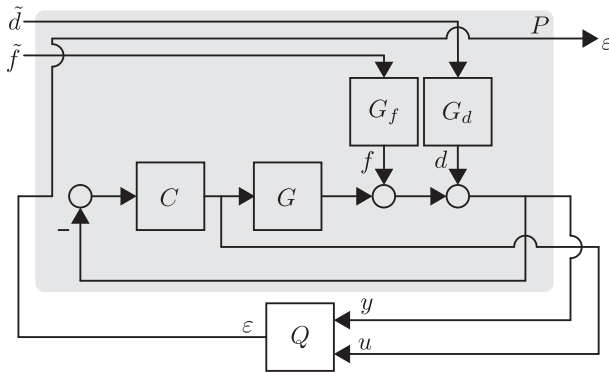
In this section, a framework is developed for the design and synthesis of optimal $\mathcal{H}_-/\mathcal{H}_\infty$ Fault Detection Filters [2].

A. Problem Formulation

Consider the block diagram depicted below, with weighted generalized disturbances \tilde{d} , weighted faults \tilde{f} , and the performance channel ε . The objective is to find an admissible residual generator Q which shapes the sensitivity to disturbances by constraining $\bar{\sigma}(T_{\varepsilon\tilde{d}}) < \gamma$, while simultaneously shaping the sensitivity to faults through constraining $\underline{\sigma}(T_{\varepsilon\tilde{f}}) > \nu$, where $\gamma, \nu > 0$. Hence, a fault diagnosis filter Q is said to satisfy $\mathcal{H}_-/\mathcal{H}_\infty$ specifications if

- 1) Q is proper and asymptotically stable;
- 2) $\|T_{\varepsilon\tilde{f}}(s)\|_- > \nu$;
- 3) $\|T_{\varepsilon\tilde{d}}(s)\|_\infty < \gamma$.

Better fault detection performance is achieved when the gap $\mathcal{J} := \frac{\nu}{\gamma}$ increases.



B. Approach

First the problem is casted into a generic framework with generalized plant P and the unknown filter Q , see the block diagram above. Next, the problem is posed as an optimization problem. The ratio \mathcal{J} is indirectly maximized through maximizing ν , while constraining γ , i.e.,

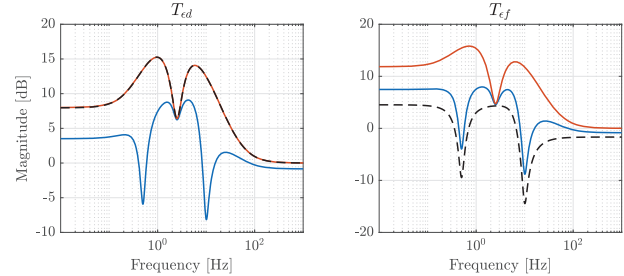
$$\begin{aligned} \max_{Q \in \mathcal{RH}_\infty, X \succ 0, \nu > 0, \gamma = \gamma_0} & \nu, \\ \text{subject to} & (*) \end{aligned} \quad (1)$$

where $\gamma = \gamma_0$. Additionally, $(*)$ indicates the minimum gain lemma and the bounded real lemma and X is a common Lyapunov variable, see [2] for details regarding the optimization. The solution is a set of matrix inequalities containing one BMI, which is solved iteratively by solving sequential LMIs.

C. Results

The developed framework is validated on a closed-loop system which is depicted as (—) without weighting filters, i.e., $T_{\varepsilon d}$ and $T_{\varepsilon f}$. The obtained bounds γG_d^{-1} and νG_f^{-1} are depicted as (---). Indeed, a filter Q is found that satisfies the

shaped upperbound and lowerbound. The residual generator is updated to compensate for the remaining gap between $T_{\varepsilon d}$ and γG_d^{-1} , i.e., $Q_2 = \frac{\gamma G_d^{-1}}{T_{\varepsilon d}} Q$, without affecting \mathcal{J} . The closed-loop system with the updated Q_2 is shown as (—).



D. Conclusion and Outlook

A new method to solve the $\mathcal{H}_-/\mathcal{H}_\infty$ problem is presented. In particular, a method is proposed to shape the minimum and maximum singular value of the closed-loop performance channels and its effectiveness is illustrated in the context of fault diagnosis. The approach can directly be implemented in combination with various multiobjective matrix inequalities and applied to synthesize filters for a wide range of control and estimation problems. Next, more emphasis will be put on including modeling uncertainty for robust fault diagnosis. In addition, the proposed fault diagnosis filters will be implemented on a next-generation wafer stage.

REFERENCES

- [1] K. Classens, W. P. M. H. Heemels, and T. Oomen, "Digital Twins in Mechatronics: From Model-based Control to Predictive Maintenance," in *2021 IEEE International Conference on Digital Twins and Parallel Intelligence*, Beijing, China, 2021.
- [2] K. Classens, W. P. M. H. Heemels, and T. Oomen, "Direct Shaping of Minimum and Maximum Singular Values: An $\mathcal{H}_-/\mathcal{H}_\infty$ Synthesis Approach for Fault Detection Filters," in *Proceedings of the IFAC 22st Triennial World Congress*, Yokohama, Japan, 2023.
- [3] K. Classens, M. Mostard, J. van de Wijdeven, W. P. M. H. Heemels, and T. Oomen, "Fault Detection for Precision Mechatronics: Online Estimation of Mechanical Resonances," in *IFAC-PapersOnLine*, vol. 55, 1, 2022, pp. 746–751.
- [4] K. Classens, W. P. M. H. Heemels, and T. Oomen, "On Nullspace-based Fault Diagnosis of Complex Mechatronic Systems," in *42nd Benelux Meeting on Systems and Control*, Eindhoven, The Netherlands, 2023.
- [5] K. Classens, W. P. M. H. Heemels, and T. Oomen, "Closed-loop Aspects in MIMO Fault Diagnosis with Application to Precision Mechatronics," in *2021 American Control Conference (ACC)*, New Orleans, Louisiana, USA, 2021, pp. 1752–1757.
- [6] K. Classens, W. P. M. H. Heemels, and T. Oomen, "On Robust Fault Diagnosis of Complex Mechatronic Systems," in *41th Benelux Meeting on Systems and Control*, Brussels, Belgium, 2022.



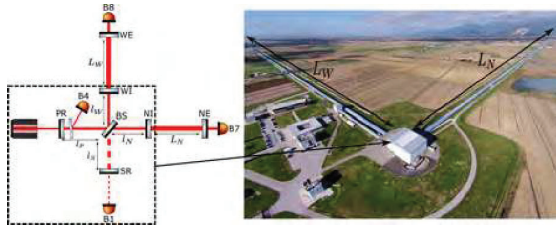
Koen Classens received the B.Sc degree (cum laude) (2016), the M.Sc degree (cum laude) (2019) in Mechanical Engineering, and the M.Sc degree (cum laude) (2019) in Systems & Control from the Eindhoven University of Technology, Eindhoven, The Netherlands. He is currently pursuing a Ph.D. degree in the Control Systems Technology group within the department of Mechanical Engineering at Eindhoven University of Technology. His research is centered around the development of fault detection and isolation systems for precision mechatronics.

Control in Gravitational Wave detectors

Mathyn van Dael^{1,2}, Gert Witvoet^{1,3}, Bas Swinkels² and Tom Oomen^{1,4}

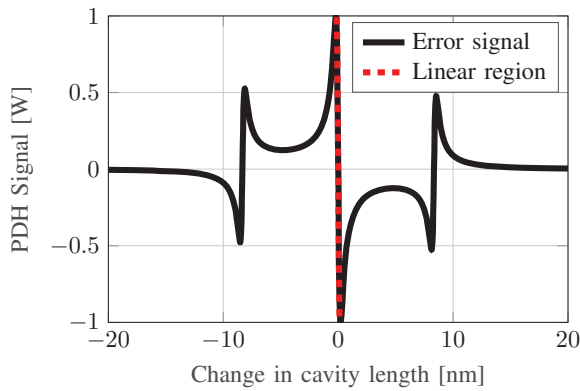
I. RESEARCH OVERVIEW

Gravitational Wave (GW) detectors measure spatial fluctuations induced by violent cosmic events such as for example the merger of black holes. Current generation detectors such as Virgo [1] and KAGRA [2] employ laser interferometry using several kilometer long arms (L_W , L_N) to measure spatial fluctuations in the order of 1×10^{-18} m. Control systems play a vital role in the operation and sensitivity of the detector.



Cavity locking

The lengths of optical cavities, i.e. distances between mirrors, have to be actively controlled for the detector to operate. The error signals for these feedback loops use the Pound-Drever-Hall (PDH) [3] method to obtain an error signal (—) that is locally linear (---). The linear region of these error signals are smaller than 1 nm, while the seismically induced motion of the mirrors before the cavities are controlled are in the order of 1 μ m.



¹ The authors are with the Control Systems Technology research section of the Eindhoven University of Technology, the Netherlands, corresponding e-mail: m.r.v.dael@tue.nl.

² Gert Witvoet is with the TNO, Delft, The Netherlands

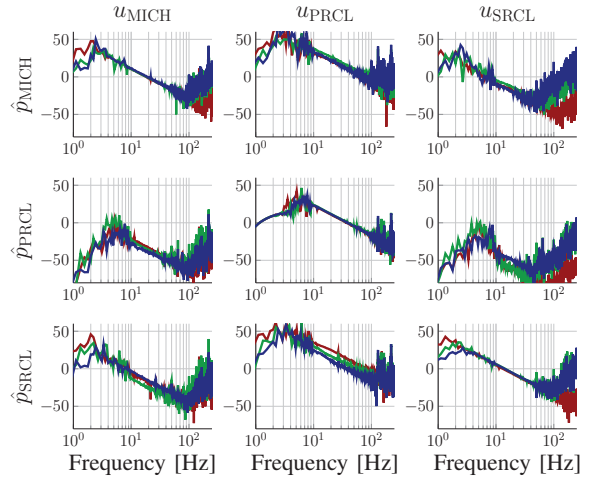
³ Bas Swinkels is with Nikhef, The Netherlands

⁴ Tom Oomen is with Delft University of Technology, The Netherlands.

Currently the cavities are locked by waiting for the error signal to be in the linear regime, at which time the linear feedback controller is engaged. Three cavities furthermore have to be locked simultaneously, requiring all three cavities to be in the linear regime of their error signal. The combination of the many degrees of freedom and poor weather conditions complicates the locking procedure and results in a reduced duty cycle of the detector. The goal of this research is to estimate the cavity lengths in a wider range of the non-linear error signal using non-linear state estimation techniques, to allow faster locking of the cavities and increase the duty cycle of the detector.

System with time-varying levels of interaction.

Three degrees of freedom in the Virgo detector exhibit strong levels of interaction and these interaction terms furthermore vary in amplitude and direction in a timespan of minutes [4]. The figure below shows the MIMO frequency response of the plant for the three loops, where the colored lines represents measurements of the frequency response, each taken one week apart. The SISO control loops require sufficient stability margins to guarantee MIMO closed-loop stability. These degrees of freedom also couple strongly to the sensitivity of the detector and low bandwidth controllers with large roll-off is therefore desired to minimize this coupling. The required stability margins therefore pose a limit on the amount of roll-off that can be achieved. The goal of this research is to develop a method maximizes the system performance in view of the varying levels of interaction.



II. SEMINAR TOPIC - Integrated Dynamic Error Budgeting and \mathcal{H}_2 synthesis

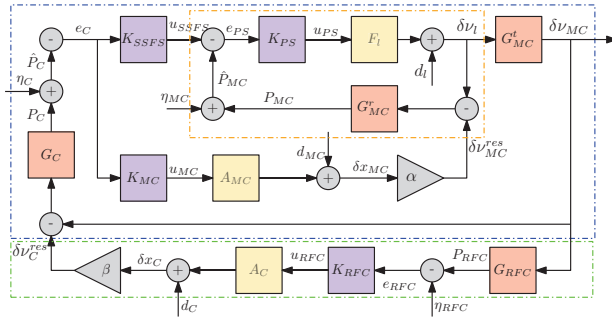
This section discusses the development of an integrated Dynamic Error Budget (DEB) and \mathcal{H}_2 synthesis.

A. Problem formulation

The arms that determine the interference pattern of the detector consist of cavities in which the light resonates up and down several hundred times in order to increase the effective length of the cavity. This resonance condition is attained when it holds that

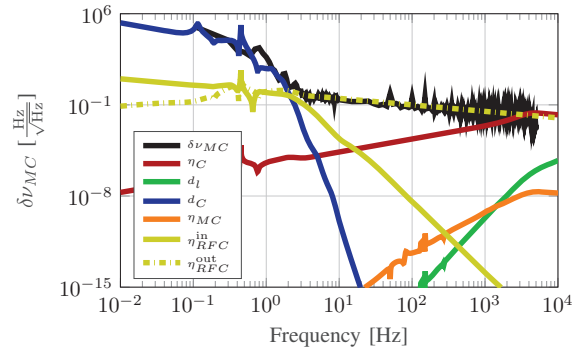
$$L_{\text{cav}} = N \cdot \frac{\lambda}{2}, \quad (1)$$

with L_{cav} the cavity length in m , λ the wavelength of the laser in m and N an integer number. Both the cavity length and laser frequency fluctuate several orders more than the required stability and are therefore actively controlled in a control system of three nested loops, each highlighted by a colored rectangular box in the block diagram below. The performance variable, the laser frequency fluctuations $\delta\nu_{MC}$, is influenced by all three loops and is furthermore subject to different disturbances coupling to the output, making it difficult to identify which controller to optimize and how.



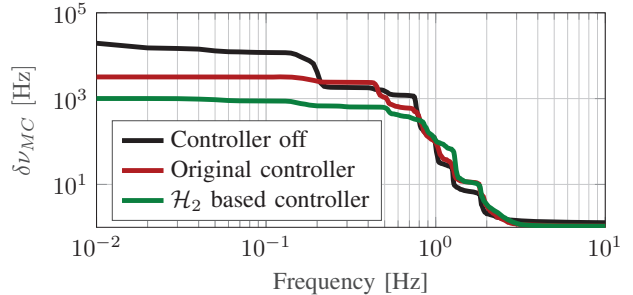
B. Approach

The approach consists of two steps. First, a Dynamic Error Budget (DEB) is developed, which consists of a spectrum of the error together with the closed-loop contributions of the modelled disturbances. This DEB is used to identify the limiting disturbances as well as how to tune the controllers to minimize this coupling. Second, the DEB is used as weighting in \mathcal{H}_2 synthesis to obtain a controller that minimizes the RMS of the performance variable.



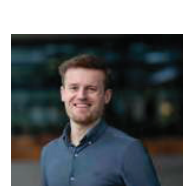
C. Experimental results

The \mathcal{H}_2 based controller is implemented on the full Virgo detector to compare the experimental performance. The \mathcal{H}_2 based controller (green) outperforms the original controller (red) in terms of Root-Mean-Square (RMS) error by a factor three. In this talk, we will present a systematic design method using dynamic error budgeting and \mathcal{H}_2 synthesis to derive the presented control design and further elaborate on the experimental results.



REFERENCES

- [1] F. Acernese *et al.*, “Advanced Virgo: a second-generation interferometric gravitational wave detector,” *Class. Quant. Grav.*, vol. 32, no. 2, p. 024001, 2015.
- [2] T. Akutsu *et al.*, “Kagra: 2.5 generation interferometric gravitational wave detector,” *Nature Astronomy*, vol. 3, pp. 35 – 40, 2018.
- [3] E. D. Black, “An introduction to Pound–Drever–Hall laser frequency stabilization,” *Am. J. of Phys.*, vol. 69, no. 1, pp. 79–87, 01 2001.
- [4] M. van Dael *et al.*, “Design for interaction: Factorized Nyquist based control design applied to a Gravitational Wave detector,” in *Proceedings of the 2022 Modelling, Estimation and Control Conference*, 2022.



Mathyn van Dael received the MSc. degree in System and Control from the Eindhoven University of Technology, in 2021. Currently, he is pursuing a Ph.D. degree at the department of mechanical engineering at the Eindhoven University of Technology. His research is focussed on improving Gravitational Wave detectors through advanced control methodologies.

High-Precision Mechatronics: from Experiment Design to Point of Interest Control

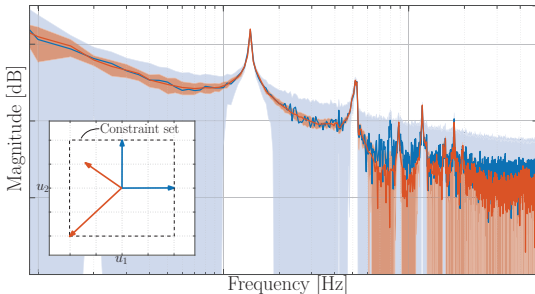
Nic Dirkx^{1,2}, Koen Tiels² and Tom Oomen^{2,3}

I. RESEARCH OVERVIEW

The performance of future high-precision mechatronics relies on advanced control strategies that can cope with the increasing system complexity, e.g., due to pronounced flexible dynamics, unmeasurable performance variables, and a large number of actuators and sensors. The availability of high-quality identified dynamic models that accurately describe these complex systems is indispensable for precision control. This research is focused on advanced identification and control of complex precision mechatronics.

Exploiting input directions enables effective identification [1].

Good design of identification experiments is crucial to obtain high-quality models, especially for complex motion systems with a large number of actuators. In classical optimal input signal design approaches, such MIMO systems are treated as a multiple of SIMO systems, leading to non-optimal model quality. In [1], it is shown that optimality is achieved by exploiting the multiplicity of the actuators, resulting in directional input signals. Optimal directional inputs significantly reduce the uncertainty region (■) compared to classical optimal input design strategies (□).



Addressing control purpose in experiment design and identification improves robust performance [2].

Addressing the control goal during the system identification procedure is crucial to ensure that the model achieves high

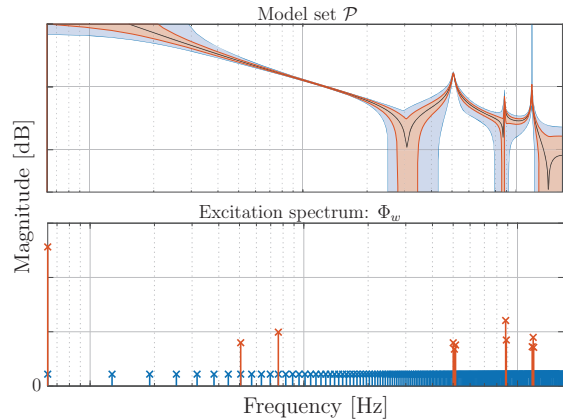
This work is part of the research programme VIDI with project number 15698, which is (partly) financed by the NWO.

¹ Nic Dirkx is with ASML, Veldhoven, The Netherlands, corresponding e-mail: nic.dirkx@asml.com.

² The authors are with the Control Systems Technology research section of the Eindhoven University of Technology, the Netherlands.

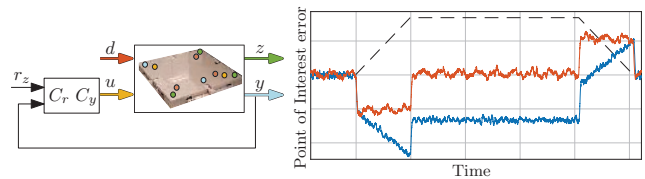
³ Tom Oomen is also with the Delft Center for Systems and Control, Delft University of Technology, Delft, The Netherlands.

control performance. In [2], a framework is developed for the identification of model sets for high-performance robust control. The key approach is to connect the criteria for robust control, identification, and experiment design through a specific robust-control-relevant (rcr) coprime factorization. Using a rcr excitation spectrum design (—), a significantly tighter model set (■) is identified, compared to the set (□) resulting from classical excitation design. This enables improving robust control performance.



Controlling the point that matters via inferential control [3].

In many motion systems, the point of interest z cannot be measured directly, but must be estimated from sensory data y in combination with a dynamic system model. The inferential aspect has large implications on the structure, the dynamics, and the design of the controller. In addition, the required inferential controller is inherently model-based, which emphasizes the need for addressing model uncertainty. In [3], a robust multivariable control design framework is developed for positioning the point of interest explicitly. Experimental results show that the inferential controller (—) suppresses the disturbance (---) significantly better than the classical control approach (—).



II. SEMINAR TOPIC - EXPLOITING WAVELETS FOR FRF IDENTIFICATION WITH MISSING SAMPLES [4]

Frequency Response Function (FRF) identification of complex systems typically requires collecting a large data amount. In practice, corrupted or missing samples in the data often occurs, which complicates FRF identification. In this section, a method is presented to accurately identify FRFs in the presence of missing samples.

A. Problem formulation

The aim is to identify the FRF model $G(\Omega_k)$ from measured input and output data u, y^m where y^m contains missing samples. The input-output relation is exactly represented in the frequency domain by

$$\begin{aligned} Y(k) &= G(\Omega_k)U(k) + T(k) + V(k), \\ Y^m(k) &= Y(k) + \Delta(k), \end{aligned} \quad (1)$$

where $U(k), Y^m(k)$ is the Discrete Fourier Transform (DFT) of the signals u, y^m at frequency bin k , term $T(k)$ denotes the transient and $V(k)$ the DFT of the measurement noise. Term $\Delta(k)$ is the global and non-smooth perturbation due to the missing samples, which affects $Y^m(k)$ as shown in Fig. 1.

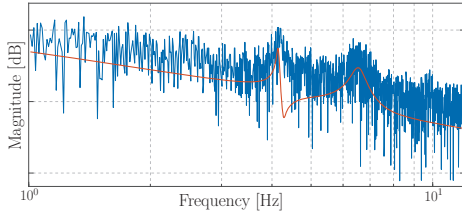


Fig. 1. Y (—) and Y^m (—). Missing samples introduce a global perturbation.

B. Approach: Wavelet-based Local Polynomial Method

The key idea is to project out the effect of the missing samples $\Delta(k)$ via a matrix M , such that

$$Y^m M = (Y + \Delta) M = YM. \quad (2)$$

To achieve (2), matrix M is selected as a bank of wavelets over a frequency grid. This enables transforming the time-domain data y^m to the time-frequency plane, in which the effect of the missing samples is local. This is shown in Fig. 2 for the same data as used in Fig. 1.

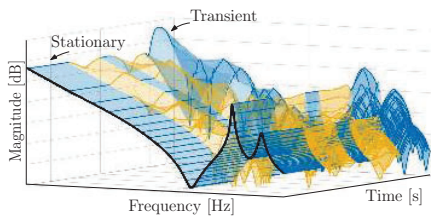


Fig. 2. Time-frequency plane representation of y^m , in which the effect of the missing samples (■) is local.

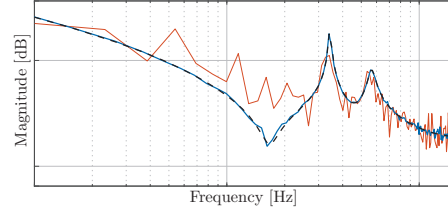
To identify the FRF $G(\Omega_k)$ from the time-frequency plane data in (■), the classical Local Polynomial Method (LPM) [5] is extended to incorporate the wavelet-based transform. The FRF estimate is obtained from the minimization problem

$$\hat{\Theta} = \arg \min_{\Theta} \|(Y^m - K\Theta) M\|_2, \quad (3)$$

where K parametrizes G and T by local polynomials as in the LPM, and Θ denotes the estimation variables.

C. Results

The developed method is applied for the identification of the simulated system with FRF in (—) in the figure below from noisy data with missing samples. The estimated FRF (—) accurately reflects the true system. In contrast, the classical LPM approach (—) fails to deliver an accurate model as a result of the missing samples.



D. Conclusions and ongoing work

The presented wavelet-based identification approach enables achieving accurate FRF models from data that is corrupted by missing samples. Future work includes uncertainty quantification, closed-loop extensions, and experimental validation.

REFERENCES

- [1] N. Dirkx, J. van de Wijdeven, and T. Oomen, "Frequency response function identification for multivariable motion control: Optimal experiment design with element-wise constraints," *Mechatronics*, vol. 71, p. 102440, 2020.
- [2] N. Dirkx and T. Oomen, "Identification and experiment design for robust control: A non-normalized coprime factor approach," *In preparation for journal submission*, 2023.
- [3] N. Dirkx, N. Moeren, and T. Oomen, "Suppressing non-collocated disturbances in inferential motion control: with application to a wafer stage," in *2021 American Control Conference (ACC)*. IEEE, 2021, pp. 4333–4338.
- [4] N. Dirkx, K. Tiels, and T. Oomen, "A wavelet-based approach to frf identification from incomplete data," *IEEE Transactions on Instrumentation and Measurement*, vol. 72, pp. 1–15, 2023.
- [5] R. Pintelon, J. Schoukens, G. Vandersteen, and K. Barbé, "Estimation of nonparametric noise and FRF models for multivariable systems—part I: Theory," *Mechanical Systems and Signal Processing*, vol. 24, no. 3, pp. 573–595, 2010.



Nic Dirkx received the MSc. degree in control systems from the Eindhoven University of Technology, in 2011. Currently, he is researcher at ASML Research Mechatronics & Control, while pursuing a Ph.D. degree at the department of mechanical engineering at the Eindhoven University of Technology. His research interests include advanced identification and control of high-precision mechatronics.

Multirate Adaptive Robust Control for Five-axis Machine Tools

CE Chenyu¹, BINH MINH NGUYEN^{1,2} and Hiroshi FUJIMOTO^{1,3}

I. RESEARCH OVERVIEW

The co-author Prof.Fujimoto proposed the multi-rate perfect tracking control in 2000. It is a powerful feedforward control method for high precision tracking control. However, it is a model based controller which means it can be largely influenced by modeling error.

To solve such problems, an online RLS estimator is used. The schematic of the machine tool, a 2DoF cradle is given as Figure.1.

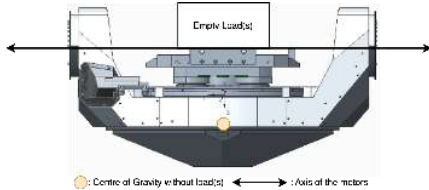


Fig. 1. The schematic of a 2DoF cradle

Such cradle like mechanism can be simplified in to a 2-inertia system, please see Figure.2. below.

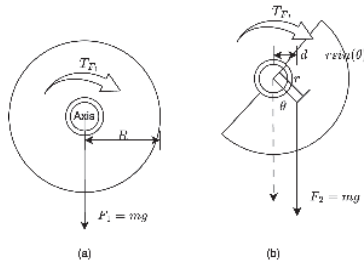


Fig. 2. (a) Schematic of a normal 2-inertia motor bench load (b) Schematic of unbalanced load

The dynamic model in Figure.2.(a) can be written as:

$$T_m = J\ddot{\theta} + D\dot{\theta} \quad (1)$$

It's easy to derive the dynamic model of Figure.2.(b) as:

$$T_m = J\ddot{\theta} + D\dot{\theta} + U \sin\theta \quad (2)$$

The goal is using RLS algorithm to estimate J , D and U online.

Supporting: Masahiro MAE and Takumi HAYASHI from The University of Tokyo. Yoshihiro ISAOKA, Yuki TERADA from DMG MORI CO., LTD.

Perfect Tracking Feedforward Control

For the PTC feedforward control, the details can be learned from [1] [4]. The schematic of single-rate PTC is shown in Figure.3.

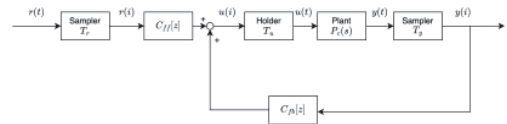


Fig. 3. The schematic of single-rate PTC

The relationship between those rates are given as Figure.4.

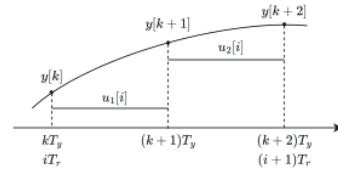


Fig. 4. The schematic of multi-rate relations

Recursive Least-square Algorithm

The continuous time RLS was originally proposed in [3]. RLS is a online parameter estimation tool that can calculate the system parameters- θ from the system input(s) u , and the system output(s) φ .

The discrete-time algorithm is represented below.

$$\hat{\theta}[k] = \hat{\theta}[k-1] + Proj_{\hat{\theta}}\{K[k](u[k] - \varphi^T[k])\hat{\theta}[k-1]\} \quad (3)$$

Where P and K are updated in every step, the update equation is given as:

$$K[k] = \frac{P[k-1]\varphi[k]}{\lambda + \varphi^T[k]P[k-1]\varphi[k]} \quad (4)$$

$$P[k] = \frac{(I - K[k]\varphi^T[k])P[k-1]}{\lambda} \quad (4)$$

The projection algorithm which guarantees that the estimated parameters do not break the designated limits, are given as below:

$$Proj_{\hat{\theta}}(H_j) = \begin{cases} 0, & \text{if } \hat{\theta}_j \geq \theta_{jmax} \quad \& \quad H_j \geq 0 \\ 0, & \text{if } \hat{\theta}_j \leq \theta_{jmin} \quad \& \quad H_j \leq 0 \\ H_j, & \text{Otherwise} \end{cases} \quad (5)$$

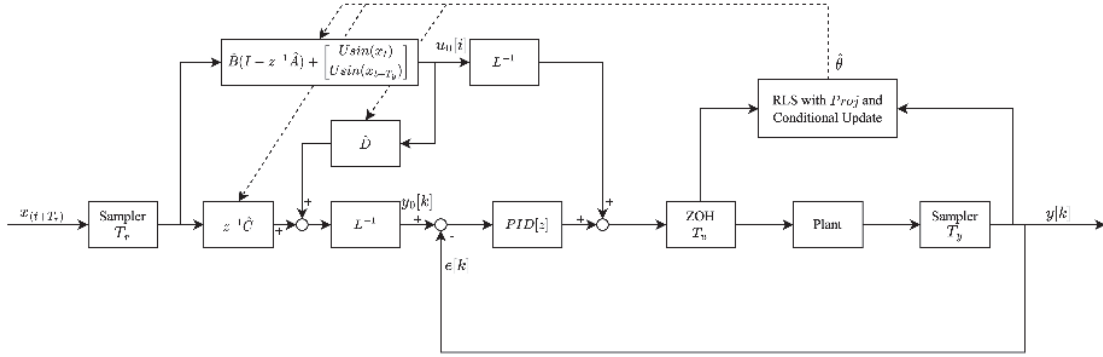


Fig. 5. Schematic of Multi-rate Adaptive Robust Control

II. SEMINAR TOPIC - *Multi-rate Adaptive Robust Control*

A. Perfect tracking Controller Design

To build a PTC controller, we need the system model. From equation (2), the continuous system state space model can be obtained as [2]:

$$\begin{aligned} \dot{x} &= A_c x + B_c(u - U \sin(\theta)) \\ y &= C_c x \end{aligned} \quad (6)$$

The discrete model of the unbalanced torque would be:

$$\begin{aligned} x[k+1] &= A_d x[k] + B_d(u[k] - U \sin(\theta[k])) \\ y[k] &= C_d x[k] \end{aligned} \quad (7)$$

Where the discrete state space can be derived as:

$$A_d = e^{A_c T_y}, \quad B_d = \int_0^{T_y} e^{A_c \tau} B_c d\tau, \quad C_d = C_c \quad (8)$$

Beyond that, the Multi-rate state space is given as:

$$\begin{aligned} x[i+1] &= Ax[i] + B(u[i] - U \sin(\theta[i])) \\ y[i] &= Cx[i] + D(u[i] - U \sin(\theta[i])) \end{aligned} \quad (9)$$

The state space matrices A, B, C, D are given in [4] [1]. The estimated system parameters coming from the RLS with projection will be used to update the PTC feed forward controller.

B. Recursive Least-square

The RLS convergence are validated through simulations:

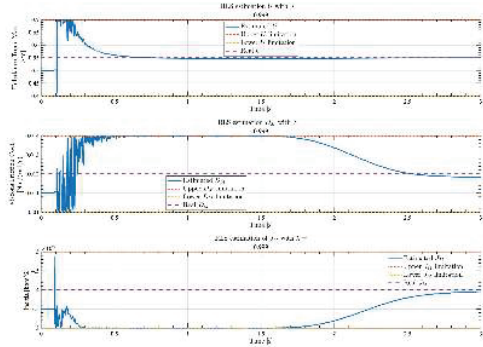


Fig. 6. The schematic of multi-rate relations

REFERENCES

- [1] Fujimoto, Hiroshi, Yoichi Hori, and Atsuo Kawamura. "Perfect tracking control based on multirate feedforward control with generalized sampling periods." *IEEE Transactions on Industrial Electronics* 48.3 (2001): 636-644.
- [2] Fujimoto, Hiroshi, and Bin Yao. "Multirate adaptive robust control for discrete-time non-minimum phase systems and application to linear motors." *IEEE/ASME Transactions on mechatronics* 10.4 (2005): 371-377.
- [3] Yao, Bin, and Andrew Palmer. "Indirect adaptive robust control of SISO nonlinear systems in semi-strict feedback forms." *IFAC Proceedings Volumes* 35.1 (2002): 397-402.
- [4] Fujimoto, Hiroshi. General framework of multirate sampling control and applications to motion control systems. Diss. PhD thesis, The University of Tokyo, 2000.



Chenyu GE received the Bachelor's degree(2021) in Nanjing University of Aeronautics and Astronautics, Nanjing, China. Currently he's in Master's Course following Prof. H.Fujimoto in the University of Tokyo, Japan.

Identification and Control for Periodic and Parameter-Varying Systems

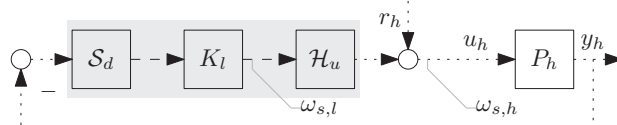
Max van Haren¹, Lennart Blanken^{1,2} and Tom Oomen^{1,3}

I. RESEARCH OVERVIEW

Increasing performance requirements for control in mechatronics leads to a situation where complex effects have to be modeled, identified and taken into account for control. For example, consider the addition of sensors, e.g., a camera, that introduces multirate sampling, and flexible dynamics that typically introduces position-dependent effects. Examples of such systems are vision-in-the-loop systems, wafer scanners and belt-driven systems. For these type of systems, performance evaluation, control and identification methods are lacking.

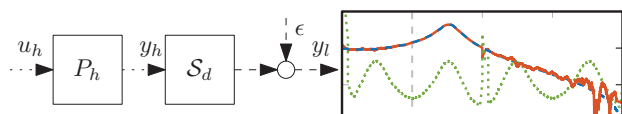
Lifting Enables Direct Evaluation of Multirate Closed-Loop Performance [1].

For multirate or sampled-data control, it is desirable to directly evaluate the closed-loop performance, that is not trivial due to the periodic effects introduced by the down- and upsampler. In [1], the performance variables are lifted, such that an LTI system is recovered and can be used for performance evaluation.



Polynomial Estimates Facilitate the Identification of Slow-Sampled Systems Above the Nyquist Frequency [2].

Frequency-Response Function (FRF) identification for slow-sampled systems is enabled through approximating the system in multiple frequency bands by a polynomial, resulting in an identified FRF (—) above the Nyquist frequency (---). Additionally, variance estimates (....) are included.



This work is part of the research programme VIDI with project number 15698, which is (partly) financed by the Netherlands Organisation for Scientific Research (NWO). In addition, this research has received funding from the ECSEL Joint Undertaking under grant agreement 101007311 (IMOCO4.E).

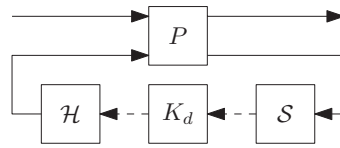
¹The authors are with the Eindhoven University of Technology, The Netherlands, corresponding e-mail: m.j.v.haren@tue.nl.

²Lennart Blanken is with Sioux Technologies, Eindhoven, The Netherlands.

³Tom Oomen is with the Delft University of Technology, The Netherlands.

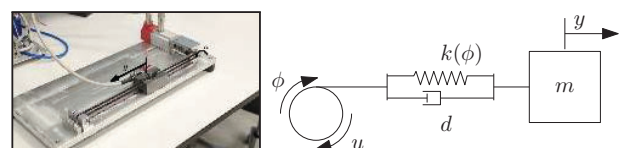
Control design for multirate and sampled-data applications.

The goal of this research topic is to design controllers for systems that have multirate sampling, and to improve intersample behavior of sampled-data systems. Ongoing research is aimed at designing controllers that directly account for the closed-loop performance of multirate systems discussed in [1], and improving intersample behavior by utilizing multirate state-tracking.



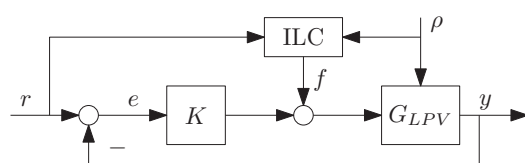
Kernel-Regularized Identification Enables Feedforward for Position-Dependent Systems [3].

Feedforward for LPV motion systems is defined by using basis functions and kernel regularized system identification, resulting in a model-free learning approach. Dependency on the derivatives of the scheduling is explicitly accounted for motion systems through a change of variables. This topic is presented in more detail in Section II.



Iterative learning techniques for LPV systems.

For Linear-Parameter Varying (LPV) systems, it is desirable to incorporate LPV feedforward into iterative learning methods. The aim in this topic is to add LPV feedforward parameters into the iterative framework, and be applied to mechatronic systems. Ongoing research is aimed at convergence results and hyperparameter optimization.



II. SEMINAR TOPIC - KERNEL REGULARIZED LPV FEEDFORWARD: APPLIED TO MOTION SYSTEMS

In this section, a framework is developed for the design and identification of LPV feedforward for motion systems [3].

A. Problem Formulation

The aim in this section is to create LPV feedforward controller F_{LPV} to minimize the tracking error $e = r - y$, as seen in Fig. 1.

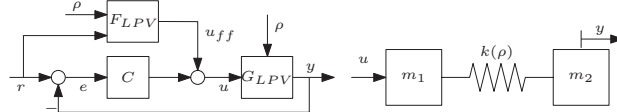


Fig. 1. Left: Feedforward structure considered. Right: Example LPV motion system.

The class of LPV motion systems are statically dependent on the scheduling sequence and have representation

$$G_{LPV} : \sum_{i=0}^{n_a} a_i(\rho) \frac{d^i}{dt^i} y = \sum_{j=0}^{n_b} b_j(\rho) \frac{d^j}{dt^j} \int \int u dt^2. \quad (1)$$

The inverse dynamics, i.e., the dynamics mapping y to u , are dynamically dependent on ρ , due to the second integral.

Example 1. The system in Fig. 1 has inverse dynamics

$$\begin{aligned} u &= \frac{d^2}{dt^2} \left(\left(\frac{m_2 m_1}{k(\rho)} \frac{d^2}{dt^2} + (m_2 + m_1) \right) y \right), \\ &= (m_1 + m_2) \ddot{y} + \frac{m_1 m_2}{k(\rho)} \dddot{y} - \frac{2m_1 m_2 \dot{\rho} k'(\rho)}{k^2(\rho)} \ddot{y} + m_1 m_2 \frac{2\dot{\rho}^2 \frac{k''(\rho)}{k(\rho)} - \dot{\rho} k'(\rho) - \dot{\rho}^2 k''(\rho)}{k^2(\rho)} \ddot{y} \end{aligned}$$

having dynamic dependency, i.e., dependency on the derivative of the scheduling, $\dot{\rho}$ and $\ddot{\rho}$. ■

B. Approach

The developed approach utilizes basis functions and LPV feedforward parameter functions and is defined as

$$F_{LPV} : \begin{cases} w_{ff} &= \sum_{i=1}^{n_\theta} \theta_i(\rho) \psi_i \left(\frac{d}{dt} \right) r, \\ u_{ff} &= \frac{d^2}{dt^2} w_{ff} \end{cases} \quad (2)$$

Example 2. The system in Fig. 1 with inverse dynamics shown in Example 1 has optimal w_{ff} as

$$w_{ff} = \int \int u_{ff} dt^2 = \left(\frac{m_2 m_1}{k(\rho)} \frac{d^2}{dt^2} + (m_2 + m_1) \right) y, \quad (3)$$

that is only statically dependent on ρ , but results in optimal feedforward u_{ff} including dynamic dependency. ■

The LPV parameter functions $\theta_i(\rho)$ are learned using data and a kernel regularized cost function [4], i.e.,

$$\hat{\Theta} = \arg \min_{\Theta} \|\bar{w} - \Phi \Theta\|^2 + \gamma \|\Theta\|_{\mathcal{H}}^2, \quad (4)$$

where more details are found in [3]. The regularization $\|\Theta\|_{\mathcal{H}}^2 = \Theta^\top K^{-1} \Theta$ specifies high-level properties of the feedforward parameters using the kernel K , e.g., smoothness or periodicity. The applied feedforward force to the system u_{ff} , see (2), leads to optimal polynomial feedforward, including dynamic dependency for LPV motion systems.

C. Results

The developed framework is validated on the system in Fig. 1 where $k(\rho) = c/(\rho(L-\rho))$, with constants c and L . The estimated parameter $\frac{m_1 m_2}{k(\rho)}$ is seen in Fig. 2. The performance is compared to traditional LTI feedforward in Fig. 3.

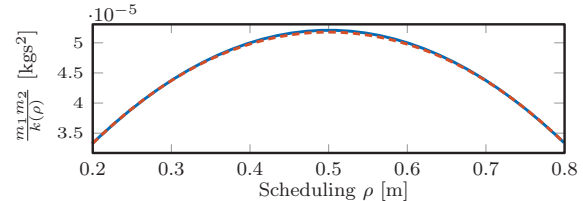


Fig. 2. True (—) and estimated (---) feedforward parameter $\frac{m_1 m_2}{k(\rho)}$.

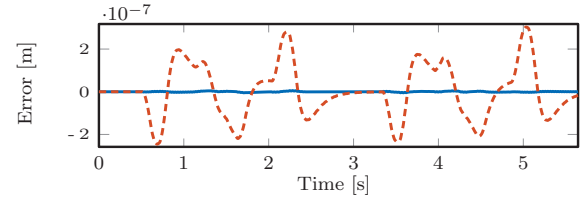


Fig. 3. Error for LTI (---) and developed (—) feedforward.

The tracking error is significantly reduced from $\|e\|_2 = 4.2 \cdot 10^{-6} \text{ m}$ to $5.8 \cdot 10^{-8} \text{ m}$.

III. CONCLUSIONS

LPV feedforward for a class of motion systems is developed, where the feedforward controller is directly identified based on input-output data, including dynamic dependency. Significant performance increase is observed for an LPV motion system. Ongoing research is aimed at experimental validation and the addition of iterative learning methods.

REFERENCES

- [1] M. van Haren, L. Blanken, and T. Oomen, "Frequency Domain Identification of Multirate Systems: A Lifted Local Polynomial Modeling Approach," in *Conf. Decis. Control*, 2022.
- [2] M. van Haren, L. Mirkin, L. Blanken, and T. Oomen, "Beyond Nyquist in Frequency Response Function Identification: Applied to Slow-Sampled Systems (To Appear)," 2023.
- [3] M. van Haren, L. Blanken, and T. Oomen, "Polynomial Feedforward for Linear Parameter-Varying Systems: a Kernel Regularized Approach," in *22nd World Congr. Int. Fed. Autom. Control*, Yokohama, 2023.
- [4] G. Pillonetto, F. Dinuzzo, T. Chen, G. De Nicolao, and L. Ljung, "Kernel methods in system identification, machine learning and function estimation: A survey," *Automatica*, vol. 50, no. 3, pp. 657–682, 2014.



Max van Haren received the MSc. degree (cum laude) in systems and control from the Eindhoven University of Technology, in 2021. Currently, he is pursuing a Ph.D. degree at the department of mechanical engineering at the Eindhoven University of Technology. His research interests include control and identification of sampled-data, multirate and linear parameter-varying systems for mechatronics.

Fast and High-Precision Temperature Control in Semiconductor Thermal Process

Akira Hirata¹, Ryosuke Shibatsuji¹, Tatsuya Yamaguchi¹, and Wataru Ohnishi²

I. RESEARCH OVERVIEW

Semiconductor technology is the basis for the affluence and convenience of the modern world and plays an important role in a low-carbon society. As the shrinking of circuit critical dimensions and the introduction of 3-dimensional integrated circuits continues, the manufacturing process should meet higher accuracy, productivity and yield.

Among various manufacturing processes, semiconductor thermal processing includes several essential steps, such as oxidation, annealing, diffusion, and chemical vapor deposition. There are mainly two equipment types for this process: batch type and single-wafer type. This section introduces the fast, high precision, and energy-friendly temperature control in the batch type vertical furnace [1]. The other section will discuss the application of iterative learning control (ILC) in the single-wafer type equipment.

The vertical furnaces must achieve even faster and more precise temperature control due to the demand for ever reducing the minimum feature size or critical dimension in semiconductor chips. Furthermore, not only these control performances, but also low energy consumption is required.

The vertical furnace is equipped with heaters and coolers, as shown in Fig. 1. For the temperature measurement, it has several thermocouples called inner TCs in the process tube near the wafers. In addition, the vertical furnace is divided into 6 zones. However, the average temperature of the inner TCs is used as the temperature output in the paper since the paper focuses on the integration of the heater and the cooler. Similarly, for the heaters, all zones are set to have the same values of heater power. This is also the case for coolers. Therefore, the paper treated the system as a two-input, one-output system with the average power of the heaters and coolers as input and the average inner temperature as output.

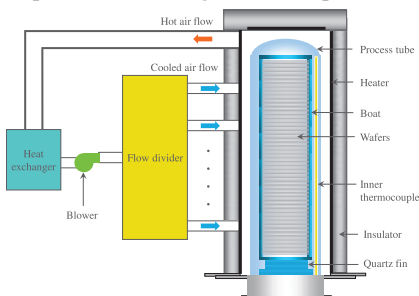


Fig. 1. Thermal plant configuration of the semiconductor vertical furnace.

¹Akira Hirata, Ryosuke Shibatsuji and Tatsuya Yamaguchi are with Tokyo Electron Technology Solutions Ltd., Japan, corresponding e-mail: akira.hirata@tel.com.

²Wataru Ohnishi is with The University of Tokyo, Japan.

The frequency response functions (FRFs) of the plant were measured using frequency domain system identification with zippered multisine signal. The FRFs indicate that the heater and the cooler characteristics are similar, except for the phase reversal and gain offset. The paper presents the heater-cooler integration method. The integrated control input u_{int} generates the heater power u_h and the cooler power u_c :

$$\begin{cases} u_h = u_{int} & u_c = 0 \quad \text{if } u_{int} \geq 0 \\ u_h = 0 & u_c = \frac{1}{k_{c \rightarrow h}} u_{int} \quad \text{else} \end{cases}$$

where $k_{c \rightarrow h}$ indicates the constant gain that brings the FRF of the cooler closer to the FRF of the heater as shown in Fig. 2. Therefore, the heater-cooler integrated controlled system is obtained as follows

$$G_{siso} = \frac{1}{2} G_{miso} \begin{bmatrix} 1 \\ k_{c \rightarrow h} \end{bmatrix}.$$

A two-degree of freedom controller was designed to control the system G_{siso} . The experimental results are shown in Fig. 3. The proposed control achieves both high control performance and low power consumption.

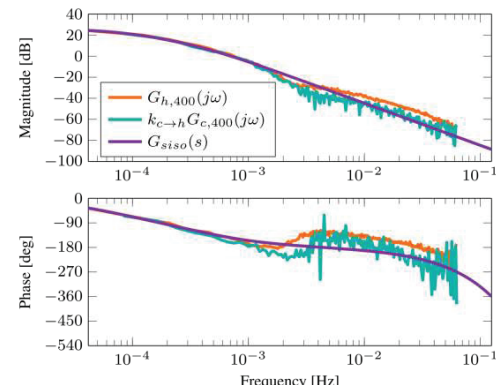
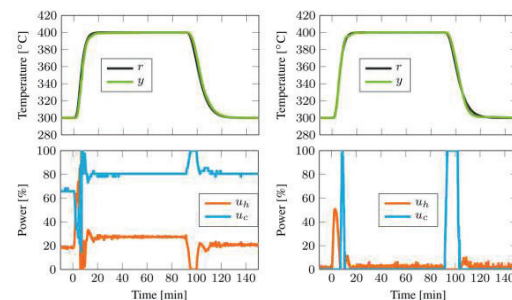


Fig. 2. Frequency response function and second-order model after the heater-cooler integration.



(a) LQG control. (b) Proposed control.

Fig. 3. Experimental results.

II. SEMINAR TOPIC – APPLICATION OF ITERATIVE LEARNING CONTROL TO TEMPERATURE CONTROL FOR SINGLE WAFER DEPOSITION SYSTEM

A single wafer deposition system has a stage heater in a chamber. A wafer near room temperature is brought in from outside the chamber and placed on the stage. This work considers the stage heater which is single-input single-output system with a heater power as input and a stage heater temperature as output. The temperature is measured by a thermocouple.

A. Purpose of This Work

This work aims to reject the temperature disturbance during the wafer loading process. During loading process, the stage temperature fluctuates greatly. This can be treated as a disturbance for the temperature control. Due to the repeatability of the disturbance, an ILC [2] could be applied for the disturbance rejection.

B. Design of ILC

An ILC input signal f_j is added to the conventional feedback control system as shown in Fig. 4. Then, the update algorithm of a frequency-domain ILC [3] is given as

$$f_{j+1} = Q(f_j + Le_j), \quad (1)$$

where, L and Q are a learning filter and robustness filter, respectively.

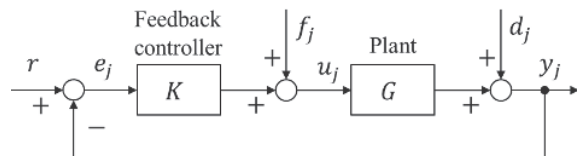


Fig. 4. Control system structure.

In this work, the FRF of GS was measured directly by using a closed-loop system identification, where S is the sensitivity function $1/(1 + GK)$. A parametric model \widehat{GS} was determined by the FRF of GS . Fig. 5 shows the FRF of GS and \widehat{GS} . Then, the learning filter L was designed as $L \approx (\widehat{GS})^{-1}$ by using the ZPETC algorithm. The robustness filter Q was designed to satisfy $|Q|^2|1 - GSL| < 1, \forall \omega$.

C. Experiments

Experiments on the stage heater temperature control using ILC were conducted in the existing single wafer deposition

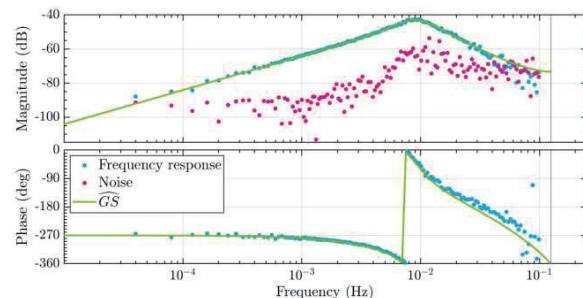


Fig. 5. Frequency response GS .

system. Fig. 6 shows the 2-norm of the error. The error decreased significantly, and the error converged even if the iteration was continued.

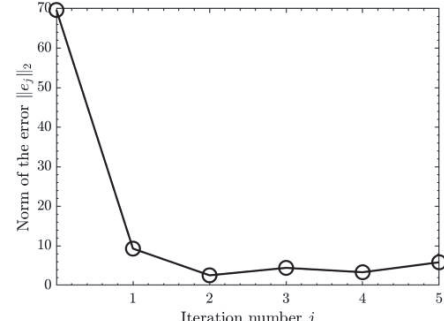


Fig. 6. Experimental results.

III. CONCLUSION

This research has contributed to the development of temperature control in semiconductor thermal process. For the batch type, proposed heater and cooler integration has been proved experimentally to reach fast and high-precision temperature control with efficient energy use. For the single-wafer type, ILC has been applied to compensate repeatable temperature disturbance, thus improve the disturbance rejection performance. Future works will continue to reach faster and more precise temperature control of both batch and single-wafer type thermal processing equipment to contribute to the development of semiconductor manufacturing sector.

REFERENCES

- [1] W. Ohnishi, A. Hirata, R. Shibatsuji, and T. Yamaguchi, "Fast and precise temperature control for a semiconductor vertical furnace via heater-cooler integration," *IEEE Trans. Semiconductor Manufacturing*, vol. 36, no. 2, pp. 197–204, May, 2023.
- [2] T. Oomen, "Learning for Advanced Motion Control," *2020 IEEE 16th International Workshop on Advanced Motion Control (AMC)*, 2020.
- [3] M. Steinbuch, and R. van de Molengraft, "Iterative learning control of industrial motion systems," *IFAC Proceedings Volumes*, vol. 33, no. 26, pp. 899-904, Sep. 2000.



Akira Hirata received the B.E. degree in multidisciplinary engineering at National Institute of Technology, Numazu College, Japan in 2018, and the M.E. degree in integrated design engineering from Keio University, Japan in 2020. Since 2020, he has been with Tokyo Electron Ltd. Since 2020, he has been assigned to Tokyo Electron Technology Solutions Ltd. He works on the design of temperature control for semiconductor equipment. He is a member of the Institute of Electrical Engineers of Japan.

Ryosuke Shibatsuji received the B.S. degree in the Department of Physics, School of Science from Nagoya University, Japan in 2015, and the M.S. degree in the Division of Material Science (Physics), Graduate School of Science from Nagoya University, Japan in 2017. Since 2019, he has been with Tokyo Electron Technology Solutions Ltd. He works on the design of temperature control for semiconductor equipment.

Tatsuya Yamaguchi received the B.E. and M.E. degrees in the Department of Mechanical Engineering from Hokkaido University, Japan in 2001 and 2003, respectively. Since 2003, he has been with Tokyo Electron Ltd. Since 2017, he has been assigned to Tokyo Electron Technology Solutions Ltd. He works on the design of temperature control for semiconductor equipment. He is a member of the Institute of Electrical Engineers of Japan.

Wind vector estimation considering the difference of propeller characteristics for fully actuated drone

Manto Kamiya¹, Sakahisa Nagai¹, and Hiroshi Fujimoto¹

I. RESEARCH OVERVIEW

Recently, business which utilizes multi-rotor Unmanned Aerial Vehicles (UAV) is rapidly developing. Conventionally, multi-rotor UAVs have been mainly used to take aerial images or to carry packages with one multi-rotor UAV. On the other hand, the demand for applications of multi-rotor UAVs to interact with the surrounding environment will increase in the future. For example, it is considered to use multi-rotor UAVs for cooperative payload transportation or contact inspection on buildings. When multi-rotor UAVs conduct such missions, it is effective to implement force control. One of the challenges to conduct force control for drones is the separation of wind disturbance from total disturbance.

Topic 1 Fully Actuated Drone

A fully actuated multi-rotor UAV is a drone whose propellers are oriented in different directions. It is currently receiving interest as one of the suitable UAVs for high-precision applications including force control. As shown in Fig. 1, mounting propellers in different directions allows the drones to control their six DOF motion separately. A fully actuated drone is expected to be used in situations where force control is required, such as contact inspections.

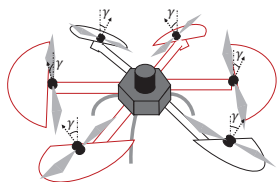


Fig. 1. Fully actuated drone.

Topic 2 Wind Vector Estimation of Multi-rotor UAV

One of the significant difficulties of force control for outdoor multi-rotor UAVs is wind disturbance. The force caused by a wind disturbance should be separated from others to recognize non-wind force accurately and to implement force control. Hence, it is important to estimate a wind vector that flows into the multi-rotor UAV.

Some methods were proposed to date to estimate wind vectors with multi-rotor UAVs as follows:

- 1) Using external wrench estimation with an Inertial Measurement Unit (IMU) [1]

- 2) Wind vector measurement by using an anemometer [2]
- 3) Considering dynamics of motors and propellers [3]

Method 1 and method 2 have difficulty in separating force caused by wind and non-wind force because the external force applied to the body frame of multi-rotor UAVs is basically considered only as a wind disturbance in those methods. Method 3 which considers the dynamics of the motor and propeller has the potential to estimate wind vector and to separate force caused by wind from other force. Reference [3] is a previous work of wind vector estimation for force control of drones which considers motor and propeller dynamics. Its method attempts to estimate three-dimensional wind velocity by combining physical models and machine learning.

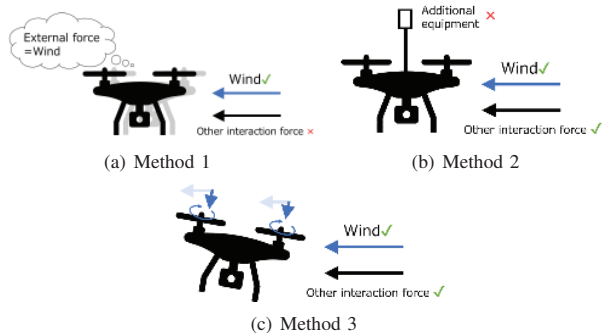


Fig. 2. Wind vector estimation methods of multi rotor UAV.

Topic 3 Wind vector estimation method for fully actuated drone

Reference [4] is our previous method. It proposed a simple wind vector estimation method only by utilizing the tilted propellers of a fully actuated drone and physical-based model. The study showed the possibility of simple wind vector estimation with the two propellers bench test in a wind tunnel.

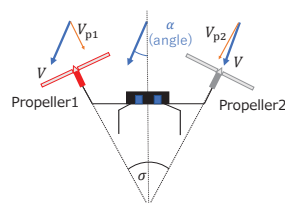


Fig. 3. Configuration of propellers of fully actuated drone.

¹ The authors are with Graduate School of Frontier Science, The University of Tokyo, 5-1-5, Kashiwanoha, Kashiwa, Chiba, 277-8561, Japan.

II. SEMINAR TOPIC - Wind vector estimation

The new wind vector estimation method for fully actuated drones which considers the difference of propeller characteristics is proposed. The proposed method requires a degree of freedom in the direction of propellers. As shown in Fig. 3 and 4, the case of two propellers is considered in this paper to simplify the situation.

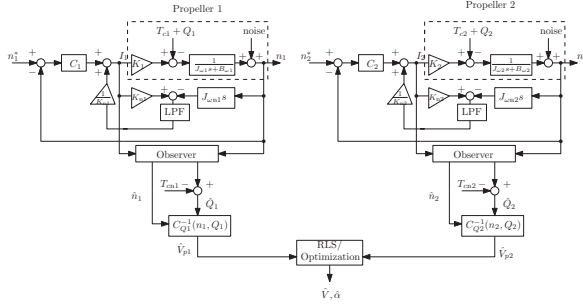


Fig. 4. Wind vector estimator.

A. Airflow Velocity Estimation

In the first step, the observer-based V_p estimation method is used. Counter torque Q of propeller is estimated by observer. Q is described with wind velocity V_p as follows:

$$Q = C_Q(J)\rho n^2 D_p^5. \quad (1)$$

Where $J = V_p/D_p n$, ρ is air density and D_p is the propeller diameter. C_Q is coefficient of torque. Therefore, V_p of each two propellers is designated by estimated Q as follows:

$$\hat{V}_p = n D_p C_Q^{-1} \left(\frac{\hat{Q}}{\rho n^2 D_p^5} \right). \quad (2)$$

V_{p1} is V_p of propeller 1 and V_{p2} is V_p of propeller 2.

B. Relationship Between Airflow Velocity Flowing in Propellers and Wind Vector

It is considered that the case where V flows in at an angle of a to the propeller. The model function of angular sensitivity of V_p to V is experimentally obtained as follows:

$$\frac{V_p}{V} = \cos(wa + \psi), \quad (3)$$

where w and ψ are fitting parameters.

C. Proposed Method: Wind Vector Estimation Considering Non-linear Simultaneous Equation

The proposed method considers the difference of the angular sensitivity function of each propeller. The optimization problem is defined as follows:

$$\min_{-\frac{\pi}{2} \leq \alpha \leq \frac{\pi}{2}, V \in \mathbb{R}} F(\alpha, V). \quad (4)$$

Where $F(\alpha, V)$ is defined as follows:

$$F(\alpha, V) = e_1^2 + e_2^2 + f_b, \quad (5)$$

$$e_1 = \hat{V}_{p1} - V \cos \left(w_1 \left(\frac{\sigma}{2} + \alpha \right) + \psi_1 \right), \quad (6)$$

$$e_2 = \hat{V}_{p2} - V \cos \left(w_2 \left(\frac{\sigma}{2} - \alpha \right) + \psi_2 \right), \quad (7)$$

Note that f_b is a barrier function to limit the searching area of α . The meaning of this optimization is to search V and α minimizing the L_2 norm of the error between the calculation value from the model and the estimation value of V_p . Estimated V and α are updated based on the steepest descent method.

D. Experimental Results of Wind Vector Estimation

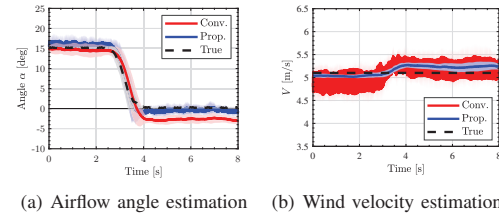


Fig. 5. Result of wind vector estimation.

From Fig. 5, it is shown that wind vector estimation with step airflow angle is achieved. Focusing on the result of Fig. 5(a), the estimation error of the proposed method is smaller than the conventional method. The reason of the result is considered that the proposed method takes into account the difference of the angular sensitivity function of each propeller.

E. Conclusion

In this study, a wind vector estimation method for large industrial fully actuated drones which can improve the accuracy of the conventional method is proposed. Note that the wind vector estimation method in this paper still has difficulty in estimating wind vectors at high rotational speed as the same in [4].

REFERENCES

- [1] T. Tomić and S. Haddadin, "Simultaneous estimation of aerodynamic and contact forces in flying robots: Applications to metric wind estimation and collision detection," in 2015 IEEE International Conference on Robotics and Automation (ICRA). IEEE, 2015, pp. 5290–5296.
- [2] A. Tagliabue, A. Paris, S. Kim, R. Kubicek, S. Bergbreiter, and J. P. How, "Touch the wind: Simultaneous airflow, drag and interaction sensing on a multirotor," in 2020 IEEE/RSJ International Conference on Intelligent Robots and Systems (IROS). IEEE, 2020, pp. 1645–1652.
- [3] T. Tomić, P. Lutz, K. Schmid, A. Mathers, and S. Haddadin, "Simultaneous contact and aerodynamic force estimation (s-cafe) for aerial robots," *The International Journal of Robotics Research*, vol. 39, no. 6, pp. 688–728, 2020.
- [4] M. Kamiya, S. Nagai, H. Fujimoto, and K. Suzuki, "Proposal of wind vector estimation using observer for multi-directional propellers drone," in proceeding of The IEEJ International Workshop on Sensing, Actuation, Motion, Control, and Optimization. IEEJ, 2023.



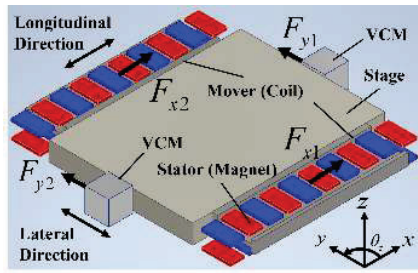
Manto Kamiya received the bachelor's degree in the department of electrical and electronic engineering in the University of Tokyo, in 2023. Currently, he is pursuing a Msc. degree at the department of advanced energy at the University of Tokyo.

Precision positioning with transverse flux linear synchronous motors

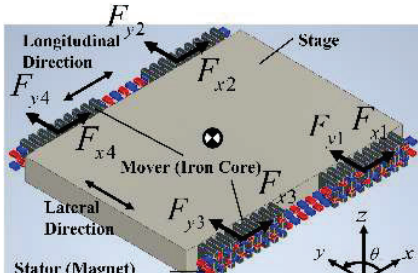
Mamoru Katayama¹, Wataru Ohnishi^{1,2}, Takafumi Koseki^{1,3}, Hwang-Joong Kim⁴ and Koichi Sakata⁵

I. SEMINAR TOPIC - PROPOSAL OF A HIGH ACCELERATION CONTACTLESS PRECISION POSITIONING STAGE WITH A PAIR OF TRANSVERSE FLUX LINEAR SYNCHRONOUS MOTORS

A. Introduction



(a) Conventional stage (coreless motors + VCMs)



(b) Proposed stage (only core-equipped motors)

Fig. 1: Comparison between a conventional stage and the proposed stage

Precision positioning stages are indispensable equipment for manufacturing semiconductor integrated circuits or flat panel displays. In recent years, linear motors are widely used for driving those stages because of their ability to provide non-contact drive. Also, the self-weight compensation mechanism includes air guides that dramatically reduce the effects of fric-

¹ The authors are with Department of Electrical Engineering, the University of Tokyo, Japan, corresponding e-mail: m.katayama@ct1.t.u-tokyo.ac.jp.

² Wataru Ohnishi is also with Department of Electrical Engineering, the University of Tokyo, Japan.

³ Takafumi Koseki is also with Department of Electrical Engineering, the University of Tokyo, Japan.

⁴ Hwang-Joong Kim is with KOVERY.

⁵ Koichi Sakata is with Nikon.

tion and floor vibration by levitating the stage in a contactless manner [1].

Conventionally, coreless motors are used in longitudinal direction and VCMs in lateral direction for precision positioning stages as seen in Figure 1(a), but core-equipped motors are more suitable for realizing higher acceleration drive and decreasing the number of actuators. However, due to the detent force and the nonlinearity of the lateral magnetic attractive force generated by the core-equipped motor, they will cause deterioration in positioning performance. So, it is necessary to redesign the motor, review the stage mechanism, and develop new control methods.

B. Structure of the Proposed Stage

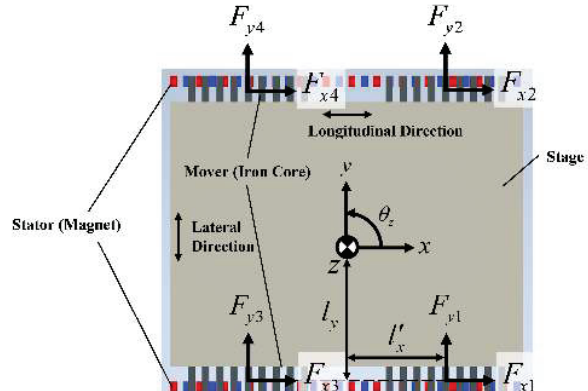


Fig. 2: Model of the proposed stage

The proposed stage uses only core-equipped linear motors to control the motion in three degrees of freedom (x , y , θ_z): F_x is generated by the q -axis current of the motors, and F_y is generated by the d -axis current, which is the difference of the lateral attractive forces by the linear motors on both sides. F_θ is mainly generated by the difference of the thrust forces by the linear motors on both sides [2].

$$\begin{bmatrix} F_x \\ F_y \\ F_\theta \end{bmatrix} = \begin{bmatrix} 1 & 0 & 1 & 0 & 1 & 0 & 1 & 0 \\ 0 & 1 & 0 & 1 & 0 & 1 & 0 & 1 \\ \frac{l_y}{2} & \frac{l'_x}{2} & -\frac{l_y}{2} & \frac{l'_x}{2} & \frac{l_y}{2} & -\frac{l'_x}{2} & -\frac{l_y}{2} & -\frac{l'_x}{2} \end{bmatrix} \begin{bmatrix} F_{x1} \\ F_{y1} \\ F_{x2} \\ F_{y2} \\ F_{x3} \\ F_{y3} \\ F_{x4} \\ F_{y4} \end{bmatrix} \quad (1)$$

C. Structure of the transverse flux linear synchronous motor

In order to stabilize the support of the stage in the z direction, the force exerted by linear motors on the stage must be sufficiently reduced. KOVERY's double-sided transverse flux linear synchronous motor with cores only on the armature side [3] are designed to reduce magnetic attractive forces in the y and the z direction [4], and detent force in the x direction [5], so this motor was adopted on the proposed stage.

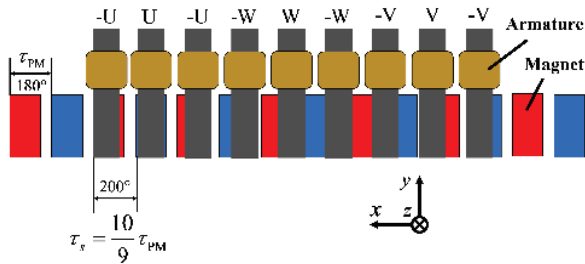
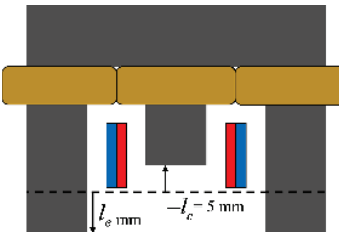


Fig. 3: Arrangement of motor armature cores and field permanent magnets

D. Redesigning of the Motor

With the current motor geometry, the lateral magnetic attractive force changes nonlinearly when the stage is displaced in the y direction. Therefore, we proposed a new motor geometry with the middle core of the conventional motor being shortened by 5 mm, and optimized the linearity by focusing on the length of the cores on both sides. As a result, the most linearized motor was obtained when $l_e = -1$ mm.



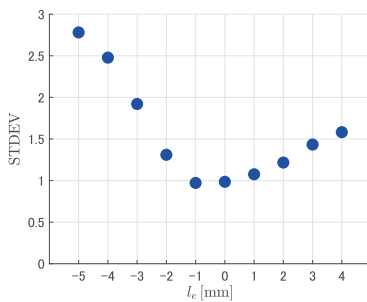
(a) Definition of the length of change of the middle core (l_e mm) and the bilateral cores (l_e mm)

REFERENCES

- [1] Wataru Ohnishi, Hiroshi Fujimoto, and Koichi Sakata, "Model-based Control Techniques for Large-Scale High-Precision Stage," IEEJ Transactions on Industry Applications, Vol.140, No.4, pp.272-280 (2017) (in Japanese)
大西亘, 藤本博志, 坂田晃一「大型超精密位置決めステージのモデルベース制御技術」電気学会論文誌 D (産業応用部門誌), Vol.140, No.4, pp.272-280 (2017)
- [2] 片山真守・大西亘・古閑隆章・金弘中・坂田晃一「非接触精密位置決めステージ高加速度駆動のための横磁束形リニア同期モータの設計」令和 5 年電気学会リニアドライブ研究会, LD-23-023 (2023)
- [3] KOVERY Motor Inc., <http://www.kovery.com/eng/main/main.php>.
- [4] 申重燮・古閑隆章・金弘中「大推力両面式横向磁束リニア同期モータの提案」平成 23 年電気学会リニアドライブ研究会, LD-11-031 (2011)
- [5] S. Ahmed, T. Koseki, and H. J. Kim, "Detent force reduction for a novel transverse flux permanent magnet linear synchronous motor without compromising stroke length," in Proc. 11th Int. Symp. Linear Drives for Ind. Appl. (LDIA), Osaka, Japan, Sep. 2017, pp.1-5, doi: 10.23919/LDIA.2017.8097256.



Mamoru Katayama received the B.Sc degree (2023) in Engineering from the University of Tokyo. Currently, he is pursuing a M.Sc. degree at the department of electrical engineering at the University of Tokyo. His research interests are centered around precision positioning using transvers flux linear synchronous motors.



(b) Standard deviation showing the variation from the approximate straight line

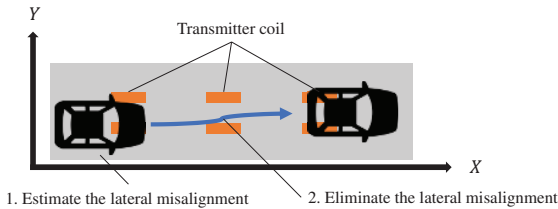
Fig. 4: Optimization of Proposed Motors

Study on Estimation and Adjustment of Lateral Misalignment in Dynamic Wireless Power Transfer with Steering Actuator and Yaw Moment

Tomoaki Koishi¹, Binh-Minh Nguyen¹, Osamu Shimizu¹, Shota Yamada¹ and Hiroshi Fujimoto¹

I. RESEARCH OVERVIEW

Recently, electric vehicles (EVs) have been gaining attention due to growing concerns about environmental issues such as global warming and air pollution caused by exhaust gas. However, the long charging time and the short cruising distance have hindered the widespread of EVs. Dynamic wireless power transfer (DWPT) has been developed to address this problem. Receiver coils are attached to EVs and run over transmitter coils embedded in the ground, which transfer electric power to EVs through magnetic resonance. To realize the DWPT, it is necessary to deal with the efficiency reduction caused by a lateral misalignment between the transmitter and receiver coils. It is well known that the lateral misalignment degrades the coupling coefficient, thereby decreasing the power transfer efficiency.

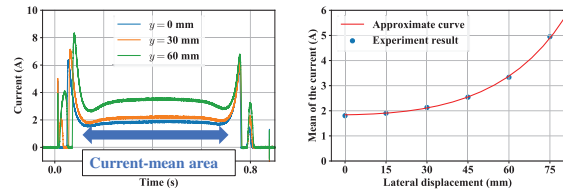


Lateral position estimation using WPT information [1].

A method is proposed to estimate the lateral misalignment of the receiver coil from the mean of the DC link current in a one-time power transfer. The method assumes that the parameters of the transmitter and receiver coils are given and uses the following approximation model using hyperbolic function and constants a , b , c :

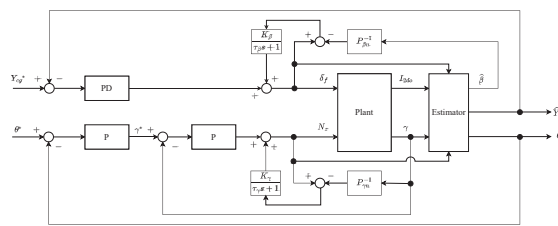
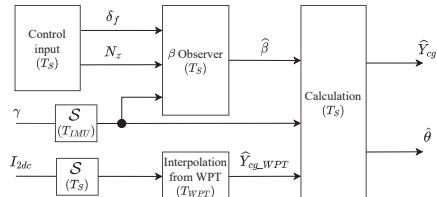
$$Y_{coil} = \frac{1}{b} \operatorname{arccosh} \left(\frac{\bar{I}_{2dc}}{a} - c \right), \quad (1)$$

where \bar{I}_{2dc} indicates the mean of the DC link current in the current-mean area, where the coupling coefficient is strong. The estimation error of this method is relatively large with a small misalignment. However, it does not affect the effectiveness since the mutual inductance is kept high with a small misalignment.



Lateral position estimation and control for vehicle [2].

This study is to further apply the method to a real experimental vehicle. To support the drive, it is not enough to compensate only for the lateral misalignment. To simultaneously control the lateral misalignment and yaw angle, this paper shows a new method to fuse the DC link current measurement with the onboard inertial measurement unit (IMU). The method uses the vehicle dynamics model to estimate the lateral misalignment and the yaw angle from the outputs of the sensors. Furthermore, the lateral misalignment and the yaw angle are controlled by integrating the rear in-wheel-motors and the front active steering mechanisms.



Neural networks for feedforward control

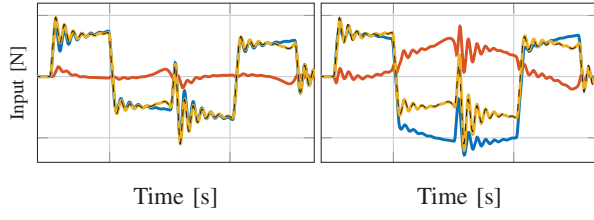
Johan Kon¹, Dennis Bruynen², Jeroen van de Wijdeven³, Marcel Heertjes^{1,3}, Tom Oomen^{1,4}

I. RESEARCH OVERVIEW

Hard-to-model dynamics limit the performance of current feedforward approaches as it is hard to describe these dynamics as a mathematical function. For example, consider the inability of a polynomial basis function feedforward to compensate nonlinear friction characteristics. This work focuses on developing more advanced feedforward controllers based on neural networks to instead learn these dynamics from data. Relevant topics within this research are i) how to combine neural networks with prior knowledge in the form of models, ii) how to guarantee stability, and iii) how to obtain consistent estimates when working with closed-loop data.

Everything that can be explained by a physical model, should be explained by this model [1], [2].

When employing neural networks for feedforward, it is common practice to ignore all prior knowledge about the systems dynamics. However, physical models are usually a very efficient representation of the dynamics, such that a purely neural network approach can introduce unnecessarily big networks. In [1] and [2], a parallel physical-model and neural-network feedforward controller is developed to utilize prior knowledge and learn unmodelled dynamics simultaneously. Through regularization, it is ensured that the neural network does not learn anything that can be captured by the physical model. The figure shows that the combined feedforward of the parallel combination (—) can learn the required input (---). However, the neural network (—) can learn parts of the physical model (—) without changing the combined feedforward (right). The proposed regularization ensures that the contributions of the physical model and neural network are complementary (left).



This work is supported by Topconsortia voor Kennis en Innovatie (TKI), and ASML and Philips Engineering Solutions.

¹: Control Systems Technology Group, Department of Mechanical Engineering, Eindhoven University of Technology, Eindhoven, The Netherlands, corresponding e-mail: j.j.kon@tue.nl.

²: Philips Engineering Solutions, Eindhoven, The Netherlands.

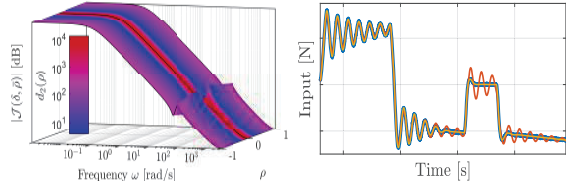
³: ASML, Veldhoven, The Netherlands.

⁴: Delft University of Technology, Delft, The Netherlands.

LPV feedforward control for position dependent zeros [3]

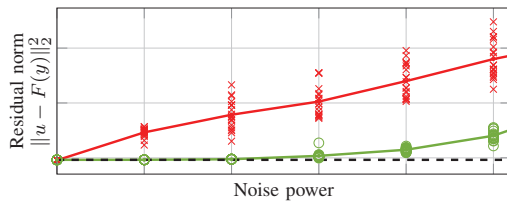
Position-dependent dynamics are omnipresent in mechatronic systems, possibly necessitating an LPV feedforward controller with 'shifting poles' to compensate for the shifting antiresonances of the position-dependent system. To learn any position-dependent function, the dependency of the controller coefficients on the scheduling variable is learned through a parallel physical model and neural network. Analytical gradient expressions combined with a second order solver allow for significantly faster optimization compared to a standard implementation in an automatic differentiation framework.

The figure shows an example system with a resonance that has a position-varying damping (left). The LPV feedforward controller (—) is able to generate the required input for perfect tracking (—) up to the approximation capabilities of the neural network, whereas a rational transfer function feedforward controller (—) cannot capture the effects of the position-dependent resonance. Current research is aimed at guaranteeing that the LPV feedforward controller is stable.



Instrumental variables for consistent estimation [4].

Input-output data for learning a feedforward controller is often obtained from a closed-loop experiment for safety concerns. Consequently, unmeasured disturbances entering the control loop end up in both input and output, creating correlations that result in inconsistent parameter estimates, degrading control performance. To obtain consistent parameter estimates, an instrumental variable neural network optimization criterion is developed. The figure shows the validation error, i.e., the norm of the predicted input and the actual input, for both a standard least-square criterion (—) and the proposed IVNN criterion (—). This validation error is shown for multiple noise realizations in the input output data (crosses and circles) and for a range of noise levels. It can clearly be seen that the bias worsens the quality of the LS estimate.



II. SEMINAR TOPIC - LEARNING FOR PRECISION MOTION OF AN INTERVENTIONAL X-RAY SYSTEM

This section illustrates research topic 1, i.e., parallel physical model and neural network feedforward control, through an experimental case study on an interventional X-ray (IX).

A. Problem Formulation

IXs are a key technology in healthcare that improve treatment quality through visualization of patient tissue. To guarantee both high imaging quality as well as patient and operator safety, accurate feedforward control is essential during operation of an IX. However, the mechanical design, constrained by the use around medical personnel, introduces nonlinear dynamics such as configuration-dependent cable forces (■) and nonlinear friction characteristics that are dependent on the normal force on the rollers in the guidance (□). These hard-to-model dynamics are only qualitatively known, and thus the aim is to learn them from data using neural networks.

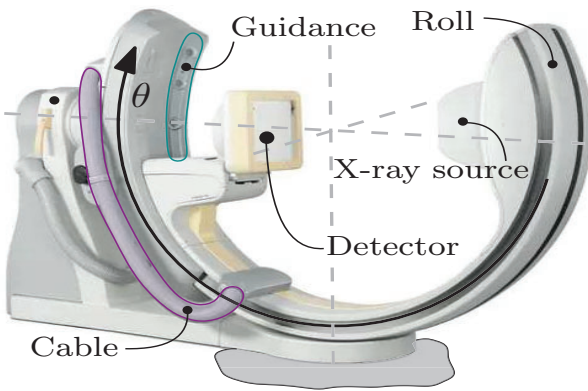


Fig. 1. Interventional X-ray system positioning the X-ray source and detector through rotating 3 axes, among which the roll axis with angle θ .

B. Feedforward Parameterization

To compensate the hard-to-model dynamics, the feedforward controller is parametrized as a parallel combination of a physical model and neural network g_ϕ such that the feedforward f for reference θ_d is given by

$$f(\theta_d(k)) = M\ddot{\theta}_d(k) + H(\theta_d) + g_\phi(T(\theta_d(k))),$$

with d the viscous damping coefficient and

$$M = m(y^2 + z^2) + J_{xx} \in \mathbb{R}_{\geq 0},$$

$$H(\theta) = mg(y \cos(\theta) - z \sin(\theta)) \cos(\zeta) \in \mathbb{R},$$

the inertia and gravity contribution. Coordinates y, z represent the offset of the center of mass with respect to the point of rotation, and ζ the known orientation of the roll axis out of the vertical plane. The neural network g_ϕ is given by

$$g_\phi(x) = W^L \sigma(W^{L-1} \sigma(\dots \sigma(W^0 x + b^0) \dots + b^{L-1}) + b^L,$$

with σ an elementwise activation function, $\phi = \{W^l, b^l\}_{l=0}^L$ weight and bias matrices. g_ϕ acts on a physics-guided input

$$T(\theta_d(k)) = [\theta_d(k) \quad \dot{\theta}_d(k) \quad \ddot{\theta}_d(k) \quad \text{relay}(\theta_d(k))]^T,$$

which encodes the prior knowledge that the required feedforward depends not only on position, but also on velocity, and the history of the direction for static friction.

The parameters m, y, z, ϕ are learned from input-output data $\{u(k), y(k)\}_{k=1}^N$ through inverse system identification, i.e., by regressing the feedforward output $f(y(k))$ on $u(k)$ as

$$\min_{m,y,z,\phi} = \sum_{k=1}^N (u(k) - f(y(k)))^2 + R(\phi).$$

$R(\phi)$ represents orthogonal projection-based regularization [1] to ensure that g_ϕ does not learn modeled effects, such that the physical model remains interpretable.

C. Results

The feedforward controller is validated experimentally on the IX setup. Fig. 2 shows the resulting tracking errors. The proposed feedforward controller (—) compensates almost all dynamics, resulting in a tracking error of a few encoder counts. In contrast, the physical-model-based feedforward controller (—) improves upon the feedback only case (—), but still contains predictable errors from uncompensated dynamics. Overall, the tracking error is reduced from 0.095 to 0.020 deg in mean absolute sense by the inclusion of a neural network.

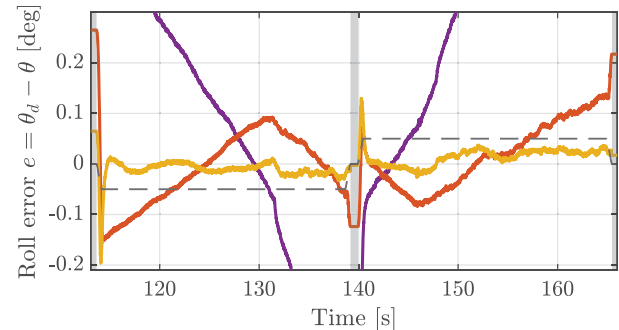


Fig. 2. Error signals for proposed (—) and physical-model-based (—) feedforward controller compared to the feedback only case (—) with scaled velocity reference (---).

REFERENCES

- [1] J. Kon, D. Bruijnen, J. van de Wijdeven, M. Heertjes, and T. Oomen, "Physics-guided neural networks for feedforward control: An orthogonal projection-based approach," in *Proc. Am. Control Conf.*, 2022.
- [2] —, "Unifying model-based and neural network feedforward: Physics-guided neural networks with linear autoregressive dynamics," in *2022 IEEE 61st Conf. Decis. Control*, 2022, pp. 2475–2480.
- [3] J. Kon, D. Bruijnen, J. van de Wijdeven, R. Tóth, M. Heertjes, and T. Oomen, "Direct learning for parameter-varying feedforward control: A neural-network approach," 2023, to appear.
- [4] J. Kon, M. Heertjes, and T. Oomen, "Neural network training using closed-loop data: Hazards and an instrumental variable (ivnn) solution," in *14th IFAC Workshop on Adaptive and Learning Control Systems*, 2022.



Johan Kon received the BSc. degree (2018) and MSc. degree (2021, cum laude) in control systems from the Eindhoven University of Technology. Currently he is pursuing a Ph.D. degree at the department of Mechanical Engineering at Eindhoven University of Technology. His research interests include feedforward control and inverse system identification with neural networks applied to high-precision mechatronic systems.

Data-Driven Auto-Tuning with Performance and Interpretability in Industrial Mechatronic Systems

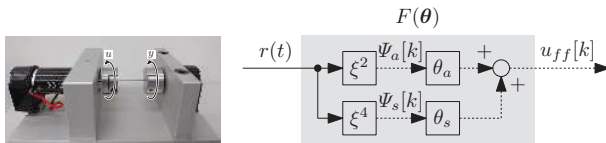
Masahiro Mae¹, Wataru Ohnishi¹ and Hiroshi Fujimoto¹

I. RESEARCH OVERVIEW

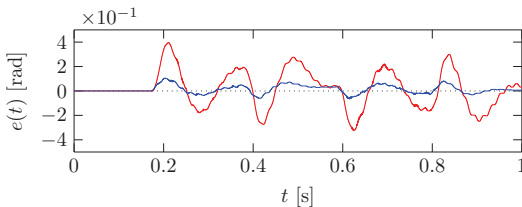
Increasing demand for industrial high-precision mechatronic systems leads to the complexity of multi-modal dynamics and multivariable tuning parameters. The aim is to develop a data-driven auto-tuning approach for industrial mechatronic systems. Data-driven auto-tuning enables performance improvement without a heuristic tuning process that is time-consuming in such multivariable systems and mass-produced products. The fully data-driven approach has a challenge in interpretability and it is not suitable for industrial mechatronic systems because the robust performance is not guaranteed and the interaction with on-site engineers is difficult. In this paper, the physics-guided data-driven auto-tuning methods to achieve both performance and interpretability are briefly introduced.

Feedforward Control using Sampled-Data Differentiator [1]

Typical multi-modal motion systems such as scanners, machine tools, and industrial robots are low-order modeled as a two-inertia system. In two-inertia systems, inertia with input and output is connected flexibly. In the feedforward controller design of the two-inertia system, acceleration and snap compensations are effective for fast and precise motion control and it can be designed easily by linear optimization.



In [1], considering the sampled-data dynamics in actual implementation, the design of the sampled-data differentiator ξ can improve the tracking performance of the feedforward controller. The differentiator design using a multirate state tracking technique (—) outperforms that using conventional backward differentiation (—) in an experimental validation.



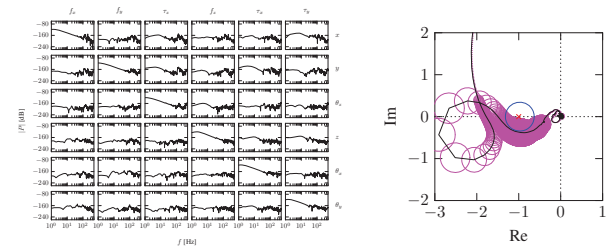
¹ The authors are with The University of Tokyo, Japan, corresponding e-mail: mmae@ieee.org.

Feedback Control with Data-Driven Loop-Shaping [2], [3]

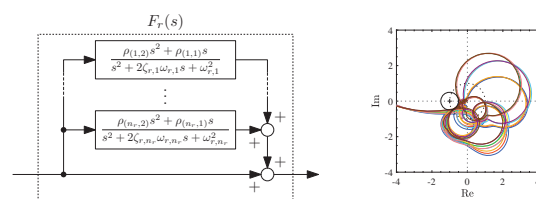
The structured modeling of the disturbances and frequency response data-based optimization enables feedback controller design with both performance and interpretability. The frequency response data-based design has several advantages in complex mechatronic systems because the parametric modeling is not necessary and the model variation can be handled directly with data sets. The approach is successfully applied in LCD scanners [2] and Hard Disk Drives (HDD) [3].



In [2], the rational peak filter is designed for a six-degrees-of-freedom high-precision scan stage. The interaction of the multi-input multi-output (MIMO) system is considered as MIMO robust stability condition (—) and the feedback controller is successfully designed with robust stability.



In [3], the multiple resonant filters are structurally parameterized corresponding to disturbance frequencies. To deal with gain and phase stability conditions in optimization constraints, the high-gained feedback controller is successfully designed with robust stability and robust performance.



II. FREQUENCY RESPONSE DATA-BASED RESONANT FILTER DESIGN APPLIED TO HARD DISK DRIVES

In this section, the approach of frequency response data-based multiple resonant filter design [3] is presented.

A. Problem formulation

To improve track-following performance, the magnetic head of the HDD is controlled by a dual-stage actuator with a Voice Coil Motor (VCM) and a PieZoelecTric (PZT) actuator, and it becomes a dual input single output system, as shown in Fig. 1.

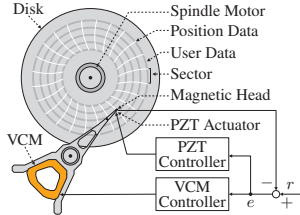


Fig. 1. Hard disk drive with a dual-stage actuator.

To minimize error e , the system and pre-designed feedback controllers are used as open-loop frequency response data G , and multiple resonant filters F are additionally designed on each actuator to reject disturbances d , as shown in Fig. 2.

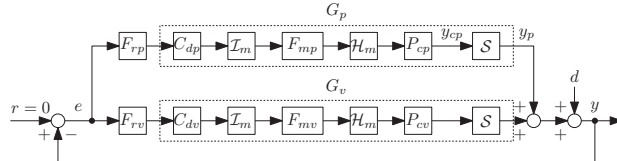


Fig. 2. Block diagram of a hard disk drive with a dual-stage actuator.

B. Approach

The designed resonant filter consists of the sum of the resonant modes and phase compensators that are defined as

$$F(s) = \frac{\kappa s^2 + \kappa \psi s}{s^2 + 2\zeta_r \omega_r s + \omega_r^2}. \quad (1)$$

To minimize the error with stroke limitation and robust stability conditions as shown in Fig. 3, the optimization problem of the multiple resonant filters is formulated as

$$\underset{\rho}{\text{minimize}} \quad \underset{\forall k_c, \forall k_f}{\max} |e_{k_c}(j\omega_{k_f})| \quad (2a)$$

$$\text{subject to} \quad |y_{p,k_c}(j\omega_{k_f})| \leq y_{p,\max} \quad (2b)$$

$$w_s(j\omega_{k_f})|S_{k_c}(j\omega_{k_f}, \rho)| \leq 1 \quad (2c)$$

$$-\frac{\pi}{2} \leq \angle(1 + L_{k_c}(j\omega_{k_f}, \rho)) - \angle(1 + G_{k_c}(j\omega_{k_f})) \leq \frac{\pi}{2}, \quad (2d)$$

where w_s is the weighting of the sensitivity function, S is the sensitivity function, L is the open-loop frequency response. Using sequential linearization, the optimization problem can be solved by iterative convex optimization, and the optimization result is shown in Fig. 4.

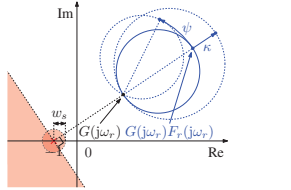


Fig. 3. Vector locus using a resonant filter with modulus margin and phase stabilization in Nyquist plot.

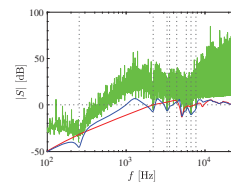


Fig. 4. Scaled inverse disturbance spectrum (green) and sensitivity function without (red) and with (blue) the optimized resonant filters.

C. Results

As shown in Fig. 5, the improvement of the track-following performance with the optimized resonant filters is validated in time-domain simulation using a dual-stage actuator HDD benchmark problem.

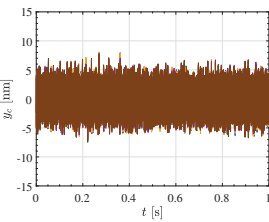
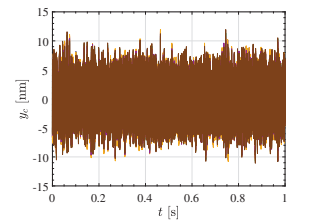


Fig. 5. Time series of head positions in dual-stage actuator HDD benchmark simulation without (left) and with (right) the optimized resonant filters.

III. CONCLUSION

The data-driven auto-tuning approach with performance and interpretability is developed for the feedforward and feedback controller design that is suitable for the applications in industrial mechatronic systems. Ongoing researches focus on the usage of both frequency-domain and time-domain data and the optimal design of the controller structure.

REFERENCES

- [1] M. Mae, M. van Haren, W. Ohnishi, T. Oomen, and H. Fujimoto, "Feed-forward with acceleration and snap using sampled-data differentiator for a multi-modal motion system," *IFAC-PapersOnLine*, vol. 55, pp. 253–258, 2022.
- [2] M. Mae, W. Ohnishi, H. Fujimoto, K. Sakata, and A. Hara, "Frequency response data-based peak filter design applied to mimo large-scale high-precision scan stage," *Mechatronics*, vol. 83, p. 102733, 2022.
- [3] M. Mae, W. Ohnishi, and H. Fujimoto, "Frequency response data-based resonant filter design considering phase stabilization and stroke limitation applied to dual-stage actuator hard disk drives," *The 22nd IFAC World Congress, FrA09*, 2023.



Masahiro Mae received the B.E., M.S., and Ph.D. degrees from The University of Tokyo, Japan in 2018, 2020, and 2023 respectively. He is currently an assistant professor at the Department of Electrical Engineering and Information Systems, Graduate School of Engineering, The University of Tokyo. He held a visiting researcher at the Eindhoven University of Technology from October 2021 to July 2022. His interests are in multivariable control and optimization of mechatronics and energy systems in industrial applications.

Identification, Calibration and Control for Motor Commutation

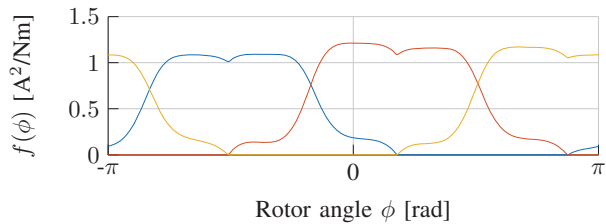
Max van Meer¹, Gert Witvoet^{1,2} and Tom Oomen^{1,3}

I. RESEARCH OVERVIEW

Switched Reluctance Motors (SRMs) [1] enable power-efficient actuation with mechanically simple designs. These actuators exhibit a highly nonlinear relationship between torque, coil currents, and rotor position, challenging position feedback control. In this abstract, some key challenges in the identification, control, and calibration of SRMs are addressed.

Optimal Commutation for Switched Reluctance Motors [2]

To allow for LTI feedback control of SRMs, the nonlinear dynamics are linearized by designing a commutation function that produces multiple coil currents based on desired torque and the rotor position. In [2], a novel approach to commutation function design through convex optimization is developed, yielding a high degree of control over and interpretability of the current waveforms.



Nonlinear Bayesian Identification for Motor Commutation

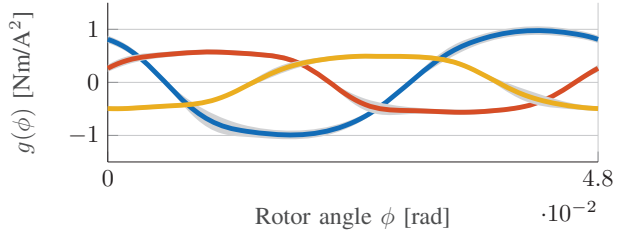
The commutation function design of SRMs relies on a model of the nonlinear torque-current-angle relationship of the system in question. This relationship is identified using Bayesian estimation. Experimental results confirm that a good model is obtained, even without torque sensors or extensive knowledge of the nonlinear structure. Moreover, an expression of the model variance is obtained, quantifying the uncertainty that results from, e.g., tooth-by-tooth variations and manufacturing tolerances.

This work is part of the research programme VIDI with project number 15698, which is (partly) financed by the Netherlands Organisation for Scientific Research (NWO). In addition, this research has received funding from the ECSEL Joint Undertaking under grant agreement 101007311 (IMOCO4.E).

¹ The authors are with the Control Systems Technology research section of the Eindhoven University of Technology, The Netherlands, corresponding e-mail: m.v.meer@tue.nl.

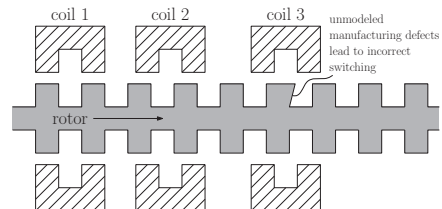
² Gert Witvoet is also with the Department of Optomechatronics, TNO, Delft, The Netherlands.

³ Tom Oomen is also with the Delft Center for Systems and Control, Delft University of Technology, Delft, The Netherlands.



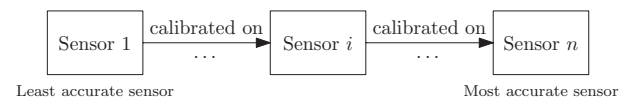
Robust Commutation Function Design

When an uncertain model of the torque-current-angle relationship of an SRM is available, this uncertainty can be explicitly taken into account in the design of commutation functions. By exploiting the optimization-based commutation design framework from [2] with a cost function that penalizes the expected value of torque ripple given the uncertain model, commutation functions are obtained that are robust to tooth-by-tooth variations and other modeling errors.



Cascaded Calibration of Mechatronic Systems via Bayesian Inference [3]

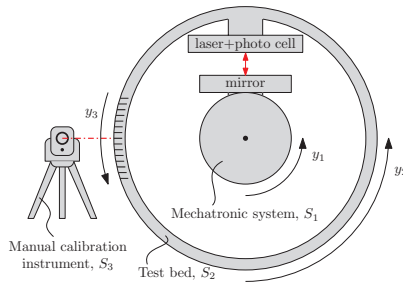
Actuators that feature a toothed rotor made from a soft magnetic material, such as SRMs, lend themselves well to Hall-effect position sensors, as these rely on the rotor teeth to yield a position measurement. However, these sensors exhibit significant position-dependent inaccuracies and hence require calibration on an external test bench. The next page summarizes a novel approach to cascaded position sensor calibration that also takes into account the calibration of the test bench to achieve more accurate calibration.



II. SEMINAR TOPIC - CASCADED CALIBRATION VIA BAYESIAN INFERENCE [3]

A. Background

The objective is to model the relationship between a low-cost, relatively inaccurate sensor (S_1) and a highly accurate manual instrument (S_3). To achieve this, a test bed is employed, incorporating a sensor (S_2) that has been calibrated against S_3 . Following this initial calibration, a diverse range of products, each equipped with its own S_1 sensor, undergoes automated calibration on the test bed. This process aims to ensure accurate mapping between S_1 and the reliable reference provided by S_3 .



B. Cascaded Calibration using Bayesian Inference

The main concept revolves around modeling the intermediate sensor calibration, denoted as $f_{2 \rightarrow 3}$, as a Gaussian Process (GP) [4]. This model captures the mapping from the readings of sensor S_2 to those of sensor S_3 as follows:

$$y_3 = f_{2 \rightarrow 3}(y_2), \quad (1)$$

where y_2 and y_3 represent the measured positions by sensors S_2 and S_3 respectively. By collecting a dataset \mathcal{D} from these sensors and employing GP models for $f_{2 \rightarrow 3}$, the posterior model variance, denoted as $\text{cov}(\hat{f}_{2 \rightarrow 3})$, can be calculated.

When readings from a low-cost sensor S_1 are compared against the intermediate calibration model and stored as $\hat{\mathcal{D}}$, the overall calibration model becomes influenced by the model uncertainty associated with the intermediate calibration:

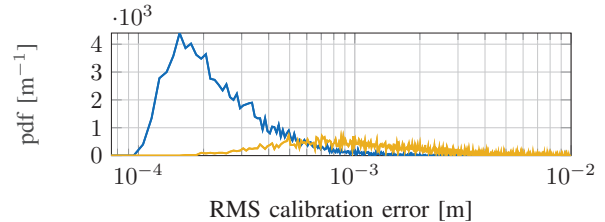
$$\hat{y}_3 = \mathbb{E}(\hat{f}_{1 \rightarrow 3}(y_1)) = g(y_1, \text{cov}(\hat{f}_{2 \rightarrow 3}), \mathcal{D}, \hat{\mathcal{D}}), \quad (2)$$

where \hat{y}_3 represents the expected true position of the mechatronic system based on the reading of the low-cost sensor S_1 , taking into account the variance of the intermediate calibration model. This expression can be evaluated in real-time to correct for repeatable sensor inaccuracies, providing an improved estimation of the true position.

C. Simulation Results

The simulation involves conducting Monte Carlo simulations with a total of 5000 scenarios. In each scenario, the calibration models $f_{1 \rightarrow 2}$ and $f_{1 \rightarrow 3}$ are randomly generated using a Fourier basis. The figure below presents a comparison between the calibration errors $\|\hat{y}_3 - y_{\text{true}}\|_2 / \sqrt{N}$ obtained from the proposed calibration approach (blue) and a lookup table

with linear interpolation (yellow). In this normalized empirical probability density function plot, a better performance corresponds with more probability mass being concentrated to the left of the figure.



The results clearly demonstrate the superior accuracy of the developed calibration approach for two main reasons: (i) The chosen model structure is better suited for extrapolation, improving accuracy beyond the measured data range, and (ii) considering the model uncertainty of the intermediate calibration model gives more weight to prior information in these regions. Consequently, the developed approach surpasses the lookup table method, significantly enhancing calibration accuracy.

D. Conclusion

The developed cascaded calibration method offers an effective solution for mitigating position sensor inaccuracies in mechatronic systems. By accurately modeling and calibrating the sensors in a cascaded manner, the method achieves enhanced calibration accuracy while minimizing resource requirements. This approach enables more precise calibration of mechatronic systems, even with limited resources, thereby improving their overall performance.

REFERENCES

- [1] T. J. E. Miller, *Switched Reluctance Motors and Their Control*. London, England: Oxford University Press, 1993, vol. 31.
- [2] M. van Meer, G. Witvoet, and T. Oomen, "Optimal Commutation for Switched Reluctance Motors using Gaussian Process Regression," *IFAC-PapersOnLine*, vol. 55, no. 37, pp. 302–307, 2022.
- [3] M. van Meer, E. Deniz, G. Witvoet, and T. Oomen, "Cascaded Calibration of Mechatronic Systems via Bayesian Inference," pp. 1–6, apr 2023. [Online]. Available: <http://arxiv.org/abs/2304.03136>
- [4] C. Rasmussen and C. Williams, *Gaussian processes for machine learning*, London, England, 2006.



Max van Meer received the MSc. degree in Mechanical Engineering (cum laude) from the Eindhoven University of Technology, in 2021. Currently, he is pursuing a Ph.D. degree at the Department of Mechanical Engineering at the Eindhoven University of Technology.

Mode Switching Algorithm to Improve Variable-Pitch-Propeller Thrust Generation for Drones Under Motor Current Limitation

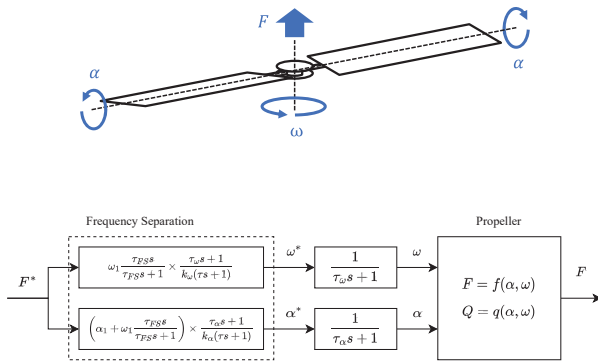
Yuto Naoki¹, Sakahisa Nagai¹ and Hiroshi Fujimoto¹

I. RESEARCH OVERVIEW

Research and development in electric vertical takeoff and landing (eVTOL) in multirotor types, including small unmanned aerial vehicles and drones, have attracted attention. Unlike the single-rotor type, the multirotor type has several propellers whose pitch is fixed, and only the rotational speed is controlled. However, in the future, multirotor is expected to be used in large vehicles for industrial applications which will require more sophisticated control. Among these requirements, the key issues are improving their motion performance, efficiency, and flying range extension. For these requirements, adding degrees of freedom (DOF) by using other rotors or actuators is one of the major solution. Methods to control such multi-DOF actuators in force dimension is lacking.

Topic 1 Response and Efficiency Improvement of Variable Pitch Propellers [1].

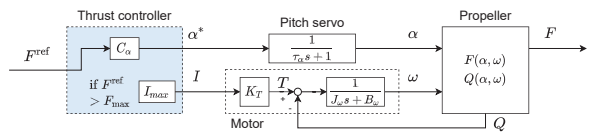
Variable pitch propellers are being studied to improve performance of the vehicles by adding DOF of mobility. However the conventional methods of variable pitch control only change the pitch angle while keeping constant rotational speed, and the efficiency of the propeller worsens. In [1], a systematic method applying frequency separation to improve steady-state efficiency while taking advantage of fast thrust response was presented. The method separate the thrust command into two actuator command values by frequency band so that the pitch angle returns to the optimum pitch angle that results in optimal propeller efficiency.



¹ The authors are with the University of Tokyo, Japan, corresponding e-mail: naoki.yuto21@ae.k.u-tokyo.ac.jp.

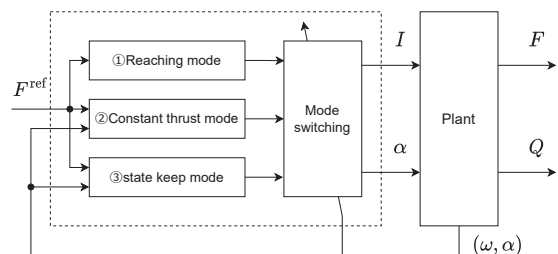
Topic 2 Achievable Thrust Expansion Control at Current Saturation of Variable Pitch Propeller [2].

The method in the previous topic allows changing the steady state operating point of the variable pitch propeller. However, the maximum thrust has limitation at the optimum pitch angle if the operating point is near to the main motor current limitation. Therefore, the maximum thrust can be expended by changing the operating point to the maximum thrust operating point, which is different from the optimum efficiency operating point. By applying the frequency separation to this case, an inverse response has caused due to the interference from the pitch angle to the rotational speed. Linearized model of a variable pitch propeller using the current and pitch angle is derived and the thrust expansion is achieved by using the model.



Topic 3 Achieve High Response and Efficiency Under Motor Current Limitation.

It is an important goal to achieve both high response and steady-state efficiency even when the main motor of the variable pitch propeller has current limitations. When the operating range varies significantly, control must take the maximum current into account. This objective can be achieved by switching between a mode in which the maximum current is used as an input to reach the target thrust and a mode in which the pitch angle is changed to the optimum pitch angle.



II. SEMINAR TOPIC - Mode Switching Algorithm to Improve Variable-Pitch-Propeller Thrust Generation Under Motor Current Limitation

In this section, mode switching algorithm is developed for the variable pitch propeller thrust control under motor current limitation [3].

A. Problem Formulation

The models of thrust and counter torque are calculated as

$$F = (b_{F0}\alpha + b_{F1})\omega^2 \quad (1)$$

$$Q = (b_{Q0}\alpha^2 + b_{Q1}\alpha + b_{Q2})\omega^2 \quad (2)$$

where each b_{FX} and b_{QX} is constant coefficient for the model. The model of the plant is shown in Fig. 1.

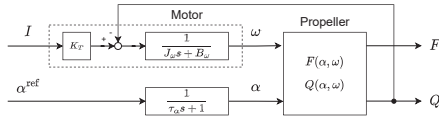


Fig. 1: Block diagram of variable pitch propeller plant model.

The controller is designed to improve the thrust tracking performance by considering the maximum motor current and its interference.

B. Maximum Current Variable Pitch Thrust Control with Switchin of Control Laws

The strategy is as follows. First, the rotational speed and pitch angle state are moved to reach the target thrust using the maximum current of the main motor. In this reaching mode, the pitch angle controller C_{reach} is designed by pole-zero cancellation.

$$C_{reach} = \frac{\frac{1}{\tau_f}s + 1}{\tau_f s + 1} \quad (3)$$

Then after the thrust is reached to the target, if the thrust is within the reachable range at the optimum efficiency pitch angle, efficiency is improved by returning to the optimum efficiency pitch angle. In this efficiency optimizing mode, pitch angle command is determined to satisfy the minute change condition of thrust as follows.

$$\frac{d\alpha}{d\omega} = \frac{F_{const}}{b_{F1}}(-2\omega^{-3}). \quad (4)$$

Finally, the states are controlled to keep the steady-state value. The flow of switching modes is shown in Fig. 2.

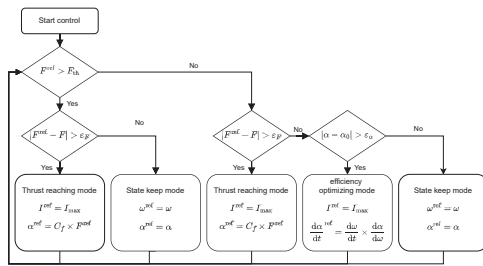


Fig. 2: The whole flow of the proposed method.

C. Results

The experiment compares the proposal to the conventional method. The condition is small step size and large step size which is different in the flow of the switching. The difference looks small in small step, but the error is reduced from $\|e\|^2 = 0.033 N^2$ to $0.015 N^2$. The performance also improved in large step about 1 s in response.

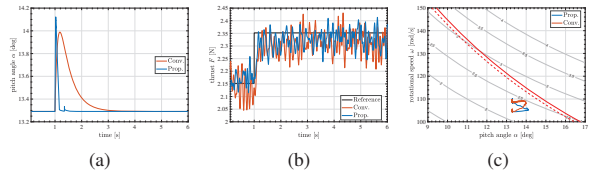


Fig. 3: Experimental result at small step. $\Delta F^{ref} = 0.2 N$
(a)Pitch angle, (b)Thrust, (c)Trajectory map

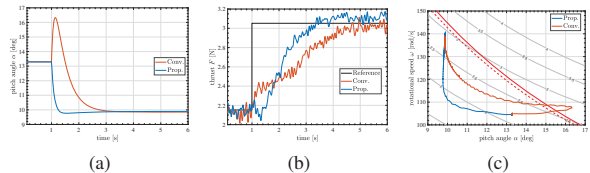


Fig. 4: Experimental result at large step. $\Delta F^{ref} = 0.9 N$
(a)Pitch angle, (b)Thrust, (c)Trajectory map

D. Conslusions

A feed-forward control method in which the maximum current is used to control the thrust by the pitch angle and rotational speed under a current limit is proposed for a variable pitch system. The response of each control law is improved by designing the pitch angle control according to the maximum value of the current used for the change in the rotational speed. Model correction of the thrust coefficient is a future work.

REFERENCES

- [1] Y. Naoki, S. Nagai, and H. Fujimoto, "Basic study on thrust control using frequency separation in variable pitch propeller mechanisms for response and efficiency improvement of drones," in the 8th IEEJ international workshop on Sensing, Actuation, Motion Control, and Optimization, 2022, pp. 480–485.
- [2] Y. Naoki, K. Yokota, S. Nagai, and H. Fujimoto, "Achievable thrust expansion control at current saturation of variable-pitch propeller for drones," in IFAC-PapersOnLine, vol. 55, no. 27, 2022, pp. 247–252, 9th IFAC Symposium on Mechatronic Systems MECHATRONICS 2022.
- [3] Y. Naoki, S. Nagai, and H. Fujimoto, "Mode-switching algorithm to improve variable-pitch-propeller thrust generation for drones under motor current limitation," IEEE/ASME Transactions on Mechatronics, pp. 1–9, 2023.



Yuto Naoki received the B.E. degree from the Department of Electrical and Electronic Engineering, The University of Tokyo, Chiba, Japan, in 2022. He is currently pursuing the M.S. degree with the Department of Advanced Energy, Graduate School of Frontier Sciences, The University of Tokyo.

His research interests includes multirotor control.

Control, Transportation, and Linear Drive for Next Generation Mechatronics

Wataru Ohnishi¹, Masahiro Mae¹, Hiroshi Fujimoto¹, and Takafumi Koseki¹

I. RESEARCH OVERVIEW

The development of modern society is significantly propelled by sophisticated and complex mechatronic systems. At the heart of these systems is automatic control, and there is a growing demand for research and development into control theories and control system design methodologies that optimizes performance and robustness. These applications span a wide range, from high-precision positioning systems like semiconductor manufacturing equipment to massive positioning systems like railways.

Koseki-Ohnishi laboratory especially focuses on research in the areas of Control, Transportation, and Linear drive, or CTL. In collaboration with industry experts facing the world's most advanced challenges, we strive for a high degree of integration between model-based [1] and data-driven designs [2], aiming for the unified optimization of both the controller and the system being controlled [3]. Specifically, we design the control system optimally based on a model that captures the physical essence, and further utilize data-driven control strategies, including learning control [4], to achieve high performance in experiments. Moreover, even for electrical [5], mechanical [6], thermal [7], and plasma [8] systems, which have completely different time constants, we aim to abstract these systems and apply the broad principles of control engineering.

Control theory and controller design

1) Non-causal feedforward and learning control for non-minimum phase systems: Constructing the inverse system of the controlled system is important in feedforward controller design and learning controller design. Design methods for inverse systems, including multirate feedforward control [9], are discussed in detail in Section II.

The effectiveness of preactuation for non-minimum phase systems was shown not only in linear time-invariant systems [1], but also in linear parameter varying systems like boost converters [5].

Supported by Japan Society for the Promotion of Science (JSPS), NEDO, Power Academy, The Telecommunication Advancement Foundation, Nagamori Foundation, Research Foundation for the Electrotechnology of Chubu, Fluid Power Technology Promotion Foundation, The Precise Measurement Technology Promotion Foundation, NSK Foundation for the Advancement of Mechatronics, Ono Charitable Trust for Acoustics, The NEC C&C Foundation, TEPCO Memorial Federation, and Takahashi Industrial and Economic Research Foundation.

¹ The authors are with the Department of Electrical Engineering and Information Systems, Graduate School of Engineering, The University of Tokyo, Japan, corresponding e-mail: ohnishi@ctl.t.u-tokyo.ac.jp.



Fig. 1. FPD lithography systems [6]



Fig. 2. Semiconductor vertical furnace [7]

2) Data-driven auto-tuning for feedback controllers: The design of high performance feedback controllers is extremely important for disturbance suppression. Since obtaining a highly accurate parametric model for a positioning system with many resonant modes and position dependence is difficult, a design method directly using frequency response data is desired. Methods for explicitly utilizing multiple sensors [10], disturbance observer design based on linear matrix inequalities [11], and convex optimization design of controllers satisfying robust performance combined with RBode and RCBode plots [12] have been explored in recent research.

3) Applications for state-of-art industrial systems: Driven by Moore's Law, the demand for control performance in semiconductor integrated circuits and flat panel display (FPD) manufacturing equipment is also increasing exponentially.

We are researching the optimal design of a peak filter for disturbance suppression, specifically for the positioning stage of a large FPD manufacturing system shown in Fig. 1. The stage possesses six degrees of freedom requiring control, making explicit consideration of inter-axis interference necessary and thus rendering the optimization problem nonlinear. Our focus lies on how to relax the original problem into convex and achieve higher positioning accuracy [6]. Additionally, we are also engaged in a study of high-speed and high-precision temperature control of a semiconductor vertical furnace shown in Fig. 2 used prior to lithography process [7].

Transportation technology

As with automobiles, there is a trend toward introducing automatic driving in railways. Recently, with the introduction of platform doors, the required positioning accuracy is ± 35 cm or even less. Given the dimensions of trains, for instance, the



Fig. 3. Actual railway vehicle

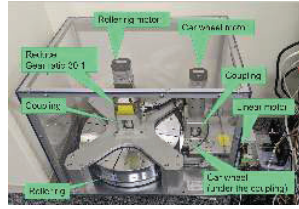


Fig. 4. Developed scale-down HILS.

longest commuter train in Japan measures 300 meters achieving this stopping accuracy requirement poses a considerable challenge.

Conducting full-scale experiments using actual railway vehicles can be extremely expensive, and purely theoretical simulations may lack persuasive power. Therefore, we have designed a Hardware-In-the-Loop System (HILS) shown in Fig. 4, which extracts friction drive dynamics of steel wheels on rails as a hardware component.

Another key innovation is the moving block system with Communications-Based Train Control (CBTC). This technology is anticipated to lower maintenance costs and boost transportation capacity in comparison to a fixed block system. Our research focus includes developing control methods to mitigate delay propagation [13] and reduce the quantity of wayside balises.

Linear drive technology

Linear drive technology, which combines linear motor design and drive technology, plays a pivotal role in semiconductor manufacturing equipment and machine tools.

We are in the process of designing magnetic levitation (maglev) linear motors. These can be of two types: attractive [14] and repulsive [15] as shown in Fig. 5 and Fig. 6. Their advantage lies in their ability to provide friction-free, highly precise propulsion systems. We're also working on a 3-DOF positioning stage that actively uses magnetic attractive force.

We're also exploring new applications of linear motors. Notably, we're investigating their use in fuse exchangers for a novel fuse-semiconductor hybrid circuit breaker [8]. Since Direct Current (DC) doesn't have a current zero point, interrupting it proves to be quite challenging, thereby hampering the broad adoption of renewable energy and the expansion of DC power grids. Our proposal aims to overcome these challenges



Fig. 5. Attractive maglev stage [14].

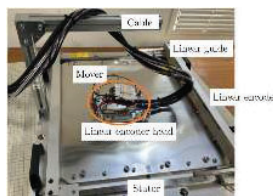


Fig. 6. Repulsive maglev stage [15].

by developing a compact and cost-effective DC circuit breaker. Our solution uses semiconductors to interrupt the fault current reduced by the fuse. Moreover, it addresses the fuse's one-time-use limitation through rapid fuse replacement facilitated by an high-acceleration linear motor.

Not only electrical linear actuator, we investigate on precision control with pneumatic cylinders for heavy positioning stages, primarily used in FPD manufacturing equipment. This is achieved by mitigating wave modes caused by compressibility [16].

II. SEMINAR TOPIC - MULTIRATE FEEDFORWARD CONTROL FOR PERFECT STATE TRACKING

A. Motivation

In digital control systems, there are sampling periods for the reference value $r(t)$, control input $u(t)$, and observed output $y(t)$, denoted as T_r , T_u , and T_y , respectively. These periods do not necessarily have to be the same due to hardware constraints or a deliberate decision to have different values - a concept known as multirate control [9]. This section specifically focuses on feedforward control and iterative learning control, which require the inversion of the system.

When designing the inverse of a system, non-minimum phase zeros can become problematic as they introduce instability to the inverse system. These zeros originate from two sources: those derived from the zeros of a continuous-time system and those generated from the discretization due to zero-order hold. Stable inversion in discrete-time systems designs inverse without distinguishing between these two types of zeros. This facilitates perfect output tracking control, provided there are no uncertainties, including disturbances.

However, as often reported, oscillations shown in Fig. 7 can occur between sampling points. Why does this happen? The reason is that the zeros produced by the zero-order hold, especially in the case of positioning control systems, are generated near $z = -1$ on the complex plane of the discrete-time domain. Consequently, the output that passes through the inverse system oscillates at the sampling frequency.

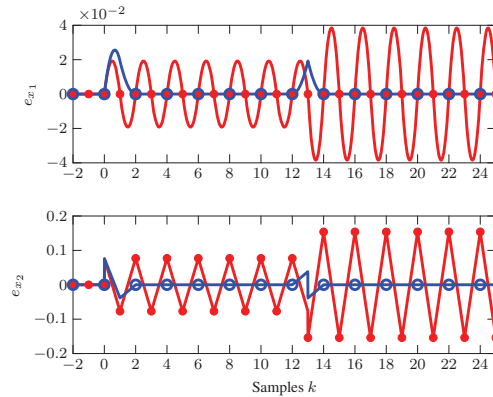


Fig. 7. Tracking error of single-rate feedforward control (—) and multirate feedforward control (—) [4].

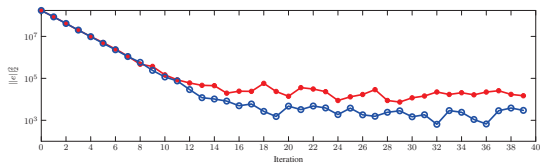


Fig. 8. Experimental results. State tracking ILC (—●—) outperforms output tracking ILC (—●—). [4]

B. Multirate feedforward control [9]

The solution to this problem is multirate feedforward control, which designs an inverse system based on the state equation of a system that has been lifted by order of the system. This method, in turn, enables perfect tracking control of the state trajectory. For instance, in a positioning control system, not only the position but also the state variable corresponding to the velocity can achieve perfect tracking, resulting in an improved intersample response. Moreover, by using the stable inverse system of continuous time to generate state trajectories, perfect tracking control of the state can be achieved even for systems that have non-minimum phase zeros in continuous time [1]. This control method has been applied in various fields, including hard disk drives (HDD) [17], stages in FPD manufacturing system [18], and machine tools [19].

C. State-tracking ILC [4]

This state tracking concept has been extended to a frequency domain ILC framework, which was shown to result in favorable inter-sample responses [4]. In this framework, the user's modeling effort can be reduced because the monotonic convergence condition for the state tracking error can be evaluated with frequency response data, which is easy to obtain. In addition, a non-causal approach was shown to be useful for estimating state variables important for state-tracking [20].

ACKNOWLEDGEMENT

The authors would like to thank all collaborators, including colleagues, former and current students, and joint research partners in academia and industry.

REFERENCES

- [1] W. Ohnishi, T. Beauduin, and H. Fujimoto, "Preactuated Multirate Feed-forward Control for Independent Stable Inversion of Unstable Intrinsic and Discretization Zeros," *IEEE/ASME Transactions on Mechatronics*, vol. 24, no. 2, pp. 863–871, 2019.
- [2] K. Tsurumoto, W. Ohnishi, and T. Koseki, "Task Flexible and High Performance ILC: Preliminary Analysis of Combining a Basis Function and Frequency Domain Design Approach," in *IFAC World Congress*, 2023.
- [3] W. Ohnishi, H. Fujimoto, K. Sakata, K. Suzuki, and K. Saiki, "Integrated Design of Mechanism and Control for High-Precision Stages by the Interaction Index in the Direct Nyquist Array Method," in *American Control Conference*, 2015.
- [4] W. Ohnishi, N. Strijbosch, and T. Oomen, "State-Tracking Iterative Learning Control in Frequency Domain Design for Improved Intersample Behavior," *International Journal of Robust and Nonlinear Control*, no. August, pp. 1–19, 2022.
- [5] S. Miyoshi, W. Ohnishi, T. Koseki, and M. Sato, "Output Voltage Precise Tracking Control for Boost Converters based on Noncausal and Nonlinear Feedforward Control," *IEEJ Journal of Industry Applications*.
- [6] M. Mae, W. Ohnishi, H. Fujimoto, K. Sakata, and A. Hara, "Frequency response data-based peak filter design applied to MIMO large-scale high-precision scan stage," *Mechatronics*, vol. 83, no. October 2021, p. 102733, 2022.
- [7] W. Ohnishi, A. Hirata, R. Shibatsuji, and T. Yamaguchi, "Fast and Precise Temperature Control for a Semiconductor Vertical Furnace via Heater-Cooler Integration," *IEEE Transactions on Semiconductor Manufacturing*, vol. 36, no. 2, pp. 197–204, may 2023.
- [8] W. Ohnishi, Y. Inada, S. Zen, R. Sasaki, Y. Takada, Y. Miyaoka, K. Tsukamoto, and Y. Yamano, "Proof-of-Concept of a Fuse-Semiconductor Hybrid Circuit Breaker With a Fast Fuse Exchanger," *IEEE Transactions on Power Delivery*, vol. X, no. X, pp. 1–10, 2022.
- [9] H. Fujimoto, Y. Hori, and A. Kawamura, "Perfect tracking control based on multirate feedforward control with generalized sampling periods," *IEEE Transactions on Industrial Electronics*, vol. 48, no. 3, pp. 636–644, 2001.
- [10] W. Ohnishi, "Data-based feedback controller tuning utilizing collocated and non-collocated sensors," in *Joint 8th IFAC Symposium on Mechatronic Systems and 11th IFAC Symposium on Nonlinear Control Systems*, no. Mechatronics, 2019, pp. 560–565.
- [11] X. Wang, W. Ohnishi, and T. Koseki, "Frequency Response Data Based Disturbance Observer Design: With Application to a Nonminimum Phase Motion Stage," *IEEE/ASME Transactions on Mechatronics*, vol. 27, no. 6, pp. 5318–5326, dec 2022.
- [12] X. Wang, W. Ohnishi, and T. Atsumi, "Systematic Filter Design by Convex Optimization for Disturbance Rejection in Dual-Stage Actuated Hard Disk Drives," in *IFAC World Congress*, 2023.
- [13] K. Sakai, W. Ohnishi, T. Koseki, K. Tanaka, S. Morita, K. Tokuhara, and K. Kasai, "Train trajectory generation method to mitigate delay propagation based on continuous train position acquisition," *IEEJ Journal of Industry Applications*, p. 22006910, 2023.
- [14] Y. Yang, W. Ohnishi, and T. Koseki, "Proposal for Estimation of the Vertical Center of Gravity and the Decoupling Control with 2-DoF for a Maglev Linear Conveyor," in *The 14th International Symposium on Linear Drivers for Industry Applications*, 2023.
- [15] N. Ito, T. Koseki, W. Ohnishi, Y. Nakamura, K. Takahashi, and H. Sekiguchi, "Practical numerical modeling approach for a design of a two-dimensional linear synchronous actuator," in *The 14th International Symposium on Linear Drivers for Industry Applications*, 2023.
- [16] W. Ohnishi, H. Fujimoto, P. H. Yang, P. W. Chang, B. Yuan, K. Sakata, and A. Hara, "Acoustic wave equation based modeling and collocated side vibration cancellation for pneumatic cylinder," *IEEJ Journal of Industry Applications*, vol. 7, no. 2, pp. 109–116, 2018.
- [17] H. Fujimoto and Y. Hori, "High-performance servo systems based on multirate sampling control," *Control Engineering Practice*, vol. 10, no. 7, pp. 773–781, 2002.
- [18] K. Saiki, A. Hara, K. Sakata, and H. Fujimoto, "A Study on High-Speed and High-Precision Tracking Control of Large-Scale Stage Using Perfect Tracking Control Method Based on Multirate Feedforward Control," *IEEE Transactions on Industrial Electronics*, vol. 57, no. 4, pp. 1393–1400, 2010.
- [19] H. Fujimoto and T. Takemura, "High-precision control of ball-screw-driven stage based on repetitive control using n-times learning filter," *IEEE Transactions on Industrial Electronics*, vol. 61, no. 7, pp. 3694–3703, 2014.
- [20] K. Tsurumoto, W. Ohnishi, and T. Koseki, "Non-Causal State Estimation for Improved State Tracking in Iterative Learning Control," *2nd Modeling, Estimation and Control Conference*, vol. 55, no. 37, pp. 7–12, 2022.



Wataru Ohnishi received the B.E., M.S., and Ph.D. degrees from The University of Tokyo, Japan, in 2013, 2015, and 2018, respectively. Presently, he is an assistant professor with the Department of Electrical Engineering and Information Systems, Graduate School of Engineering, The University of Tokyo. He held a visiting position at the Eindhoven University of Technology. His research interests include high-precision motion control and optimization. He is a senior member of The Institute of Electrical Engineers of Japan.

Learning in Machines: From Data to Models, Control Performance, and Monitoring

Tom Oomen^{1,2}, Leontine Aarnoudse¹, Lennart Blanken¹, Koen Classens¹,
 Mathyn van Dael¹, Nic Dirkx¹, Rodrigo González¹, Max van Haren¹,
 Johan Kon¹, Max van Meer¹, Maurice Poot¹, Paul Tacx¹, Koen Tiels¹, Gert Witvoet¹

I. RESEARCH OVERVIEW: COMPLEXITY IN FUTURE DATA-INTENSIVE HIGH-TECH SYSTEMS

Future high-tech systems are subject to increasing performance demands [1], including accuracy, throughput, and versatility. Important examples of such systems in the manufacturing domain include wafer stages for integrated circuit production, see Fig. 1(a), and the generic substrate carrier for industrial production, see Fig. 1(b). Important examples of scientific instruments include large scale telescopes with deformable mirrors, see Fig. 1(c) and the gravitational wave detector in Fig. 1(d).

Radically new (opto-)mechatronic system designs and control approaches are envisaged to meet increasing performance requirements, including the following examples.

1) The use of additional actuators and sensors to increase performance and enable innovative designs [2]. Spatially-distributed actuators control flexible mechanics in new lightweight designs, see Fig. 1(a). Individually controlled segmented rollers are used in carriers for extreme positioning accuracy, see Fig. 1(b). Deformable mirrors are controlled using a large number of actuators, see Fig 1(c). Additional actuators enhance accuracy in gravitational wave detectors, see Fig 1(d).

2) Directly addressing overall system performance goals. In traditional approaches, the control problem is subdivided into manageable subproblems associated with system submodules, leading to suboptimal performance. Directly addressing the overall performance requirements leads to unparalleled performance at the price of an extreme increase in complexity, e.g., the integrated control of the two motion stages in Fig. 1(a), see [3]. Relevant aspects also include unmeasurable performance variables [4], intermittent sampling [5], and sampled-data aspects [6]. Furthermore, multi-physics control problems are addressed, including the thermo-mechanical control system in Fig 1(a), see [7], and the opto-mechatronic systems in Fig. 1(c)-1(d), see [8] and [9], respectively.

The key step to enable the envisaged future data-intensive equipment lies in control design, where the major challenge lies in dealing with the extreme complexity.

Supported by NWO VIDI 15698 and ECSEL 101007311 (IMOCO4.E).

¹ The authors are with the Control Systems Technology research section of the Eindhoven University of Technology, the Netherlands, corresponding e-mail: t.a.e.oomen@tue.nl.

² Also with the Delft Center for Systems and Control, Delft University of Technology.

From Data to Models for Control

Models are essential to provide performance and robustness guarantees in future data-intensive machines. To this end, major developments have been made to identify complex mechatronic systems from data, including

- nonparametric models for complex [10], multi-physics [7], operating-condition-dependent [11], slowly-sampled [12], missing-data [13], and Lebesgue-sampled [14] systems; and
- parametric models for complex [2] and operating-condition-dependent [15], [8] systems.

These models are essential for subsequent feedback control design, see [2] for an overview.

From Data to Control Performance via Learning

The availability of ubiquitous data in future data-intensive systems provides major opportunities for performance enhancement through learning. Essentially, all predictable behavior can be fully compensated. First, disturbances are typically present that are accurately modelled as a stochastic process.

- Feedback control, [2], is essential to suppress these stochastic disturbances. These disturbances cannot be predicted before the task starts, yet typically these have a certain spectrum. Feedback can suppress these disturbances leading to an optimal error that is white noise.

Second, many motion systems have repeating signals that disturb the system, often of a deterministic nature. A large range of approaches are relevant.

- Iterative learning control and repetitive control [16], [17].
- Batch-to-batch feedforward [18], including recursive [19], [20], data-driven [21], and hysteresis [22] variants.
- Gaussian process models for position-dependent and task-flexible feedforward [23].
- Neural-networks [24] as add-on inverse model completion of the explainable models in the previous subsection.

From Data and Models to Monitoring

Any physical system degrades due to wear, ageing, etc. Feedback, feedforward, and learning algorithms provide a large amount of data on the state of the system during operation. Besides these data, accurate models are readily available from control design. These models can be re-purposed and integrated with data, enabling fault identification, isolation, and predictive maintenance, leading to drastic downtime minimization and increasing productivity [25], [26].

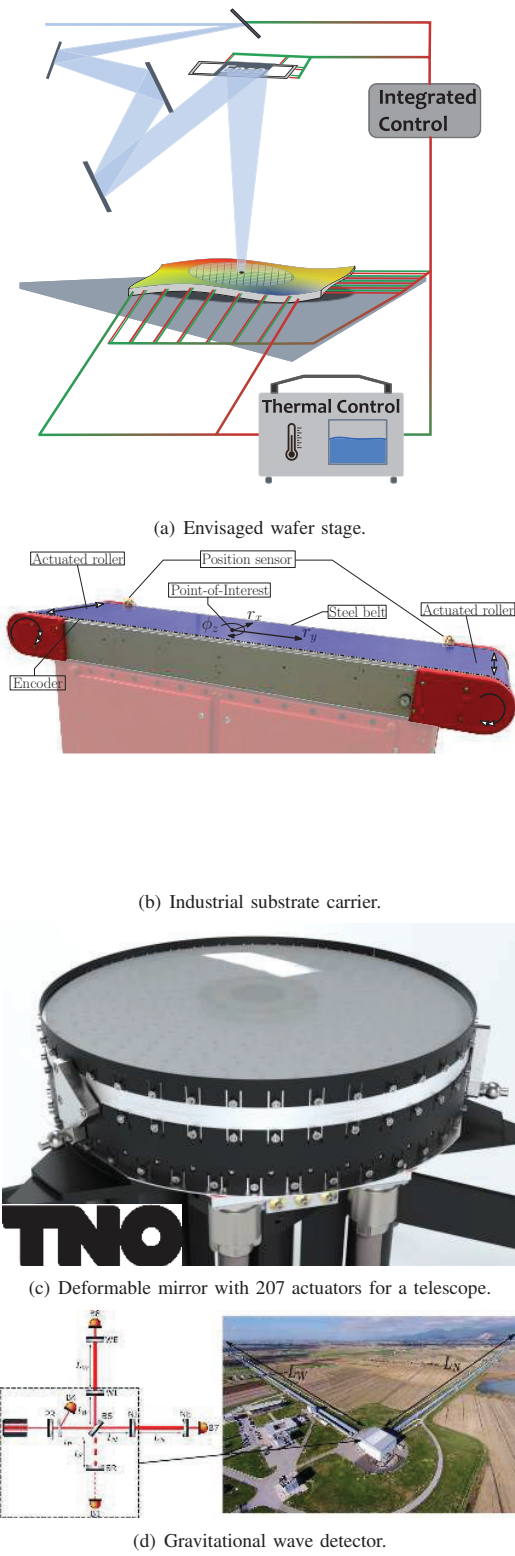


Fig. 1. Selection of complex data-intensive (opto-) mechatronic systems.

II. SEMINAR TOPICS

A. Gaussian Processes for Advanced Motion Control

Manufacturing equipment and scientific instruments are subject to increasing speed, accuracy, and flexibility requirements. Examples of such systems include wafer scanners, printing systems, pick-and-place machines, and microscopes. Learning from data provides huge opportunities in these future data-intensive mechatronic systems to meet increasing speed, accuracy, and functionality requirements. To this end, learning techniques are presented, including Gaussian Processes (GPs). Successful applications of GPs for feedforward and learning control, including identification and learning for noncausal feedforward, position-dependent snap feedforward, motor force constants (Fig. 2), nonlinear feedforward, and GP-based spatial repetitive control, are outlined. Experimental results on various systems, including a desktop printer, wirebonder, and substrate carrier, confirm that data-based learning can significantly improve the accuracy of mechatronic systems.

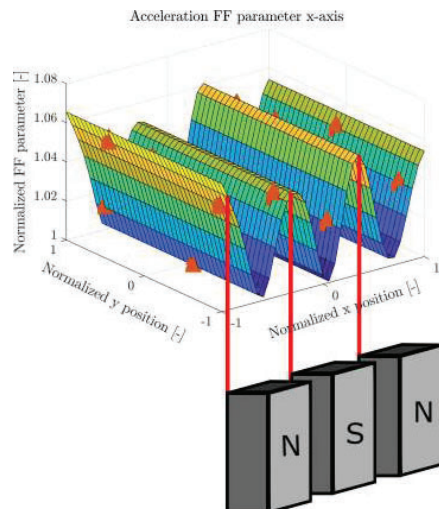


Fig. 2. Data-driven learning of Gaussian-Process based motor force compensation.

B. Learning for Precision Motion Control

Iterative Learning Control (ILC) can achieve perfect tracking performance for mechatronic systems. The aim is to present an ILC design tutorial for industrial mechatronic systems. First, a preliminary analysis reveals the potential performance improvement of ILC prior to its actual implementation. Second, a frequency domain approach is presented, where fast learning is achieved through noncausal model inversion, and safe and robust learning is achieved by employing a contraction mapping theorem in conjunction with nonparametric frequency response functions. The approach is demonstrated on a desktop printer, see Fig. 3. Finally, a detailed analysis of industrial motion systems leads to several shortcomings that obstruct the widespread implementation of ILC algorithms. An overview of recently developed algorithms is given, in-

cluding extensions using machine learning algorithms. These are aimed to facilitate broad industrial deployment.

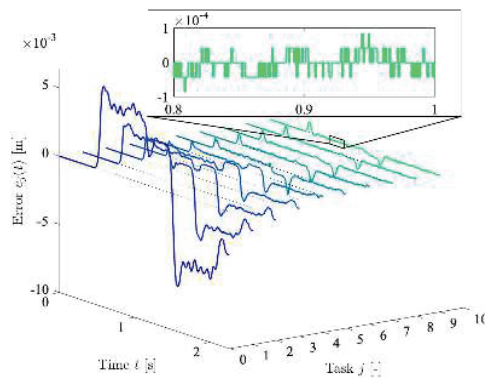


Fig. 3. Performance enhancement on a desktop printer through iterative learning control

ACKNOWLEDGEMENT

The authors would like to thank all collaborators, including colleagues, former students, and visitors from both academia and industry.

REFERENCES

- [1] M. Steinbuch, T. Oomen, and H. Vermeulen, "Motion control, mechatronics design, and Moore's law," *IEEJ Transactions on Industry Applications*, vol. 11, no. 2, pp. 245–255, 2022.
- [2] T. Oomen, "Advanced motion control for precision mechatronics: Control, identification, and learning of complex systems," *IEEJ Transactions on Industry Applications*, vol. 7, no. 2, pp. 127–140, 2018.
- [3] E. Evers, M. van de Wal, and T. Oomen, "Beyond decentralized wafer/reticle stage motion control design: A double-Youla approach for enhancing synchronized motion," *Control Engineering Practice*, vol. 83, pp. 21–32, 2019.
- [4] T. Oomen, E. Grassens, and F. Hendriks, "Inferential motion control: An identification and robust control framework for unmeasured performance variables," *IEEE Transactions on Control Systems Technology*, vol. 23, no. 4, pp. 1602–1610, 2015.
- [5] N. Strijbosch and T. Oomen, "Iterative learning control for intermittently sampled data: Monotonic convergence, design, and applications," *Automatica*, vol. 139, p. 110171, 2023.
- [6] W. Ohnishi, N. Strijbosch, and T. Oomen, "State-tracking iterative learning control in frequency domain design for improved intersample behavior," *International Journal of Robust and Nonlinear Control*, vol. 33, pp. 4009–4027, 2023.
- [7] E. Evers, B. de Jager, and T. Oomen, "Incorporating prior knowledge in local parametric modeling for frequency response measurements: Applied to thermal/mechanical systems," *IEEE Transactions on Control Systems Technology*, vol. 30, no. 1, pp. 142–155, 2022.
- [8] P. Tacx, M. Teurlings, R. Habraken, G. Witvoet, M. Heertjes, and T. Oomen, "Spatio-temporal analysis of overactuated motion systems: A mechanical modeling approach," in *IFAC 22nd Triennial World Congress*, Yokohama, Japan, 2023.
- [9] M. van Dael, J. Casanueva Diaz, G. Witvoet, B. Swinkels, M. Pinto, D. Bersanetti, M. Mantovani, C. de Rossi, P. Spinicelli, and T. Oomen, "Integrating H_2 synthesis and dynamic error budgeting for improved gravitational wave detection," in *IFAC 22nd Triennial World Congress*, Yokohama, Japan, 2023.
- [10] R. Voorhoeve, A. van der Maas, and T. Oomen, "Non-parametric identification of multivariable systems: A local rational modeling approach with application to a vibration isolation benchmark," *Mechanical Systems and Signal Processing*, vol. 105, pp. 129–152, 2018.
- [11] R. de Rozario and T. Oomen, "Frequency response function identification of periodically scheduled linear parameter-varying systems," *Mechanical Systems and Signal Processing*, vol. 148, p. 107156, 2021.
- [12] M. van Haren, L. Mirkin, L. Blanken, and T. Oomen, "Beyond Nyquist in frequency response function identification: Applied to slow-sampled systems," *IEEE Control Systems Letters (L-CSS)*, 2023.
- [13] N. Dirkx, K. Tiels, and T. Oomen, "A wavelet-based approach to FRF identification from incomplete data," *IEEE Transactions on Instrumentation and Measurement*, vol. 71, pp. 1–15, 2023.
- [14] R. A. González, K. Tiels, and T. Oomen, "Identifying lebesgue-sampled continuous-time impulse response models: A kernel-based approach," in *IFAC 22nd Triennial World Congress*, Yokohama, Japan, 2023.
- [15] R. Voorhoeve, R. de Rozario, W. Aangenent, and T. Oomen, "Identifying position-dependent mechanical systems: A modal approach with applications to wafer stage control," *IEEE Transactions on Control Systems Technology*, vol. 29, no. 1, pp. 194–206, 2021.
- [16] T. Oomen, "Learning for advanced motion control," in *International Workshop on Advanced Motion Control*, Agder, Norway, 2020, pp. 65–72.
- [17] ———, "Learning in machines," *Mikroniek*, vol. 6, pp. 5–11, 2018.
- [18] L. Blanken, F. Boeren, D. Bruijnen, and T. Oomen, "Batch-to-batch rational feedforward control: from iterative learning to identification approaches, with application to a wafer stage," *IEEE/ASME Transactions on Mechatronics*, vol. 22, no. 2, pp. 826–837, 2017.
- [19] N. Mooren, G. Witvoet, and T. Oomen, "From batch-to-batch to online learning control: Experimental motion control case study," in *Joint Conference 8th IFAC Symposium on Mechatronic Systems and Proceedings of the 12th IFAC Symposium on Nonlinear Control Systems*, Vienna, Austria, 2019, pp. 1013–1018.
- [20] T. van Keulen, T. Oomen, and M. Heemels, "Online feedforward parameter learning with robustness to set-point variations," in *IFAC 22nd Triennial World Congress*, Yokohama, Japan, 2023.
- [21] L. Aarnoudse and T. Oomen, "Automated MIMO motion feedforward control: Efficient learning through data-driven gradients via adjoint experiments and stochastic approximation," in *2022 Modeling, Estimation and Control Conference (MECC)*, Jersey City, New Jersey, United States, 2022.
- [22] N. Strijbosch, K. Tiels, and T. Oomen, "Memory-element based hysteresis: Identification and compensation of a piezoelectric actuator," *IEEE Transactions on Control Systems Technology*, To appear.
- [23] M. Poot, J. Portegies, N. Mooren, M. van Haren, M. van Meer, and T. Oomen, "Gaussian processes for advanced motion control," *IEEJ Transactions on Industry Applications*, vol. 11, no. 3, pp. 396–407, 2022.
- [24] J. Kon, N. de Vos, D. Bruijnen, J. van de Wijdeven, M. Heertjes, and T. Oomen, "Learning for precision motion of an interventional X-ray system: Add-on physics-guided neural network feedforward control," in *IFAC 22nd Triennial World Congress*, Yokohama, Japan, 2022.
- [25] K. Classens, M. Heemels, and T. Oomen, "A closed-loop perspective on fault detection for precision motion control: With application to an overactuated system," in *IEEE International Conference on Mechatronics*, Tokyo, Japan, 2021.
- [26] M. Čech, A.-J. Beltman, and K. Ozols, "Digital twins and AI in smart motion control applications," in *27th IEEE International Conference on Emerging Technologies and Factory Automation (ETFA)*, Stuttgart, Germany, 2022, pp. 1–7.



Tom Oomen is full professor with the Department of Mechanical Engineering at the Eindhoven University of Technology. He is also a part-time full professor with the Delft University of Technology. He is a recipient of the 7th Grand Nagamori Award, the IFAC 2019 TC 4.2 Mechatronics Young Research Award, the 2019 IEEJ Journal of Industry Applications Best Paper Award, and recipient of a Veni and Vidi personal grant. He is currently a Senior Editor of IEEE L-CSS.

Feedforward Control using Gaussian Processes for Semiconductor Manufacturing Equipment

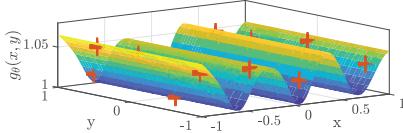
Maurice Poot¹, Dragan Kostić², Jim Portegies³, and Tom Oomen^{1,4}

I. RESEARCH OVERVIEW

The increasing demands on throughput and accuracy of semiconductor manufacturing equipment necessitate accurate feedforward motion control that is able to compensate for unmodeled parasitic effects. These effects include position-dependent dynamics and motor force constants, base-frame vibrations, magnetic saturation in the actuators, and point-of-interest dynamics. In this research, iterative learning control (ILC) and Gaussian processes (GPs) [1] are employed to tackle these effects in a wirebonder by ASMPt.

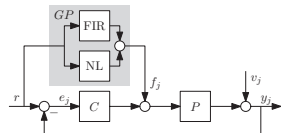
Gaussian Processes for Advanced Motion Control: Position Dependent Feedforward [2]

Interpretable and task-flexible position-dependent feedforward is achieved through modeling the feedforward parameters as function of position using a GP. A framework for experiment design in the sense of automatically determining the training positions is presented by exploiting the uncertainty estimates of the GP. The position-dependent acceleration parameter of a wirebonder modeled by a GP compensates for the variation of the motor force constant.



Gaussian Processes for Advanced Motion Control: Task-Flexible Feedforward [3]

To achieve task-flexibility in ILC, a non-causal high-order FIR regularized by a kernel is learned simultaneously with pre-specified nonlinear basis functions (BF) in closed-loop. The kernel incorporates prior knowledge, enforcing model complexity and non-causality to deal with NMP systems.



This work is supported by ASMPt.

¹Maurice Poot and Tom Oomen are with CST, Eindhoven University of Technology, corresponding e-mail: m.m.poot@tue.nl.

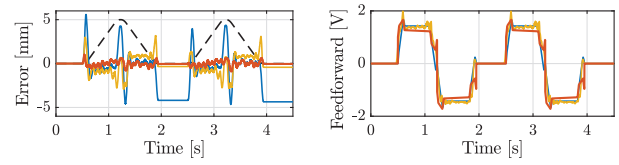
²Dragan Kostić is with ASMPt, The Netherlands.

³Jim Portegies is with CASA, Eindhoven University of Technology.

⁴Tom Oomen is also with the Delft Center for Systems and Control, Delft University of Technology.

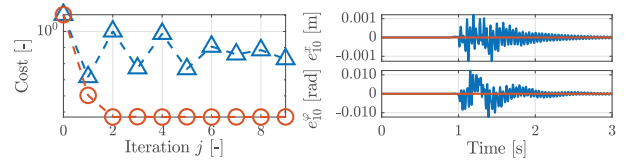
Gaussian Processes for Advanced Motion Control: Nonlinear Feedforward [4]

In contrast to ILC with BF [5] (—) and the linear non-causal FIR with pre-specified nonlinearities [3] (—) as seen above, here, no knowledge about the nonlinearity is required. By utilizing input-output data, a GP models the inverse system dynamics as an NFIR to compensate for unknown nonlinear effects (—), as demonstrated on an A3 printer.



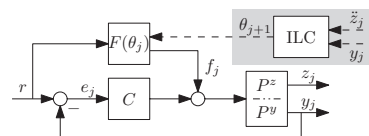
Rational Basis Functions in ILC for Multivariable Systems [6]

To address base-frame vibrations in multivariable systems, rational feedforward in ILC for noncommutative MIMO systems is developed (—). By rewriting the optimization problem a weighted least-squares problem is obtained that can be solved after each experiment, avoiding the exploitation of the commutation property of the pre-existing SISO approach extended for MIMO systems (Δ), yielding better convergence and lower error in an Arizona printer simulation.



Data-Driven and Task-Flexible Point-of-Interest Control

Ongoing research focuses on offline inference of the point-of-interest with an accelerometer and exploiting the batch-to-batch process of ILC (—). By employing rational basis functions, the flexible dynamics between encoder and point-of-interest can be compensated, resulting in enhanced tracking performance for the bondhead in a wirebonder simulation.



II. SEMINAR TOPIC - FEEDFORWARD CONTROL IN THE PRESENCE OF INPUT NONLINEARITIES [7]

To achieve high tracking accuracy and task flexibility for nonlinear systems, extensions to ILC with BF [5] are necessary that compensate input nonlinearities, e.g., magnetic saturation in linear actuators.

A. Problem formulation

The aim of this research is to develop a data-driven feedforward tuning approach consisting of a Wiener feedforward, i.e., linear parameterization $F(\theta)$ with an output nonlinearity $h(\cdot, \phi)$, see Fig. 1, for Hammerstein systems [8].

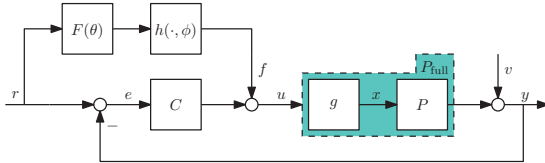


Fig. 1. Proposed closed-loop control scheme with Wiener feedforward $f = h(F(\theta)r, \phi)$.

B. Approach

The developed approach exploits norm-optimal iterative learning control (NOILC) to learn a feedforward signal f^{NOILC} from data that minimizes the error. The setpoint is persistently exciting, i.e., a concatenated setpoint with varying maximum accelerations, see Fig. 2. The parameters $\theta^{\text{opt}}, \phi^{\text{opt}}$ are jointly optimized using a nonconvex optimization procedure with

$$\{\theta^{\text{opt}}, \phi^{\text{opt}}\} = \underset{\{\theta, \phi\}}{\operatorname{argmin}} \|\widehat{SP}(f^{\text{NOILC}} - h(F(\theta)r, \phi))\|^2, \quad (1)$$

where the model $\widehat{SP} : f \rightarrow e$ is introduced to make the cost function control-relevant, as it relates the feedforward signal to its contribution to the error, see [9]. See [7] for cost landscape.

C. Results

Experimental results on a commercial wirebonder show a reduction in tracking error using the developed approach with

$$f = h(F(\theta)r, \phi) = \phi \cdot \operatorname{atanh}\left(\frac{\dot{r}\theta_1 + \ddot{r}\theta_2}{\phi}\right), \quad (2)$$

where compensation for magnetic saturation and rigid-body dynamics is applied, see Fig. 2. The tracking error of the developed approach is lower and more consistent for increasing setpoint acceleration than only linear rigid-body feedforward.

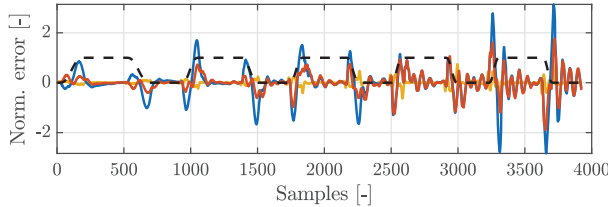


Fig. 2. Error signals of linear (—), the developed (—), and NOILC (—) approach for a setpoint with varying maximum acceleration (---).

Moreover, for setpoints with varying maximum accelerations and motion distances, the relearned mass parameter is significantly more consistent in the developed approach, indicating task flexibility, see Fig. 3.

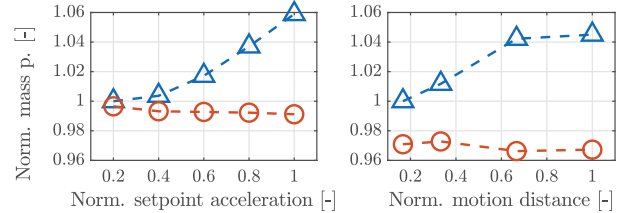


Fig. 3. Mass parameter per setpoint acceleration (left) and motion distance (right) of the linear (Δ) and the developed (○) approach.

D. Conclusion and outlook

The developed Wiener feedforward approach achieves high tracking accuracy and task flexibility for Hammerstein systems. Ongoing research focuses on compensating other nonlinear and position dependent effects in the wirebonder.

REFERENCES

- [1] M. Poot, J. Portegies, N. Mooren, M. van Haren, M. van Meer, and T. Oomen, "Gaussian Processes for Advanced Motion Control," *IEEE J. Ind. Appl.*, vol. 11, no. 3, pp. 396–407, 2022.
- [2] M. Poot, M. V. Haren, D. Kostić, J. Portegies, and T. Oomen, "Position-Dependent Motion Feedforward via Gaussian Processes: Applied to Snap and Force Ripple in Semiconductor Equipment," *To Appear*, 2023.
- [3] M. Poot, J. Portegies, and T. Oomen, "Kernel-Based Learning Control for Iteration-Varying Tasks Applied to a Printer With Friction," in *2021 IEEE/ASME Int. Conf. Adv. Intell. Mechatronics*, Delft, 2021, pp. 1052–1057.
- [4] M. van Meer, M. Poot, J. Portegies, and T. Oomen, "Learning nonlinear feedforward: a Gaussian Process Approach Applied to a Printer with Friction," in *Model. Estim. Control Conf.*, Jersey City, New Jersey, 2022.
- [5] J. van de Wijdeven and O. Bosgra, "Using basis functions in iterative learning control: analysis and design theory," *Int. J. Control.*, vol. 83, no. 4, pp. 661–675, apr 2010.
- [6] M. Poot, J. Portegies, D. Kostić, and T. Oomen, "Rational Basis Functions in Iterative Learning Control for Multivariable Systems," *To Appear*, 2023.
- [7] M. Poot, J. V. Hulst, K. W. Yan, D. Kostić, J. Portegies, and T. Oomen, "Feedforward Control in the Presence of Input Nonlinearities: With Application to a Wirebonder," in *2023 IFAC World Congr.*, Yokohama, 2023.
- [8] J. van Hulst, M. Poot, D. Kostić, K. W. Yan, J. Portegies, and T. Oomen, "Feedforward Control in the Presence of Input Nonlinearities: A Learning-based Approach," in *Model. Estim. Control Conf.*, Jersey City, New Jersey, 2022.
- [9] L. Aarnoudse, W. Ohnishi, M. Poot, P. Tacx, N. Strijbosch, and T. Oomen, "Control-Relevant Neural Networks for Intelligent Motion Feedforward," *Accept. to IEEE Int. Conf. Mechatronics 2021*, 2021.



Maurice Poot received the M.Sc. degree in Systems & Control from the Eindhoven University of Technology in 2019. Currently, he is pursuing a Ph.D. degree at the department of Mechanical Engineering at the Eindhoven University of Technology and his research is in collaboration with ASMPT. His research interest includes learning control and Gaussian processes for precision mechatronics. In his free-time, he enjoys meditation, running, swimming, and wild camping.

State-Variable Dependent Disturbance Compensation Signal Generation Using Gaussian Process Regression

Reon Sasaki, Wataru Ohnishi

I. INTRODUCTION

IN recent years, DC power transmission technology has attracted more and more attention. The introduction of DC system requires a circuit breaker to interrupt the current in the event of an accident as shown in Fig.I,1. In addition, since the impedance of transmission lines is lower than that of alternating current, faults propagate easily, so high-speed interruption is also required.



Fig. 1. Explosion when fuse and IGBT cutoff failure. In order to prevent this situation, it is necessary to improve the performance of the circuit breaker.

This research shows the effect of applying the actuator as a high-speed fuse changer in the new DC circuit breaker proposed by our research group, instead of using it for the electrode opening operation.

II. OPERATION PRINCIPLE

A. Mechanism of current interruption

As shown in Fig.II-A, the basic structure of the circuit breaker proposed by our research group consists of a FUSE, which is an inexpensive and compact current limiting device,

R. Sasaki is with the Department of Electrical Engineering and Information Systems Graduate School of Engineering, The University of Tokyo, e-mail: r.sasaki@ctf.t.u-tokyo.ac.jp

W. Ohnishi is with the Department of Electrical Engineering and Information Systems Graduate School of Engineering, The University of Tokyo, e-mail: ohnishi@ieee.org

an Insulated Gate Bipolar Transistor (IGBT) that can interrupt limited current at high speed, and a VARISTOR whose resistance value changes according to the applied voltage and protects IGBT.

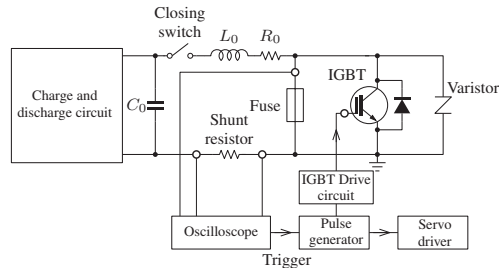


Fig. 2. Equivalent circuit diagram of the new circuit breaker.

The advantage of this circuit breaker is that there is no heat generation due to the ON resistance of the semiconductor. While semiconductor circuit breakers are capable of high-speed current interruption, they generate Joule heat due to ON resistance even during rated operation, requiring a cooling mechanism. The new circuit breaker does not generate heat because current flows through the fuse during rated operation.

Furthermore, since the fault current is limited by the fuse and then cut off, the current load flowing into the system when a fault occurs is small. Since the IGBT has a low breaking current, there is no need to use a large semiconductor device, and further cost reduction and miniaturization can be expected.

B. Role of linear motor

The new circuit breaker uses a fuse, it cannot be used again once the current is interrupted, and it is necessary to replace the fuse with a new one in order to restore the state of the circuit before the accident occurred. Therefore, using a linear motor, reclosing the circuit can be achieved by replacing the fuse at high speed. A new fuse is introduced into the circuit by sliding the fuse after the fuse is shut off and the system is restored.

III. DISTURBANCE COMPENSATION

Replacing the fuse, disturbance occurs during contact between the electrodes and the fuse due to reclose. Due to this disturbance, the re-closing by the fuse, that is, the time until power restoration becomes uncertain. Since the time to

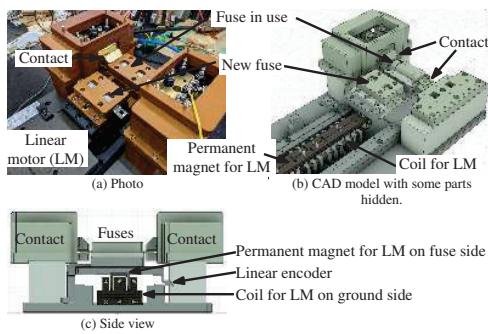


Fig. 3. Structure of fuse changer equipped with transverse flux linear motor.

recovery from an accident is a very important performance indicator for protecting precision equipment, highly reproducible control that compensates for disturbances is required. To compensate this, estimation of disturbance by Gaussian Process Regression(GPR) as shown in Fig.III.

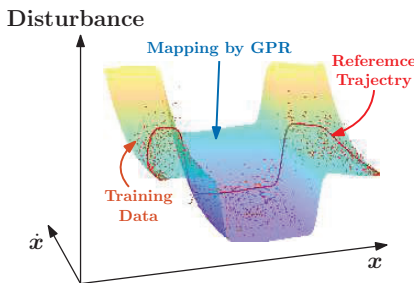


Fig. 4. Disturbance mapping using Gaussian process regression.

The disturbance based on the previously measured linear model is estimated from the Kalman Smoother using the position, velocity, and control input data during a feedback control experiment.

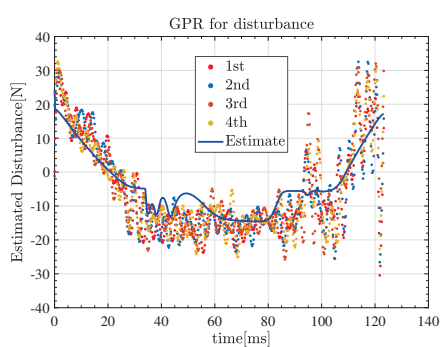


Fig. 5. Time-series data of acquired data and disturbance compensated signal.

Then, GPR is performed with the position and velocity as input and the magnitude of the disturbance as output, and the input-output relationship is regressed. Then, by estimating the magnitude of the disturbance expected from the position and velocity on the target trajectory and providing a signal

to compensate for it (Fig.III), the Saidai tracking error was reduced by 66.2%.

IV. FUTURE WORK

A new control method has been proposed that combines Iterative Learning Control(ILC), which applies a learning filter to the tracking error to determine the most effective control and performs highly accurate control with repeated experiments, and GPR as shown in Fig.IV.

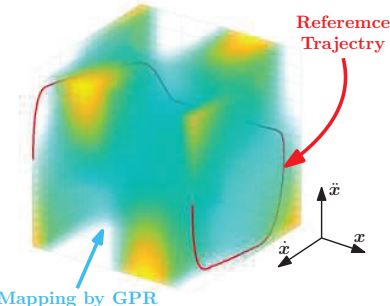


Fig. 6. Combination of ILC and GPR.

REFERENCES

- [1] W. Ohnishi, Y. Inada; S. Zen; R. Sasaki, et al. "Proof-of-Concept of a Fuse-Semiconductor Hybrid Circuit Breaker With a Fast Fuse Exchanger," *IEEE Transactions on Power Delivery*, 2023
- [2] R. Sasaki, W.Ohnishi, et al. "Compensation for state variable dependent disturbances in linear motor using gaussian process regression" 2022
- [3] R. Sasaki, W.Ohnishi, et al. "Basic study of high-speed fuse replacement using a linear motor in the fuse semiconductor hybrid circuit breaker" 2021.



Reon Sasaki received the B.E., M.S. degrees from The University of Tokyo, Japan, in 2021, and 2023, respectively. Presently, he is currently enrolled in the doctoral program at the University of Tokyo Graduate School of Engineering, Department of Electrical Engineering. Mainly engaged in research on motion control using Machine Learning.



Wataru Ohnishi received the B.E., M.S., and Ph.D. degrees from The University of Tokyo, Japan, in 2013, 2015, and 2018, respectively. Presently, he is an associate professor with the Department of Electrical Engineering and Information Systems, Graduate School of Engineering, The University of Tokyo. He held a visiting position at the Eindhoven University of Technology. His research interests include high-precision motion control and optimization. He is a senior member of The Institute of Electrical Engineers of Japan.

Identification for Multivariable Precision Mechatronics

Paul Tacx¹, Matthijs Teurlings¹, Roel Habraken^{1,4}, Gert Witvoet^{1,4}, Marcel Heertjes^{1,3}, Tom Oomen^{1,2}

I. RESEARCH OVERVIEW

Stringent demands regarding performance in mechatronic systems require the flexible dynamic behavior to be addressed explicitly in the control design.

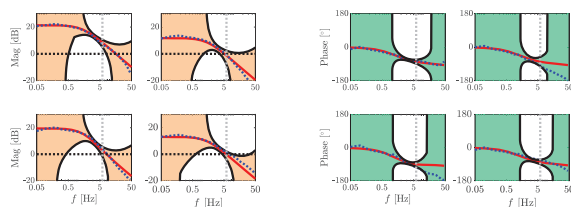


Data-based \mathcal{H}_∞ -norm estimation [1]

Accurate \mathcal{H}_∞ -norm estimation is of critical importance for robust control design. The main idea is to estimate the global \mathcal{H}_∞ norm by estimating the finite-frequency L_∞ norm of the local models through the generalized KYP lemma.

Visualizing & Comparing Multivariable Uncertain Systems [2]

The availability of reliable and systematic robust control algorithms has spurred the development of uncertainty structures of multivariable model sets for robust control. A unified approach is developed for generating element-wise and multivariable Bode plots for both the magnitude and phase of multivariable uncertain systems.



One-step Centralized Overactuation [3]

A systematic one-step robust control design approach to go beyond the conventional performance limits through explicit control of the flexible dynamical behavior using additional actuators and sensors.

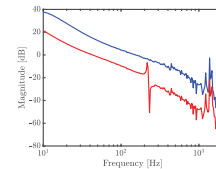
Funding: This work is part of the research programme VIDI with project number 15698, which is (partly) financed by the Netherlands Organisation for Scientific Research (NWO). Corresponding e-mail: p.j.m.m.tacx@tue.nl.

¹Eindhoven University of Technology, Department of Mechanical Engineering.

²Delft University of Technology, Delft Center for Systems and Control, Delft, The Netherlands.

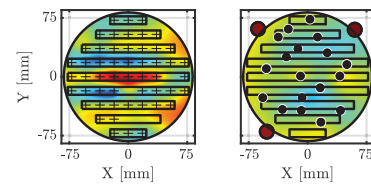
³ASML, Mechatronic Systems Development, Veldhoven, the Netherlands

⁴TNO, Optomechatronics Department, Delft, the Netherlands



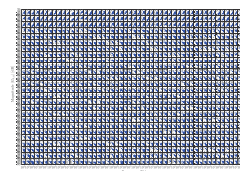
Spatio-Temporal Modeling for Next-gen Motion Control [4]

The proposed approach exploits the modal modeling framework and the overactuated setting to enhance the estimation of the modeshape. The enhanced spatial resolution of the modeshape is used to estimate the spatial system behavior.



Design Analysis of Future Deformable Mirrors [4]

Modeling the flexible dynamic behavior of next-generation deformable mirrors is essential for the design analysis and control. An unified approach is developed for the identification of deformable mirrors with a large number of spatially distributed actuators and a limited number of sensors.



References

- [1] Paul Tacx and Tom Oomen, Accurate H-infinity-norm estimation via finite-frequency norms of local parametric models, ACC 2021, New Orleans, Louisiana, 2021.
- [2] Paul Tacx and Tom Oomen, Bode analysis of uncertain multivariable systems, In 2022 ACC, 5056-5061, Atlanta, Georgia, 2022.
- [3] Paul Tacx and Tom Oomen, A one-step approach for centralized overactuated motion control of a prototype reticle stage, In 2022 MECC, Jersey City, New Jersey, 2022.
- [4] Paul Tacx, Matthijs Teurlings, Roel Habraken, Gert Witvoet, Marcel Heertjes, and Tom Oomen, Spatio-temporal analysis of overactuated motion systems: A mechanical modeling approach, IFAC WC, Yokohama, Japan, 2023.

II. SEMINAR TOPIC - Spatio-Temporal Modeling for Next-Generation Motion Control

A. Background

Flexible dynamics in next-generation motion systems lead to inherent spatio-temporal system dynamics. Inevitably, next-generation control techniques increasingly rely on accurate modeling techniques that capture the spatio-temporal nature of the flexible dynamic behavior [1]. Two case studies are being investigated: adaptive optics and mechanical stage control.

B. Problem Formulation

A key challenge for next-generation motion systems is the modeling of the spatio-temporal flexible dynamics. Traditional parametric and nonparametric identification approaches aim to identify the temporal behavior of the flexible dynamics. As a result, the flexible dynamic behavior is estimated at a limited spatial grid which limits the understanding of the position-dependency of the flexible dynamic behavior [2]. The aim of this paper is to identify and reconstruct the spatio-temporal behavior for spatio-temporal control of next-generation motion systems with a large number of spatially distributed actuators.

C. Approach

Given a motion system $G_m : [u_1 \dots u_{n_a}]^\top \mapsto [y_1 \dots y_{n_s}]^\top$ with a large amount n_a of spatially distributed actuators and a limited amount of n_s sensors, i.e. $n_s \ll n_a$. The aim is to model the spatio-temporal nature of the flexible dynamic behavior. The approach includes the identification of modal models [2]. The modal system description is exploited by including mechanical systems knowledge [3]. The proposed approach allows enhancing the estimation of the spatial system behavior [4].

D. Results

The proposed approach is illustrated on an experimental beam setup, see Figure 1. The approach proposed in this paper allows identifying the full response G_m while only having access to the first sensor by exploiting the proposed approach. In particular, the approach allows analyzing the spatio-temporal behavior with limited sensing capabilities, see Figure 2. In particular, the full system G_m is identified while only having access to the first sensor.

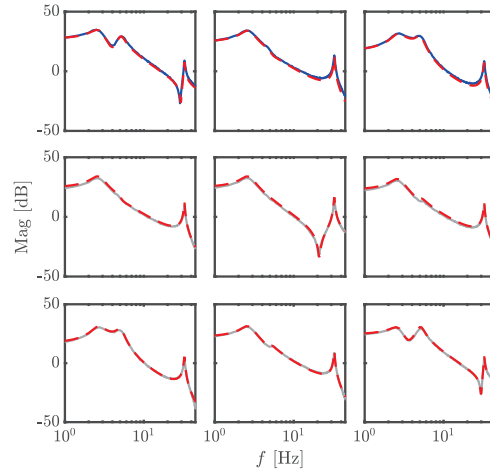


Fig. 3: Experimental overactuated beam setup. The three voice-coil actuators are indicated in red. The flexible beam system G_m is actuated by three voice coil actuators (red) and the displacement is measured by three sensors (blue and grey). The proposed method only considers the first sensor (blue) to estimate the full system G_m .



Fig. 4: Element-wise Bode magnitude plot of the non-parametric estimate of the full system G_m (grey), the non-parametric estimate of subsystem G_o (blue), and extended plant G_m (dashed red).

REFERENCES

- [1] T. Oomen, R. van Herpen, S. Quist, M. van de Wal, O. Bosgra, and M. Steinbuch, "Connecting system identification and robust control for next-generation motion control of a wafer stage," *IEEE Trans. on Contr. Sys. Tech.*, vol. 22, no. 1, pp. 102–118, 2013.
- [2] R. Voorhoeve, R. de Rozario, W. Aangenent, and T. Oomen, "Identifying position-dependent mechanical systems: A modal approach applied to a flexible wafer stage," *IEEE Trans. on Contr. Sys. Tech.*, vol. 29, no. 1, pp. 194–206, 2020.
- [3] A. Ghali and A. Neville, "Structural Analysis: A unified classical and matrix approach," CRC Press, 1981.
- [4] P Tacx, R. Habraken, M. Teurlings, G. Witvoet, M. Heertjes, T. Oomen, "Spatio-Temporal Analysis of Overactuated Motion Systems: A Mechanical Modeling Approach," Under review.

Nonlinear system identification for high-tech systems

Koen Tiels¹

I. RESEARCH OVERVIEW

Increasing demands on future high-tech systems for increased throughput, increased accuracy, and reduced costs lead to lightweight designs that show significant nonlinear behavior. Capturing this nonlinear behavior can be beneficial for accurate simulation and for designing feedforward controllers.

New challenges in linear model identification

Linear models are still very useful to provide insight into the dynamics of the system or as initialization for a nonlinear model. Moreover, new challenges in linear system identification pop up. One example is due to non-conventional sampling, e.g., Lebesgue sampling [1], moving away from traditional equidistant sampling. Another example is due to thermal aspects of the system becoming important for accurate modeling of the system behavior. Since thermal dynamics are slow, typically long data records are observed that cannot be captured without interruptions, eventually leading to missing samples [2].

Nonlinear behavior in high-tech systems

Increasing requirements necessitate and justify the use of nonlinear models and their subsequent use in motion control. One aspect that is often present in motion systems is hysteretic behavior. Accurately modeling (the inverse of) this behavior and compensating for it with feedforward control can lead to significant improvements in tracking performance [3].

Supported by NWO VIDI 15698 and ECSEL 101007311 (IMOCO4.E).

¹ The author is with the Control Systems Technology research section of the Eindhoven University of Technology, the Netherlands, corresponding e-mail: k.tiels@tue.nl.

Linear time-invariant solutions for enhancing iterative learning control theory

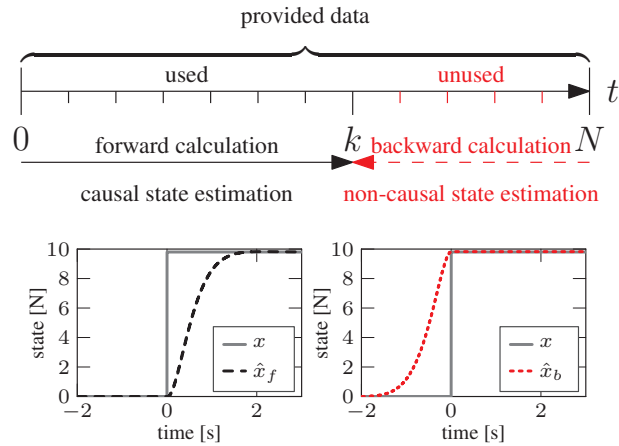
Kentaro Tsurumoto¹, Wataru Ohnishi¹ and Takafumi Koseki¹

I. RESEARCH OVERVIEW

High precision motion systems require fast, precise, and reliable control. Iterative learning control (ILC) is a powerful method meeting all of these requirements for high precision motion systems with repeating tasks. This research is positioned at enhancing the strength of ILC theory with negligible compromise. First, an overview of two research topics utilizing non-causality for state estimations is given, and secondly the synergy of combining ILC frameworks is elaborated.

Non-causal filtering improves off-line state estimation [1]

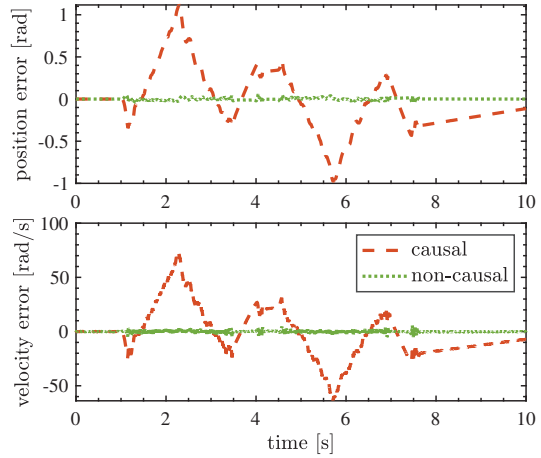
During off-line analysis, unlike on-line, full experiment data is provided in advance. This motivates utilizing the full data when making a state estimation for each point of time.



To make full use of the data, in addition to a standard causal state observer (—), an unstable state observer with the same bandwidth as the causal observer is constructed. By applying stable inversion to the unstable state observer and filtering the unused data backwards in time, a stable non-causal state estimation (···) is obtained. Finally, by combining both state estimations based on their covariance matrix, an improved state estimation is acquired.

Results of non-causal filtering lead to significant state estimation error reduction (—), compared to a causal estimate (—) with the same bandwidth.

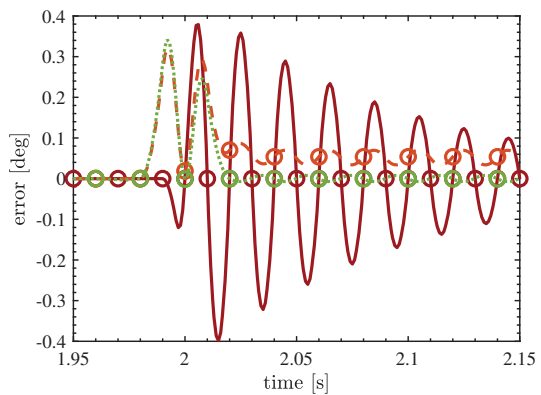
¹ The authors are with the Department of Electrical Engineering and Information Systems, The University of Tokyo, 7-3-1 Hongo, Bunkyo-ku, Tokyo, Japan,
corresponding e-mail: k.tsurumoto@ctl.t.u-tokyo.ac.jp.



Non-causal state estimation improves inter-sample behaviour of iterative learning control [2]

ILC can theoretically achieve perfect on-sample tracking performance (○). However, due to discretization, systems often have zeros near the stability limit. This leads to an oscillatory inter-sample behavior (—). Although state-tracking ILC [3] has introduced the idea of state-tracking to deal with this problem, the previous research does not take the advantage of off-line learning and uses causal state estimations. This leads to a steady state error caused by modeling error of the system (—○).

By using non-causal state estimation for state-tracking ILC, on-sample state error (○) is significantly improved and inter-sample tracking performance (---) is further enhanced.



II. SEMINAR TOPIC - Combined ILC: Achieving Both Task Flexibility and Higher Tracking Performance in ILC [4]

The use of basis functions in iterative learning control (B-ILC) enhances task flexibility for ILC [5]. However, B-ILC has a compromise in achievable tracking performance when compared to other ILC frameworks such as frequency-domain ILC (F-ILC). The aim of this research is to develop an ILC framework combining the frequency-domain design and basis function approach, enhancing tracking performance against repeating tasks while achieving task flexibility.

A. Problem Formulation

The control objective is to minimize the tracking error $e_j = r_j - y_j$ for trial j as possible for both when same tasks are repeated and tasks have been changed. The supposed close-loop setup is shown in Step 0 of Fig. 1.

B. Approach

As shown in Fig. 1, the developed framework consists of parallel feedforward update of basis function component f_j^θ and frequency-domain component f_j^{ILC} .

Step 1: Learning of basis function component f_{j+1}^θ

Instead of minimizing e as the validation function, minimizing $e^\theta := e + SGf^{\text{ILC}} = Sr - SGF(\theta)r$ is proposed. Due to this modification, f^θ will be able to learn an accurate inverse model G^{-1} , without interacting with the learning of f_j^{ILC} .

Step 2: Learning of frequency-domain component f_{j+1}^{ILC}

The feedforward update law is defined as

$$f_{j+1}^{\text{ILC}} = Q(f_j^{\text{ILC}} + Le_j) + f_j^\theta - f_{j+1}^\theta. \quad (1)$$

With an assumption of an asymptotic FF controller $F(\theta_\infty) = \lim_{j \rightarrow \infty} F(\theta_j)$ and

$$|Q(e^{i\omega})||1 - G(e^{i\omega})S(e^{i\omega})L(e^{i\omega})| < 1, \quad \forall \omega, \quad (2)$$

the asymptotic error $e_\infty = \lim_{j \rightarrow \infty} e_j$ for C-ILC becomes,

$$e_\infty = \frac{(1 - Q)S}{1 - Q(1 - SGL)} (1 - GF(\theta_\infty)) r. \quad (3)$$

This achieves $(1 - GF(\theta_\infty))$ times performance improvement than that of standard F-ILC. Note that in this implementation f_{j+1}^{ILC} is reset to zero when task is changed.

C. Results

Tracking performance per iteration of C-ILC is compared with traditional F-ILC and B-ILC in Fig. 2. From the result, C-ILC exceeds the performance of F-ILC for repeating tasks, while ensuring the same task flexibility as that of B-ILC.

D. Conclusions

An ILC framework for combining a frequency-domain design and basis function approach is developed, where parallel learning of each component is achieved without interacting with each other. Ongoing research is aimed at consideration of external disturbance and extension to MIMO systems.

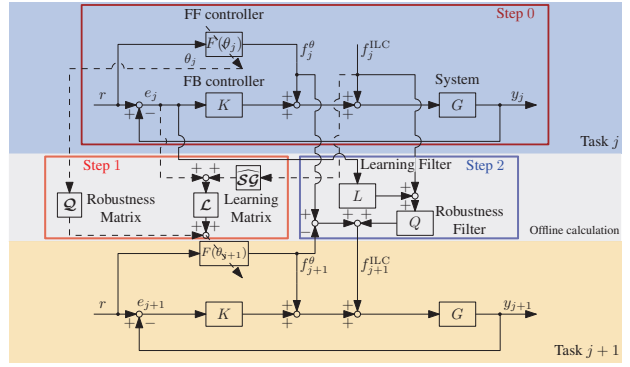


Fig. 1. Proposed Combined ILC (C-ILC) structure.

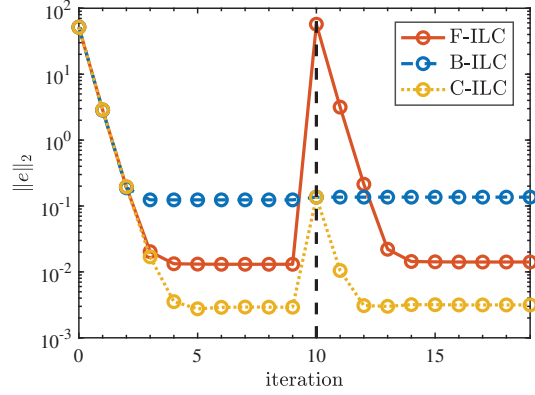


Fig. 2. Comparison of F-ILC (red circles), B-ILC (blue circles), and C-ILC (yellow circles) tracking performance. From the 10th trial and on, the task is changed to a different reference trajectory from the 0th to 9th trial.

REFERENCES

- [1] K. Tsurumoto, W. Ohnishi, T. Koseki, N. Strijbosch, and T. Oomen, "Improved state estimation by non-causal state observer," in *8th IEEJ International Workshop on Sensing, Actuation, Motion Control, and Optimization*, 2022.
- [2] K. Tsurumoto, W. Ohnishi, T. Koseki, N. Strijbosch, and T. Oomen, "Non-causal state estimation for improved state tracking in iterative learning control," in *2022 Modeling, Estimation, and Control Conference*, 2022.
- [3] W. Ohnishi, N. Strijbosch, and T. Oomen, "State-tracking iterative learning control in frequency domain design for improved intersample behavior," *International Journal of Robust and Nonlinear Control*, 2022.
- [4] K. Tsurumoto, W. Ohnishi, and T. Koseki, "Task flexible and high performance ILC: Preliminary analysis of combining a basis function and frequency-domain approach," in *22nd IFAC World Congress*, 2023.
- [5] "Fixed structure feedforward controller design exploiting iterative trials: Application to a wafer stage and a desktop printer," *Journal of Dynamic Systems, Measurement and Control, Transactions of the ASME*, vol. 130, no. 5, pp. 1–16, 2008.



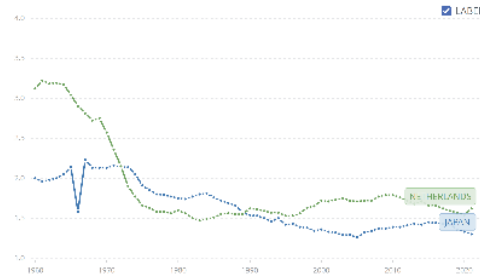
Kentaro Tsurumoto received the BSc. degree in electrical engineering from The University of Tokyo, in 2022. Currently, he is pursuing a MSc. degree at the department of Electrical Engineering and Information Systems, Graduate School of Engineering, The University of Tokyo. His research interests include non-causal estimation, high-precision motion control and learning control.

A Proposal for a Simulated Running Environment for Railway Vehicle Control Engineering Tests Using a Scaled Roller Rig that Simulates High-Speed Friction Fluctuations

So Ueno^{1,2}, Wataru Ohnishi¹ and Takafumi Koseki¹

I. RESEARCH OVERVIEW

Demand for automated railroad operation is increasing due to the expected decrease in the number of railroad workers in the future caused by birthrate decrease shown in figure below. (Figure by the World Bank [1])



However, there are several factors that make automated operation of rail vehicles difficult. For example, tolerance of stop position error are limited by platform door as shown in figure.



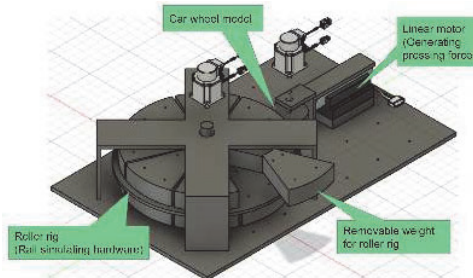
Hence, precise automatic operation control technology is required, but it is not easy to use actual railcars for the evaluation of technology.

Therefore, "roller rig devices," in which wheels are rotated on a disk that simulates rails to simulate the running of a vehicle, are used in research [2], and in addition to full-scale devices, scaled-down devices are also being used [3].

Since rolling stock runs repeatedly on the same track, it is expected that learning control that takes into account variations in the maximum adhesion force between the wheels and rails due to running conditions will be useful. However, there is no research on high-speed simulation of adhesion force fluctuations in actual railroads.

Proposal for roller rig system simulating high-speed friction fluctuations [4]

A 1/10 scale roller rig device was fabricated, featuring a linear motor thrust to control the pressing force between the wheel and the roller rig, which can simulate the variation of maximum adhesion force quickly.



Measurement of adhesion by a scaled roller rig [5].

We measured the adhesion characteristics of the manufactured roller rig system using methods described in next page.



¹ Koseki Ohnishi Laboratory, The University of Tokyo
² Corresponding e-mail: s.ueno@ctl.t.u-tokyo.ac.jp

II. SEMINAR TOPIC - ROLLER RIG SYSTEM ADHESION CHARACTERISTICS MEASUREMENT

A. Necessity of adhesion characteristics measurement

A 1/10 scale roller rig device featuring a linear motor to control the pressing force between the wheel and the roller rig to simulate the fluctuations in adhesion at high speed.

In order to verify that this device successfully simulates the basic adhesion characteristics of a real railway vehicle, it is necessary to measure the relationship between the "slip speed", which corresponds to the difference between the wheel speed and body speed of a real vehicle, and the "adhesion force between wheel and roller rig", which is the speed difference between the wheel and roller rig contact area.

B. Measurement of adhesion characteristics using disturbance observer

1) Measurement Procedure:

- 1) Determine the transfer function from the output torque of the roller rig and car wheel motor to the angle of rotation, respectively.
- 2) Build a disturbance observer to determine the adhesion force from the wheel rotation angle information.
- 3) Measure the relationship between slip speed and adhesive force by pressing the wheel and the track wheel together with a linear motor and then increasing the torque of the wheel motor in this state.
- 2) System identification of car wheel simulating parts: The transfer characteristic from the torque of the wheel motor to the angle of rotation of the wheel is assumed to be the sum of three shown below.

- 1) Pure integration (depending on inertia moment)
- 2) Viscous resistance torque proportional to rotational speed
- 3) Frictional resistance torque with a constant magnitude independent of rotational speed

Inertia moment is measured using chirp signal injected to car wheel motor torque command value.

Viscous and frictional resistance parameters are measured using car wheel motor torque command value under the condition car wheel is rotating in constant speed.

3) Constructing disturbance observer: Using parameters indicating characteristics of car wheel measured with methods above, disturbance observer for measuring adhesive force between car wheel and roller rig is constructed as shown in Fig.1.

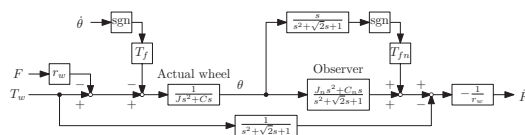


Fig. 1. Disturbance observer for measuring adhesion force \hat{F}

C. Results

In actual railcars, when the "slip speed," defined as the difference in speed between the car body and the wheel, is small, the adhesive force increases with the sliding speed, and when the sliding speed exceeds a certain level, the adhesive force begins to decrease. As shown in figure, the same characteristics were obtained in this experimental apparatus.

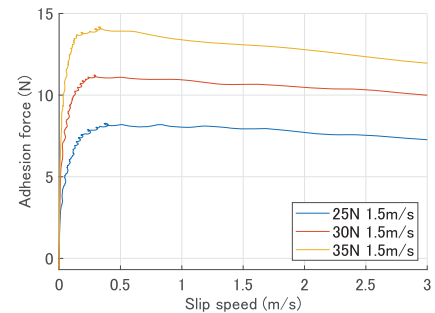


Fig. 2. Results of seminar topic.

III. CONCLUSIONS

The adhesion characteristics between the wheel and the roller rig of the experimental system have the same characteristics as those of a real vehicle.

REFERENCES

- [1] The World Bank, "Fertility rate, total (births per woman) - Japan, Netherlands," <https://data.worldbank.org/indicator/SP.DYN.TFR.TIN?end=2021&locations=JP-NL&start=1960&view=chart>.
- [2] Y. Yamanaga, "蛇行動限界速度評価の精度向上に向けた研究," *JSME Transportation & Logistics Newsletter*, no. 56, 2018.
- [3] T. MATSUDAIRA, "Nosing of 2-axle Railway Cars and its Prevention : 2nd Report, Model Experiment," *Transactions of the Japan Society of Mechanical Engineers*, vol. 19, no. 87, pp. 146–153, 1953.
- [4] S. Ueno, W. Ohnishi, and T. Koseki, "A proposal for a simulated running environment for railway vehicle control engineering tests using a scaled roller rig that simulates high-speed friction fluctuations," *Joint Technical Meeting on Transportation and Electric Railway/Linear Drives*, January 2023, TER-23-011 LD-23-011.
- [5] —, "Measurement of adhesion by a scaled roller rig device to emulate fast change of it for evaluating performance of railway traction control technology," *Joint Technical Meeting on Transportation and Electric Railway/Linear Drives*, May 2023, TER-23-049.



So Ueno received the MEng. degree from the University of Tokyo, in 2021. Currently, he is pursuing a Ph.D. degree at the department of electrical engineering at the University of Tokyo.

Direct Yaw Moment Control for Electric Vehicles Based on Adaptive Driving Force Control

Takumi Ueno¹, Binh-Minh Nguyen^{1,2} and Hiroshi Fujimoto^{1,3}

I. RESEARCH OVERVIEW

Electric vehicles are not only environmentally friendly in terms of transportation but also novel motion control systems, thanks to their fast and accurate torque generation capacity. In addition, in-wheel-motor vehicles can control each wheel independently. Due to this merit, direct yaw moment control (DYC) has been proposed to control the yaw-rate and improve the lateral stability. However, there is still an open issue with merging the DYC and traction control. Thus, this paper proposes new yaw moment control based on adaptive driving force control. Note that this paper is an abridged version of [1], and the details can be found there.

Topic 1 Vehicle Dynamics Model.

Fig. 1 shows the vehicle dynamics model. The lateral motion of the vehicle is described as

$$MV \left(\frac{d\beta}{dt} + \gamma \right) = 2(Y_f + Y_r + Y_d) \quad (1)$$

$$I\dot{\gamma} = N_z - N_t - N_d. \quad (2)$$

The rotational motion of each wheel is described as

$$J_{ij}\dot{\omega}_{ij} = T_{ij} - r_{ij}F_{dij}. \quad (3)$$

When the vehicle accelerates or decelerates, the wheel velocity $V\omega = r\omega$ differs from the vehicle velocity V because of the tire's elastic deformation. The slip ratio λ is defined as

$$\lambda_{ij} = \frac{V\omega_{ij} - V}{\max(V\omega_{ij}, V, \epsilon)}. \quad (4)$$

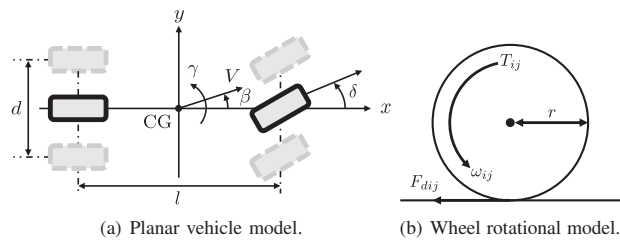


Fig. 1. Vehicle model.

This work was partly supported by Industrial Technology Research Grant Program from New Energy and Industrial Technology Development Organization (NEDO) of Japan (number 05A48701d), the Ministry of Education, Culture, Sports, Science and Technology grant (number 22246057 and 26249061).

^{1,2,3} The authors are with the University of Tokyo, Japan, corresponding e-mail: ueno.takumi22@ae.k.u-tokyo.ac.jp.

Topic 2 Yaw Moment Control.

Fig. 2 shows the block diagram of yaw-rate controller [2]. The yaw-rate reference can be calculated as

$$\gamma^* = \frac{1}{1+AV^2} \frac{V}{l} \delta. \quad (5)$$

To improve the robustness of the yaw-rate control under the uncertainty of road conditions and the unknown disturbances, the yaw moment observer is utilized. Through the YRC, in case the vehicle is a rear-drive system, the force distribution law (FDL) is designed as

$$\begin{bmatrix} F_{dRR}^* \\ F_{dRL}^* \end{bmatrix} = \begin{bmatrix} 1/2 & 1/d \\ 1/2 & -1/d \end{bmatrix} \begin{bmatrix} F_{dall}^* \\ N_z^* \end{bmatrix}. \quad (6)$$

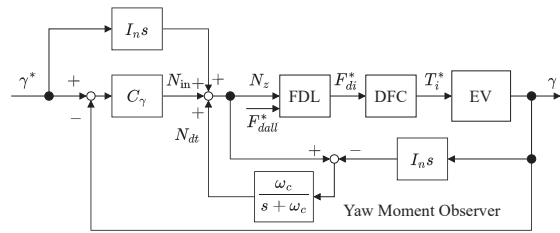


Fig. 2. Block diagram of the YRC.

Topic 3 Driving Force Control.

Fig. 3 shows the block diagram of the driving force controller (DFC) [3]. The DFC has a cascade configuration, including an integral force controller and a proportional-integral wheel speed controller. The driving force is feedbacked thanks to the driving force observer, which utilizes the motor torque and the angular velocity of the wheel.

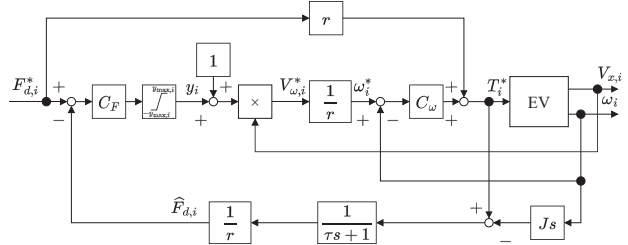


Fig. 3. Block diagram of the DFC.

II. SEMINAR TOPIC - DESIGN OF THE VARIABLE-RATE-SLIP-RATIO-LIMITER: APPLIED TO DFC

A. Problem Formulation

The slip ratio limiter in DFC is used to prevent excessive tire slippage. The conventional DFC uses the limiter as a constant value. However, the situation is quite different when the vehicle turns. The driving force F_d is limited by the vertical force. Due to the load transfer, the vertical forces of the left and right sides change with the situation. Therefore, the optimal driving force also changes in real-time. Consequently, the limited value of the slip ratio would be adaptively calculated in real-time to optimize the yaw moment generation capability of the vehicle.

B. Approach

In the situation that the wheels slip and slip ratio reaches the limited value, the driving forces of the rear left and rear right wheels are expressed as

$$F_{di} = \lambda_{limi} D_{si} \quad (7)$$

(8)

Let k be the rate between the left and right limiters, and it can be given as

$$k(t) = \frac{\lambda_{limR}}{\lambda_{limL}}. \quad (9)$$

In this study, assuming that the road conditions are the same between both wheels, the driving stiffness of both wheels is treated as $D_{sL} = D_{sR}$. Thus, a various-rate-slip-ratio-limiter $k(t)$ can be updated in real-time as

$$k(t) = \begin{cases} 1 + \frac{2N_z^*}{d\hat{F}_{dRL}} & (V \geq V_t) \\ 1 & (V < V_t) \end{cases}, \quad (10)$$

where N_z^* is given by the outer-layer, and \hat{F}_{dRL} is given by the DFO.

C. Experiment

a) *Experimental Setup:* The FPEV2-Kanon, which was developed by our research group, is used as an experimental vehicle. We use the vehicle as a rear-drive system. The vehicle runs straight at the speed of 10 km/h and makes a tip-in accelerated turn from 1 s. Under this condition, three

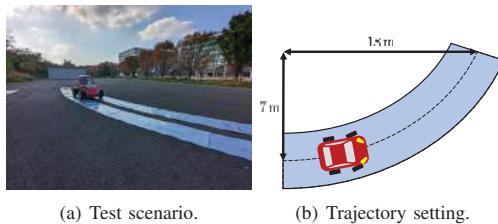


Fig. 4. Experimental setup.

test cases are conducted as follows.

- Case-1: The vehicle is handled by the driver (Without DYC).
- Case-2: The vehicle is controlled by the DYC that utilizes the DFC with a fixed-slip-ratio-limiter.
- Case-3: The vehicle is controlled by the proposed DYC.

In Case-2, λ_{lim} of both wheels are set as 0.06. On the other hand, in Case-3, λ_{limL} is set as 0.06 and λ_{limR} is set as $k(t) \times 0.06$.

b) *Experimental Result:* Fig. 5 shows the experimental result. To evaluate the effectiveness of the proposed system, the root mean square deviation (RMSD) of the yaw-rate control errors is calculated from 1 to 5 s. In comparison with Case-1, Case-2 can reduce the tracking error by 23.8 %. Remarkably, the tracking error can be reduced by about 86.5 % by Case-3.

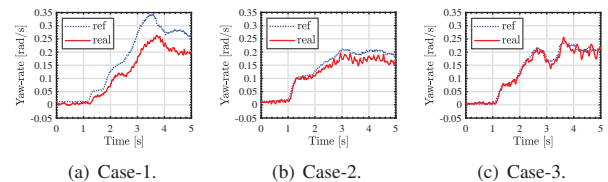


Fig. 5. Experimental result.

TABLE I
RMSD OF YAW-RATE.

Method	RMSD of yaw-rate rad/s	Rate of decrease %
Case 1	7.97×10^{-4}	0
Case 2	6.07×10^{-4}	23.8
Case 3	1.07×10^{-4}	86.5

III. CONCLUSION

In this paper, the DYC system based on adaptive driving force control is proposed. The boundary of the slip ratio limiter is updated in real-time by utilizing the yaw moment command and the estimated driving force. The experimental results show that the proposed method can operate effectively even when cornering with acceleration on the low friction surface. In the future, we will develop separate limiters for both the left and right wheels and consider the split- μ scenario.

REFERENCES

- [1] T. Ueno, B.-M. Nguyen, and H. Fujimoto, "Direct yaw moment control for electric vehicles with variable-rate-slip-ratio-limiter based driving force control," in *2023 IEEE International Conference on Mechatronics (ICM)*. IEEE, 2023, pp. 1–6.
- [2] H. Fujimoto, T. Saito, and T. Noguchi, "Motion stabilization control of electric vehicle under snowy conditions based on yaw-moment observer," in *The 8th IEEE International Workshop on Advanced Motion Control, 2004. AMC'04*. IEEE, 2004, pp. 35–40.
- [3] M. Yoshimura and H. Fujimoto, "Driving torque control method for electric vehicle with in-wheel motors," *Electrical Engineering in Japan*, vol. 181, no. 3, pp. 49–58, 2012.

Next-Generation Opto-mechatronic systems: control for free-space optical communication

G. Witvoet^{1,2}, M. van Dael¹, R. Geraldes^{1,3}, M. van Meer¹, N. Mooren^{1,4}, P. Tacx¹ and T. Oomen^{1,5}

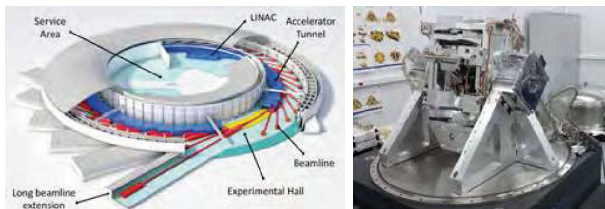
I. RESEARCH OVERVIEW

Opto-mechatronics is a multidisciplinary field of expertise in which physics and engineering come together to create novel instruments and systems. Nowadays, opto-mechatronic instruments can be found in many semiconductor, astronomy or space applications, and it is gaining popularity both in research and industry; both in high- and low-tech domains.

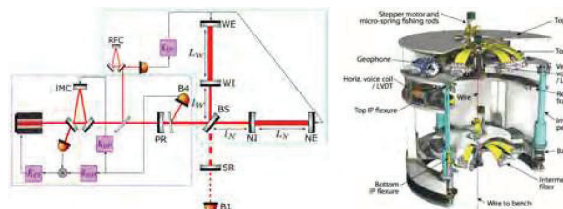
In our research we focus on two different trends that we recognize in recent developments in opto-mechatronics. As discussed next, these trends are partly motivated by the domain in which opto-mechatronics is employed.

Novel complex concepts and systems

In many scientific applications there is a trend towards novel and more complex opto-mechatronics concepts, with larger complexity in e.g. the optical and mechanical designs.



One example is our work on systematic design philosophies for a High-Dynamic Double-Crystal Monochromator for the Sirius synchrotron [1], in which, among others, dynamic error budgeting techniques have been employed to design and create an opto-mechatronic machine concept with unsurpassed accuracy and scanning possibilities.



¹ The authors are with the Control Systems Technology research section of the Eindhoven University of Technology, the Netherlands; corresponding e-mail: g.witvoet@tue.nl.

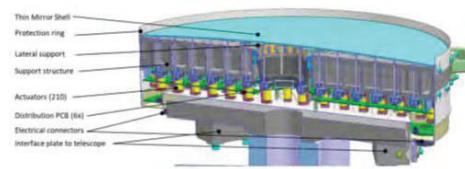
² Also with the Optomechatronics dept. at TNO, Delft, the Netherlands.

³ Also with Brazilian Synchrotron Light Laboratory, Campinas, Brazil.

⁴ Currently with Sioux, Eindhoven, the Netherlands.

⁵ Also with the Delft Center for Systems and Control, Delft University of Technology, the Netherlands.

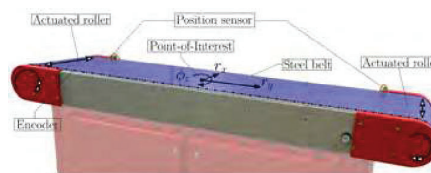
Controller design for such systems is not straightforward, e.g. due to their multi-variability and non-linearities. In our work for the Virgo gravitational wave detector [2] we offer systematic controller design procedures, which have delivered improved performance on the sensitivity of the detector.



Multi-variability comes to an extreme in Adaptive Optics (AO), which utilizes deformable mirrors (DMs) with hundreds of actuators. Our work on DMs [3] focuses on the dynamic identification and systematic control synthesis of such massive-MIMO systems.

Maintaining performance with lower costs

In industrial applications we see a cost-reduction trend, in which opto-mechatronic products need to be built with cheaper, less-performing components, while system performance needs to be maintained.



Our work on a substrate carrier led to novel Gaussian Process (GP) repetitive control approaches [4] to compensate for imbalances introduced by non-perfect mechanics.



This technique has also been employed to improve communication of Coarse Pointing Assemblies (CPAs), while GPs have also been successfully applied in calibration of test benches [5] meant for mass production of such CPAs.

II. SEMINAR TOPIC - Free-space optical communication

In free-space optical communication (FSOC) both opto-mechatronic trends come together, especially in the space domain, where optical links need to be established between terminals hundreds (e.g. for LEO-to-ground) or ten thousands (e.g. for GEO-to-ground) of kilometers apart, using laser beams with divergences of only 10 to 100 μrad . For successful fast data transfer between such terminals, absolute laser pointing accuracies of just a few μrad need to be achieved, even in the presence of vibrations and atmospheric turbulence. This introduces challenges both in the opto-mechatronic concept itself, as well as on the control design.

A. FSOC developments at TNO

Space-relevant FSOC is still heavily under development by many parties world-wide; Netherlands Organization for Applied Scientific Research (TNO) is contributing to these developments by designing, realizing and testing various prototype FSOC terminals for different use cases. This includes both ground stations, as well as space- and airborne terminals.

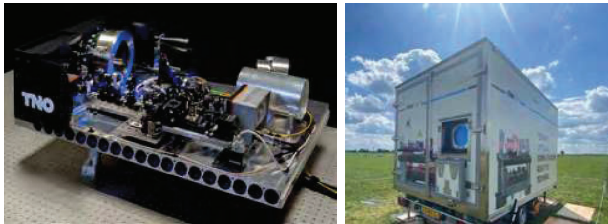


Fig. 1. The TOnCAT optical bench (left) and test trailer (right).

One of the demonstrator ground stations is TOnCAT, shown in Fig. 1, which is the outcome of a feasibility study for terabits/second feederlinks, by utilizing both AO for high-order compensation of atmospheric turbulence, and multiplexing multiple beams of different wavelength. This technology has been demonstrated in an actual field test over 10 km, during which TOnCAT was built into a portable trailer.



Fig. 2. Ultra-Air (left) and LEOCAT (right) demonstrator terminals.

Flight hardware comes with different challenges. For example, for the airborne Ultra-Air terminal (Fig. 2, left) vibrations from the airplane it is installed in form a huge challenge to meet the extreme pointing requirements to be able to communicate with a GEO satellite 36 000 km away. For spaceborne terminals, such as LEOCAT (Fig. 2, right), designed for

data relay between LEO satellites), the tight volume, mass and cost constraints are often the most important design drivers.

B. The CubeCAT DTE terminal

In this seminar talk we will discuss some technical details of another space-borne terminal, called CubeCAT, shown in Fig. 3. CubeCAT is a direct-to-earth (DTE) terminal designed for commercial cubesats and fits all its functionality in just $10 \times 10 \times 10 \text{ cm}$, i.e. not only the complete optical head, but also the laser, and all electronics.

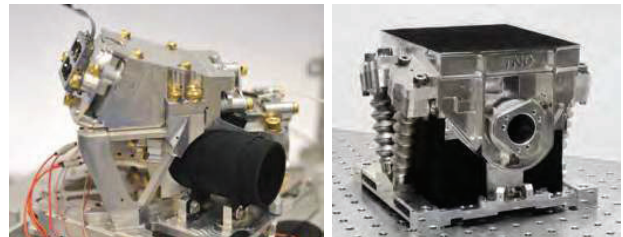


Fig. 3. The CubeCAT optical head (left) and final state before launch (right).

CubeCAT measures the angle of the incoming beacon light via a sensitive quadrant detector, and uses that information in real-time to control a Fine Steering Mirror (FSM), such that the transmitted data laser is perfectly aligned with the incoming beacon, and is thus properly pointed to the ground station. CubeCAT has been launched into orbit in April 2023, and is currently being commissioned. In this talk the opto-mechatronic design of CubeCAT will be discussed, as well as the feedback control trade-offs and verification tests.

REFERENCES

- [1] R. Geraldes, M. Moraes, G. Witvoet, and H. Vermeulen, "Predictive modeling through dynamic error budgeting applied to the High-Dynamic Double-Crystal Monochromator for Sirius light source," *Precision Engineering*, vol. 77, pp. 90–103, 2022.
- [2] M. van Dael, J. Casanueva Diaz, G. Witvoet, B. Swinkels, M. Pinto, D. Bersanetti, M. Mantovani, C. de Rossi, P. Spinicelli, and T. Oomen, "Integrating H_2 synthesis and dynamic error budgeting for improved gravitational wave detection," in *IFAC 22nd Triennial World Congress*, Yokohama, Japan, 2023.
- [3] P. Tacx, M. Teurlings, R. Habraken, G. Witvoet, M. Heertjes, and T. Oomen, "Spatio-temporal analysis of overactuated motion systems: A mechanical modeling approach," in *IFAC 22nd Triennial World Congress*, Yokohama, Japan, 2023.
- [4] N. Mooren, G. Witvoet, and T. Oomen, "Gaussian process repetitive control: beyond periodic internal models through kernels," *Automatica*, vol. 140, p. 110273, 2022.
- [5] M. van Meer, E. Deniz, G. Witvoet, and T. Oomen, "Cascaded calibration of mechatronic systems via Bayesian inference," in *IFAC 22nd Triennial World Congress*, Yokohama, Japan, 2023.



Gert Witvoet is a senior dynamics and control specialist at the Netherlands Organisation for Applied Scientific Research (TNO), Delft, The Netherlands, and a part-time associate professor with the Mechanical Engineering department at the Eindhoven University of Technology. His research interests are in the application of advanced motion and learning control techniques on high-tech instruments and equipment, with applications in the semiconductor, astronomy, and space markets.

Control Scheme of RRO Compensation for Track Mis-registration in HDDs

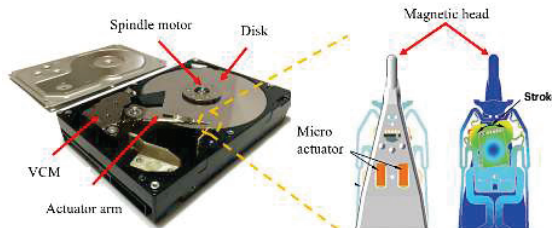
Shota Yabui¹, Takenori Atsumi² and Atushi Okuyama³

I. RESEARCH OVERVIEW

Hard disk drives (HDDs) which can store of large amount of digital data are supporting information society. To read/write the digital data on the disk, the magnetic head must be controlled precisely. The data is recorded as concentric orbits called as tracks on the disk. In the controller design, servo engineer must evaluate track mis-registration (TMR) for the reliability [1]. The TMR is one of criteria of relative positioning accuracy for the tracks for risk assessment of data incorrectly writing. The risk means that the magnetic heads write on the different track from the target track. The relative positioning accuracy in the tracks should be improved to decrease the risk.

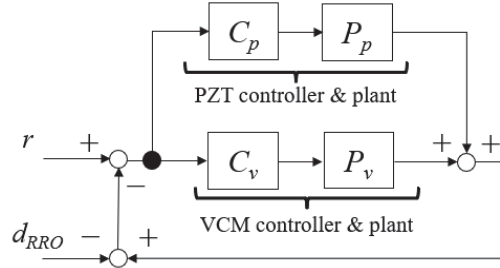
Head positioning system of HDDs

To read/write digital data on disks, the HDDs has a positioning system to control magnetic heads. The magnetic head positioning control system using the dual-stage actuator system is shown below figure. The dual-stage actuator system uses two actuators, a voice coil motor (VCM) and a micro-actuator. Coarse movement is controlled by the VCM attached to the base of the actuator arm, and fine movement is controlled by the micro-actuator attached to the tip [2].



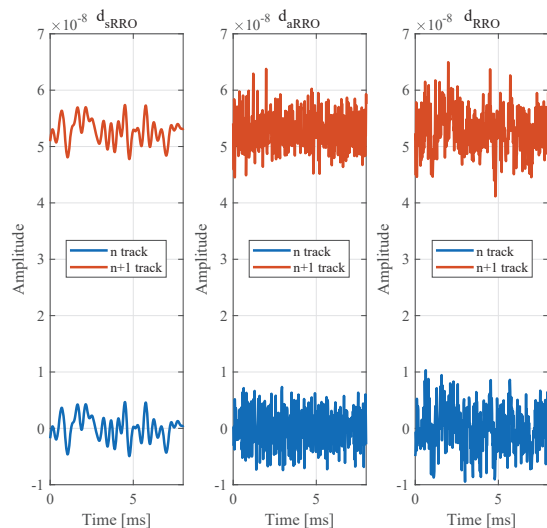
Block diagram of the head positioning control system

The block of the dual-stage control system is shown in the below figure. Where, P_v is the control object of the VCM side, P_p is the control object of the micro-actuator side, and C_v is the control for the VCM, C_p is the controller for the micro-actuator. d_{RRO} is RRO which is distort the reference signal r .



The characteristic of RRO

d_{RRO} is assumed to consist of the synchronous RRO and asynchronous RRO. The synchronous RRO d_{sRRO} is mainly caused by unbalanced force or harmonic vibrations of the rotating disk. Shapes of the vibrations are dependent on the disk location, that is, trajectories of the vibration are similar between the tracks. The asynchronous RRO d_{aRRO} is mainly caused by noise or mechanical vibration. These are random vibrations, that is, the trajectories are no regularity between the tracks. Time responses on the circumference of d_{sRRO} , d_{aRRO} , and $d_{RRO} = d_{sRRO} + d_{aRRO}$ in number n and $n+1$ tracks are shown in below figure. The reference signal is $r = 0$ for n track, and $r = 52.7 \times 10^{-9}$ for $n+1$ track (52.7nm is inter-track distance in 482000TPI).



¹ First author is with Tokyo City University, Japan, corresponding e-mail: yabuis@tcu.ac.jp.

² Author Two is with Chiba Institute of Technology.

³ Author Three is with Tokai University.

II. SEMINAR TOPIC - *Relative positioning accuracy in the head positioning control system of HDDs*

The TMR indicates statistical data for the evaluation of relative positioning accuracy for the tracks. It estimates a risk that the magnetic heads accidentally write on the different track of the target track, namely destroying the original data. In this study, we propose a control scheme in the head positioning control system for RRO compensation for the TMR.

A. A Problem formulation

To evaluate the relative positioning accuracy, the control system is following for the reference r distorted by the RRO d_{RRO} of nine tracks from n to $n+8$ in this simulation. After that, we evaluate the closest distance of the head position y_c . The time responses of the d_{RRO} are shown in Fig.1.

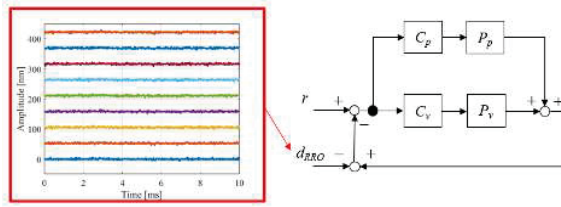


Fig. 1. Simulation model in this study.

B. B Proposed control system

The proposed control system is shown in Fig.2. We employ the adaptive feedforward cancellation (AFC) which can compensate for the RRO adequately.

$$u_{i,j}(k) = p_{i,j}(k) \cos(\omega_{i,j}Tk) + q_{i,j}(k) \sin(\omega_{i,j}Tk) \quad (1)$$

$$p_{i,j}(k) = p_{i,j}(k-1) + \lambda_{i,j}e(k) \cos(\omega_{i,j}Tk + \theta_{i,j}) \quad (2)$$

$$q_{i,j}(k) = q_{i,j}(k-1) + \lambda_{i,j}e(k) \sin(\omega_{i,j}Tk + \theta_{i,j}) \quad (3)$$

Here, $p_{i,j}$ and $q_{i,j}$ are the adaptive parameters, $\lambda_{i,j}$ is the step size parameter, and $\theta_{i,j}$ is the phase parameter (subscript i for d_{sRRO} , subscript j for d_{aRRO}). $p_{i,j}$ and $q_{i,j}$ are updated by the recurrence formula as equations (2) and (3).

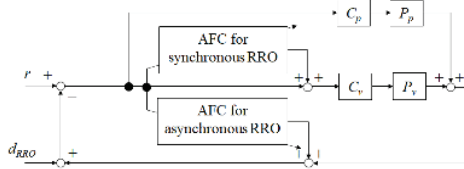


Fig. 2. Simulation model in this study.

Although the original algorithm as shown in equations (1) - (3) are recurrence formula, the formula can be transformed to a transfer function [3]. Based on the transfer function model, the frequency responses of open loops are shown in Fig.3. The gain of open is increased at the harmonic frequency of d_{sRRO} . AFCs works to follow strongly for the distorted reference including d_{sRRO} . The gain of open is decreased

at the harmonic frequency of d_{aRRO} . AFCs works to remove the influence of d_{aRRO} for the control system.

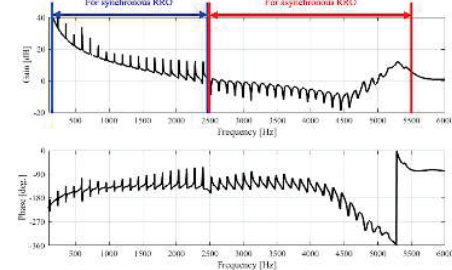


Fig. 3. Frequency response of the open loop

C. Subsection C

For comparison study, we simulate the three cases of the control system: all-tracking system (conventional method) [3], proposed control system. Figure 4 indicates the time responses of y_c close up $n+6$ track and $n+7$ track in the range from 1.4ms to 1.6ms. The relative position around 1.5ms in three cases, the case of the all-tracking system is 34.5 nm, the case of the proposed control system is 52.5 nm. The proposed control system can improve the relative positioning accuracy.

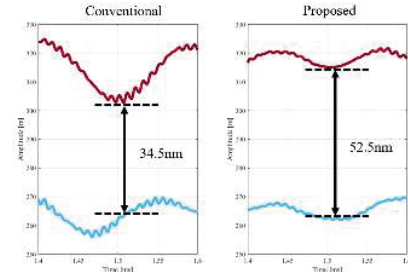


Fig. 4. Simulation result in critical point

REFERENCES

- [1] Maman, A., Guo, G., and Bi, C. (2007). Hard Disk Drive Mechatronics and Control. CRC Press
- [2] HGST, "TECH BRIEF: HGST Micro Actuator," TB02-HGST-Micro-Actuator-EN-US-0917-02, 2017 URL: <https://www.westerndigital.com/> (accessed May 31, 2023).
- [3] S. Yabui, A. Okuyama, M. Kobayashi, and T. Atsumi Optimization of adaptive feedforward repeatable run-out cancellation for positioning control system of hard disk drives, *Microsystem Technologies*, Vol. 18, No. 9-10, 2012, pp.1703-1709.

Shota Yabui received the B.S. and M.S. degree in electrical engineering from Mie University, Tsu, Japan, in 2007 and 2009, respectively, and the Ph.D. degrees in mechanical engineering from Hokkaido University, Sapporo, Japan, in 2014. From 2009 to 2015, he has worked for Hitachi Ltd. and HGST Japan. At 2016, he has worked for Mitsubishi Space Software Co.,Ltd. Since 2021, he has been associate professor with the Mechanical Systems Engineering, Faculty of Science and Engineering, Tokyo city university.. His research interests include adaptive feed-forward control technologies, integrated design method of control and mechanics and analysis of rotor dynamics.



A survey of robust controller design for stage positioning with ball screw feed drive system

Shogo Yamada¹ and Hiroshi Fujimoto¹

I. RESEARCH OVERVIEW

Ball screw feed drive system is a mechanism that converts the rotational motion of a motor into the translational motion with a ball screw and nut, and it is widely used in micron scale positioning or motion trajectory control [1] [2].

As shown in the figure below, the ball screw drive consists of a screw supported by thrust bearings at both ends and a nut with recirculating balls [1].

Ball screw feed drive system is characterized by high efficiency, low friction, low heating, low sensitivity to external forces and inertia changes and high service life. Therefore, ball screw feed drives are widely used in various fields such as machine tools, semiconductor manufacturing equipment, aerospace equipment, vehicles, various elevating mechanisms, textile machinery and some other equipment [1] [2].

As important drives and transmission element, ball screw drives need to be faster with high tracking accuracy [2]. One of the challenges to improve tracking performance of ball screw feed drives is parameter variation.



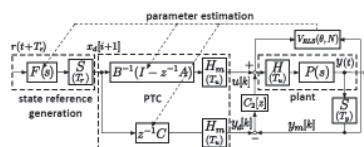
Topic 1 Adaptive vibration suppression perfect tracking control

In our laboratory, an adaptive perfect tracking control (AVSPTC) method for system with time-varying modes was proposed [3].

This study focuses on the changes of the workpiece mass and table position. AVSPTC is a method which combines the recursive least squares algorithm with multirate feedforward.

The block diagram is shown in the figure below.

However, this study has not been able to verify the online estimation against load mass variation in actual machine experiments.



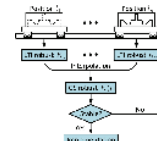
¹ The authors are with the University of Tokyo, 5-1-5, Kashiwanoha, Kashiwa, Chiba, 277-8561, Japan

Topic 2 My research topic

I surveyed research on Gain-scheduling robust control which takes into account both the workpiece mass changes and table position-dependent dynamics [4], and research on robustness of Final-state control [5].

The proposed control strategy in [4] is illustrated below. This method would be a good comparative candidate for my research.

As for my future research, I would like to take over [3], and design perfect tracking controller which have robustness, and implement it on actual equipment. I am wondering if I can incorporate the method which is used in [5].



REFERENCES

- [1] Y. Altintas, A. Verl, C. Brecher, L. Uriarte, and G. Pritschow, "Machine tool feed drives," *CIRP Annals*, vol. 60, no. 2, pp. 779–796, 2011.
- [2] T. Huang, Y. Kang, S. Du, Q. Zhang, Z. Luo, Q. Tang, and K. Yang, "A survey of modeling and control in ball screw feed-drive system," *The International Journal of Advanced Manufacturing Technology*, vol. 121, no. 5-6, pp. 2923–2946, 2022.
- [3] T. Beauquin, H. Fujimoto, and Y. Terada, "Adaptive vibration suppression perfect tracking control for linear time-varying systems with application to ball-screw feed drives," in *2016 IEEE 14th International Workshop on Advanced Motion Control (AMC)*, 2016, pp. 245–250.
- [4] T. Zhong, R. Nagamune, D. Bao, and W. Tang, "Gain-scheduling robust control with guaranteed stability for ball screw drives with uncertain load mass and varying resonant modes," *Precision Engineering*, vol. 80, pp. 198–207, 2023.
- [5] M. Hirata and K. Nonami, "Seek control of hard disk drives based on final-state control - a study for the robustness -," *IJC*, vol. 2, no. 91, pp. 35–40, 2002.



Corresponding Author is pursuing a bachelor's degree at the department of electrical and electronic engineering at the University of Tokyo.

Identification and Motion Control for a Maglev Linear Synchronous Motor

Yueying Yang¹, Wataru Ohnishi¹ and Takafumi Koseki¹

I. RESEARCH INTRODUCTION

The rapid development of technology and industrial manufacturing has created a growing demand for super-high-speed, high-precision, and dust-free precision devices. Thanks to their frictionless advantages and unique operational direction, Maglev linear motors have emerged as an up-and-coming solution for conveyors in these industries. Our research group has successfully developed an Iron-core Transverse Flux Permanent Magnet Linear Synchronous Motor(TF-PMLSM), incorporating attractive EMS technology. This design ensures high thrust density and substantial load capacity [1], [2]. However, this design also presents challenges as it amplifies the system's inherent instability due to the attractive forces between the permanent magnets and the core. Therefore, this research focuses on designing a robust controller for the maglev system to enhance disturbance rejection performance and overall robustness.

II. RESEARCH TOPICS

The structure and dynamic modeling for TF-PMLSM [2]

The 3D model of the TF-PMLSM is shown in Fig.1a. The propulsion system consists of nine C-shaped armature cores at each side that embed the permanent magnet. The mover can be driven in the x -direction by applying three phase current into the armature coils. The levitation system consists of two E-shaped electromagnets. We can actively control three degrees of freedom, heave z , pitch θ_y , and roll θ_x by the DC in the levitation coils.

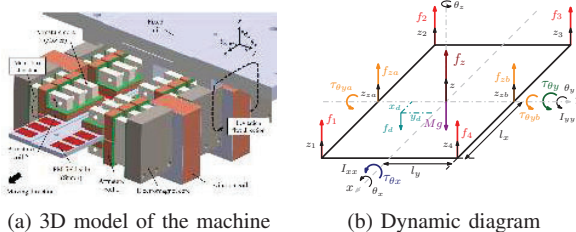


Fig. 1: The structure of TF-PMLSM

We simplify the complex coupled system into a single-input, single-output(SISO) system. This approach allows us to derive an approximate linear model of the levitation system through a series of steps, including the building magnetic circuit model

¹ The authors are with the Department of Electrical Engineering and Information Systems Graduate School of Engineering, The University of Tokyo, Japan, corresponding e-mail: y.yang@ctl.t.u-tokyo.ac.jp .

of the E-type electromagnet, coordinate transformation, and linearization.

$$\begin{cases} g_z(s) = \frac{\Delta z(s)}{\Delta i_z(s)} = \frac{k_{izz}}{Ms^2 - (k_{zz} + k_{zp})} \\ g_{\theta_y}(s) = \frac{\Delta \theta_y(s)}{\Delta i_{\theta_y}(s)} = \frac{k_{iyy}}{I_{yy}s^2 - (k_{yy} + k_{yp})} \\ g_{\theta_x}(s) = \frac{\Delta \theta_x(s)}{\Delta i_{\theta_x}(s)} = \frac{k_{ixx}}{I_{xx}s^2 - (k_{xx} + k_{xp})} \end{cases} \quad (1)$$

Feedback Control Design for a 3-DOF Magnetic Levitation System based on I-PD Closed-Loop System Identification [3]

For three independent models in (1). We employed the I-PD feedback controllers as the position control strategy. By repeatedly tuning the parameters of the controller, we achieve a stable levitation of the system. In addition, we conducted identification experiments of the frequency domain using Chirp-Sine signals for the maglev system to modify the mathematical model.

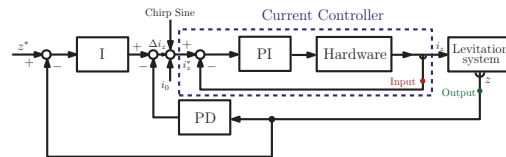


Fig. 2: I-PD feedback control strategy

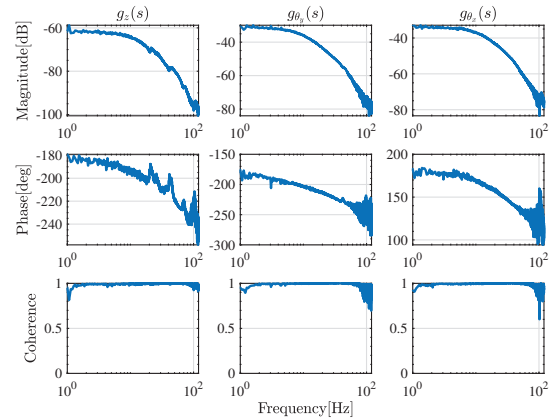


Fig. 3: Three SISO Frequency Response Functions of Eq (1)

The frequency response functions of three degrees of freedom obtained by the system identification experiments are shown in Fig. 3. And with this nominal model, we redesigned

the parameters of the I-PD controller to improve the levitation performance with the open-loop Nyquist plots and sensitivity functions.

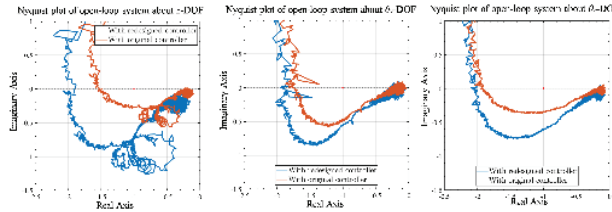


Fig. 4: Open-loop Nyquist plots with different controllers

Proposal for Estimation of the Vertical Center of Gravity and the Decoupling Control with thrust and pitch 2-DoF [4]

For linear motors with large thrust density, if there is a shift of the center of gravity in the vertical direction, the stability performance of the maglev system may be deleteriously affected by the thrust. This not only restricts the load capacity but also significantly impacts the control precision. Therefore, this topic will aim to estimate the vertical center of gravity using the recursive least squares method and eliminate the coupling between thrust and pitch by designing a pre-compensator.

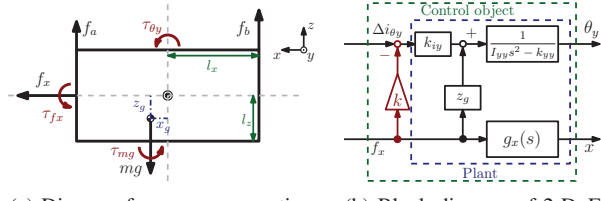


Fig. 5: Diagram of estimation \hat{z} and decoupled control

After adding the propulsion system, the free body diagram for 2-DoF in the x - y cross-section is shown in Fig.5a, which is the side view of Fig.1a. $\tau_{\theta y}$ is the torque generated by attractive levitation force in θ_y direction. f_x is the thrust produced by the propulsion system. Because the change of the vertical center gravity z_g , f_x produces a torque on θ_y DoF, which is τ_{fx} . The dynamic equations of the system in the x and θ_y directions with the expression of z_g are as follows.

$$\begin{cases} I_{yy}\ddot{\theta}_y = \tau_{\theta y} + \tau_{fx} + \tau_{mg} + \tau_{py} \\ m\ddot{x} = f_x \end{cases} \quad (2)$$

$$\Rightarrow f_x z_g = I_{yy}\ddot{\theta}_y - \tau_{\theta y} - \tau_{mg} - \tau_{py}$$

Without considering the case of x_g , we could derive the linear magnetic torque $\tau_{\theta y}$ as (3). When bringing (3) into dynamic functions (2), we can deduce the new expression about the direction of θ_y as (4). Finally, the coupling influence between the x and the θ_y DoF could be suppressed by inserting a pre-compensator as in Fig. 5b.

$$\tau_{\theta y} = k_{yy}\theta_y + (k_{iy} + k_{yp})i_{\theta y} \quad (3)$$

$$\begin{aligned} \Delta\theta_y(s) &= \frac{k_{iy}\Delta i_{\theta y}(s) + z_g f_x(s)}{I_{yy}s^2 - (k_{yy} + k_{yp})} \\ &= g_{\theta y}(s)\Delta i_{\theta y}(s) + g_{x\theta y}(s)f_x(s) \end{aligned} \quad (4)$$

Finally, we verify the proposal of the vertical center of gravity estimation and the decoupling control by simulation as follows. The results contain the different cases with and without the pre-compensator. The first half of the experiment, $t \in [0, 0.9]$, focused on the situation where the vertical center of gravity changes. In contrast, the second part, $t \in [0.9, 1.5]$, checked the situation of varying thrust. Compared to the case without the pre-compensator, both the estimation of \hat{z}_g and the state of the θ_y DoF showed noticeable improvements.

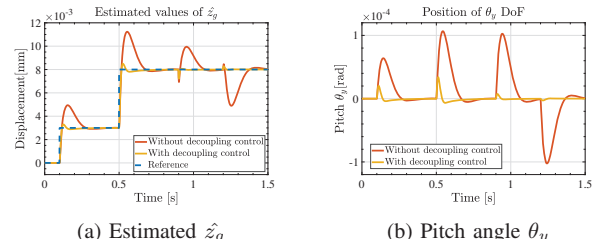


Fig. 6: Estimation and decoupling results verification

III. FUTURE WORKS

In the future, our next steps involve conducting physical experiments to verify the impact of the vertical center of gravity specification and decoupling control. Additionally, we will explore the coupling relationship between the three degrees of freedom: z , θ_y , and θ_x , within the maglev system. Our aim is to design an optimal MIMO control system to realize better stability performance.

REFERENCES

- [1] S. Ahmed, C. Grabher, H. J. Kim, and T. Koseki, "Multifidelity surrogate assisted rapid design of transverse-flux permanent magnet linear synchronous motor," *IEEE Transactions on Industrial Electronics*, vol. 67, pp. 7280–7289, 9 2020.
- [2] S. Ahmed, T. Koseki, and H. Kim, "Proposal of a compact magnetically levitated transverse flux permanent magnet linear synchronous motor as a 6-dof transport carrier," *The Journal of Engineering*, vol. 2019, pp. 4420–4425, 6 2019.
- [3] Y. Yang, W. Ohnishi, and T. Koseki, "Feedback control design for a 3-dof magnetic levitation system based on i-pd closed-loop system identification," *IEEJ, Joint Technical Meeting on Transportation and Electric Railway/Linear Drives*, pp. 83–88, 2023.
- [4] ———, "Proposal for estimation of the vertical center of gravity and the decoupling control with 2-dof for a maglev linear conveyor," *The 14th International Symposium on Linear Drivers for Industry Applications (LDIA)*, 2023.



Yueying Yang received the B.Sc degree in Electrical Engineering from Jiangsu University, China, in 2021. Now, he is pursuing an M.Sc degree at the Department of Electrical Engineering and Information Systems Graduate School of Engineering, The University of Tokyo, Japan.

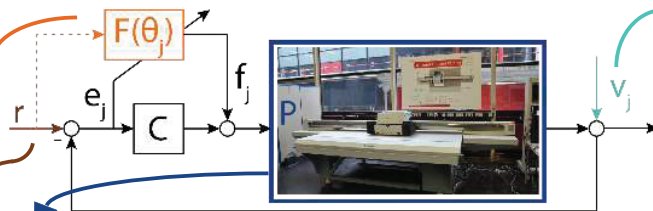
Part II

Submitted Posters

(Machine) learning for feedforward in precision mechatronics

Leontine Aarnoudse¹ and Tom Oomen^{1,2}¹Eindhoven University of Technology, Eindhoven, The Netherlands,²Delft University of Technology, Delft, The Netherlands

l.i.m.aarnoudse@tue.nl



What if P is MIMO and unknown?
use randomized learning to efficiently learn feedforward parameters

- 1) Measure e_j for $f_j(r, \theta_j) = \psi(r)^T \theta_j$
- 2) Use 1 experiment to obtain an unbiased gradient estimate:

$$\begin{bmatrix} e_j^1 \\ e_j^2 \\ \vdots \\ e_j^{n_o} \end{bmatrix} \xrightarrow{T^{n_o}} \begin{bmatrix} 0 & \cdots & 1 \\ 1 & \cdots & 0 \\ \vdots & \ddots & \vdots \\ 0 & \cdots & 0 \end{bmatrix} \xrightarrow{C} \begin{bmatrix} a_j^{11} & \cdots & 0 \\ 0 & \cdots & a_j^{11} \\ \vdots & \ddots & \vdots \\ 0 & \cdots & a_j^{1n_o} \end{bmatrix} \cdots \begin{bmatrix} a_j^{1n_o} & \cdots & 0 \\ 0 & \cdots & a_j^{1n_o} \\ \vdots & \ddots & \vdots \\ 0 & \cdots & a_j^{1n_o} \end{bmatrix} \xrightarrow{P} \begin{bmatrix} a_j^{n_o 1} & \cdots & 0 \\ 0 & \cdots & a_j^{n_o 1} \\ \vdots & \ddots & \vdots \\ 0 & \cdots & a_j^{n_o n_o} \end{bmatrix} \cdots \begin{bmatrix} a_j^{n_o n_o} & \cdots & 0 \\ 0 & \cdots & a_j^{n_o n_o} \\ \vdots & \ddots & \vdots \\ 0 & \cdots & a_j^{n_o n_o} \end{bmatrix} \xrightarrow{A_j} \begin{bmatrix} T^{n_i} \\ \vdots \\ T^{n_i} \end{bmatrix} \xrightarrow{-2\psi(r)} \hat{g}(\theta_j)$$

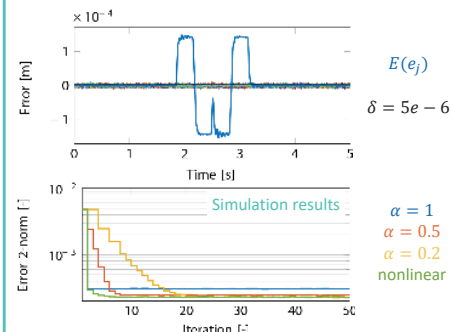
- 3) $E(\hat{g}(\theta_j)) = -2\psi(r)((1 + PC)^{-1}P)^T e(\theta_j) = g(\theta_j)$
- 4) Find optimal step size ε_j using 1 experiment
- 5) Update θ_j using stochastic gradient descent: $\theta_{j+1} = \theta_j - \varepsilon_j \hat{g}(\theta_j)$

How to avoid amplifying v_j ?
use a nonlinear ILC algorithm with a deadzone to create variable learning gains

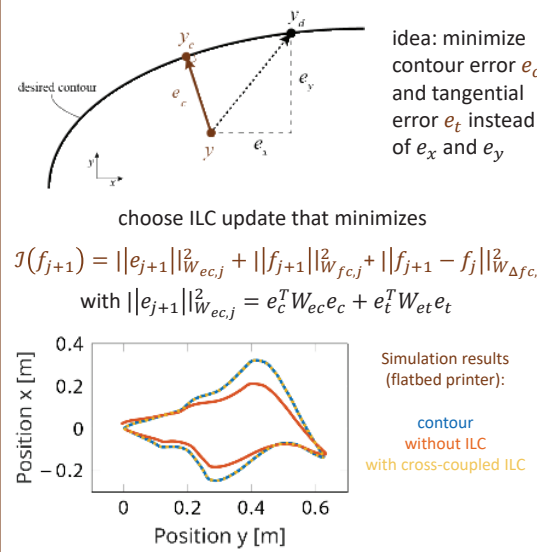
- ILC may amplify disturbances up to a factor 2
- Amplification is reduced by smaller learning gain α , which also slows down convergence
- Solution: nonlinear ILC update

$$f_{j+1} = Q(f_j + \alpha L e_j + L \varphi(e_j))$$

$$\varphi(e_j(k)) = \begin{cases} 0, & \text{if } |e_j(k)| \leq \delta \\ (\gamma - \frac{\gamma \delta}{|e_j(k)|}), & \text{if } |e_j(k)| > \delta \end{cases}$$

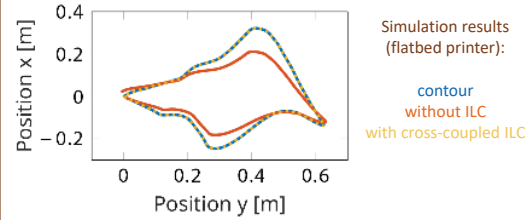


What if r is a contour and tracking matters?
weight deviation from contour in cross-coupled ILC



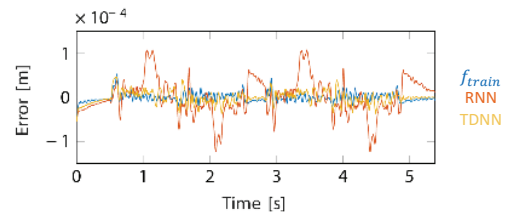
$$\mathcal{J}(f_{j+1}) = \|e_{j+1}\|_{W_{ec,j}}^2 + \|f_{j+1}\|_{W_{fc,j}}^2 + \|f_{j+1} - f_j\|_{W_{\Delta fc,j}}^2$$

with $\|e_{j+1}\|_{W_{ec,j}}^2 = e_c^T W_{ec} e_c + e_t^T W_{et} e_t$



What if we make F a neural network?
neural networks lead to performance and flexibility, but cost function, model structure and data set matter!

- Control-relevant cost function: minimize $\|e_{fnn}\|$ instead of $\|f_{train} - f_{nn}\|$ because similar signals $\not\Rightarrow$ similar errors. Use $\mathcal{J} = \|\mathcal{S}\mathcal{P}(f_{train} - f_{nn})\|$
- Non-causal neural networks enable preview
- Training data (references + feedforward signals) should be generated in closed-loop, e.g., using ILC



Experimental results (Arizona flatbed printer):
a non-causal time-delay neural network outperforms a non-causal recurrent neural network, which overfits the data



Study of Current Command Generation Method for Iron Loss Reduction in Permanent Magnet Synchronous Motors

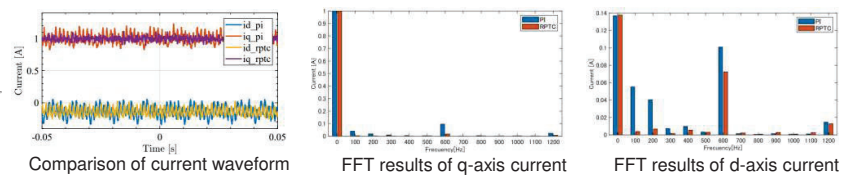
Kaiki Akizuki, Toshiyuki Fujita, Sakahisa Nagai, Hiroshi Fujimoto (The University of Tokyo)

Low-order harmonic current suppression

- Harmonic currents are considered one of the factors that increase iron loss.
- Repetitive Perfect Tracking Control (RPTC) [1] is used to suppress low-order harmonic currents.**
- The features of RPTC**
 - RPTC is composed of Perfect Tracking Control (PTC)[2] and Periodic Signal Generator (PSG).
 - Memory in PSG can record and compensate for errors to suppress periodic disturbances.

[1] Y. Inagaki, M. Mae, O. Shimizu, S. Nagai, H. Fujimoto, T. Miyajima, Y. Yasuda, A. Yanagawa, "Effect of Harmonic Current Suppression on Iron Loss of IPMSM Using Repetitive Perfect Tracking Control," IEEJ Journal of Industry Applications, Vol. 11, No. 2, pp. 317-326, 2022.

[2] H. Fujimoto, Y. Hori, A. Kawamura, "Perfect tracking control based on multi-step forward control with generalized sampling periods," IEEE Transactions on Industrial Electronics, Vol. 48, No. 5, pp. 636-644, 2001.

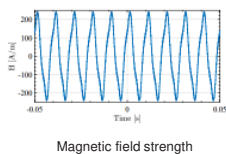


H-coil method

- The structure of motor bench**
 - In motor side, there are **search coils** to measure the electrical signal of **magnetic flux density(B)**.
 - H-coil** is used to measure the electrical signal of **magnetic field strength(H)**.
- Data processing method**
 - Data processing using software such as matlab
 - Calculating the electrical signal using the following equation, it is possible to obtain the waveforms of B and H.

$$H = \frac{1}{\mu_0 S_H N_H} \int_0^T e_H dt$$

$$B = \frac{1}{S_B N_B} \int_0^T e_B dt$$



*Odd order components are extracted to obtain hysteresis characteristics.

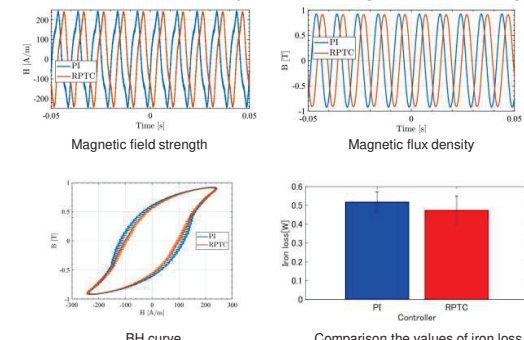
Evaluation of iron loss by H-coil method

- Experimental conditions**
 - Rotation per minute : 3000rpm
 - Current command value
d-axis : -0.137 A q-axis 1A (MTPA)
 - Carrier frequency : 10kHz
- Comparison of iron loss using PI control and RPTC**
 - It is possible to draw the **BH curve** using H-coil method.
 - Comparing with the average of three times measurement results.

PI control : 0.5178 W RPTC : 0.4740 W

8.45 % reduction !

Low-order current harmonics are suppressed, which reduces **low-order components of magnetic field strength**.

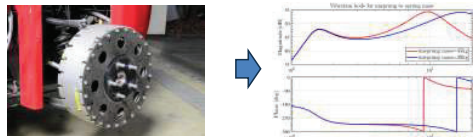


Vertical Vibration Suppression Control Using Disturbance Observer for In-wheel Motor EV Considering Under-sprung Motion

Qi Chen, Binhmin Nguyen, Sakahisa Nagai, and Hiroshi Fujimoto  THE UNIVERSITY OF TOKYO

Background

- Vertical vibration of vehicle

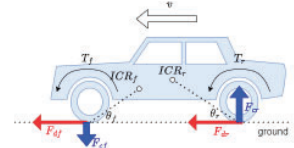


Under-sprung mass increase



Vertical vibration under 10Hz increases

- Suspension reaction force



Horizontal driving force generated by torque output



Vertical suspension reaction force

$$F_c = F_d \tan \theta$$

- Quarter car model

$$\begin{cases} m_1 z_1 s^2 = -[c_s s + k_s](z_1 - z_2) + [c_s s + k_s](z_0 - z_1) - F_c \\ m_2 z_2 s^2 = [c_s s + k_s](z_1 - z_2) + F_c \end{cases}$$

$$z_2 = \frac{c_s s + k_s}{m_2 s^2 + c_s s + k_s} z_1 + \frac{1}{m_2 s^2 + c_s s + k_s} F_c$$

Method

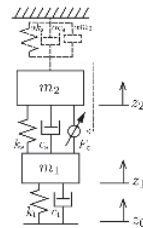
- Conventional triple skyhook control

Suppress the sprung vibration by pole-zero cancellation

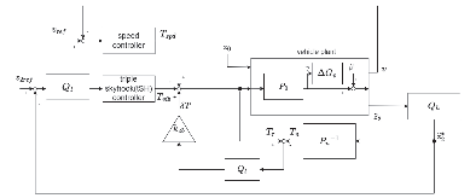
$$F_c = -\alpha(m_2 s^2 + c_s s + k_s)z_2$$

$$z_2 = \frac{1}{1 + \alpha m_2 s^2 + c_s s + k_s} z_1$$

- Weak to parameter variation
- Perform bad in low frequency with HPF



- Proposal tSH+DOB method



Novelty: new designed nominal model against bad performance of low frequency

$$P_{ndc}^{-1} = \frac{T}{z_2} = \frac{r}{\tan \theta} m_2$$

$$P_{ndp}^{-1} = \frac{T}{z_2} = \frac{r}{\tan \theta} (m_2 + \frac{c_s}{s} \frac{m_1 + m_2}{m_1} + \frac{k_s}{s^2} \frac{m_1 + m_2}{m_1})$$

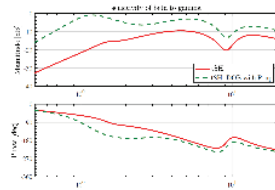
Simulation and Experiments



(a) FPEV2-Kanon for experiment

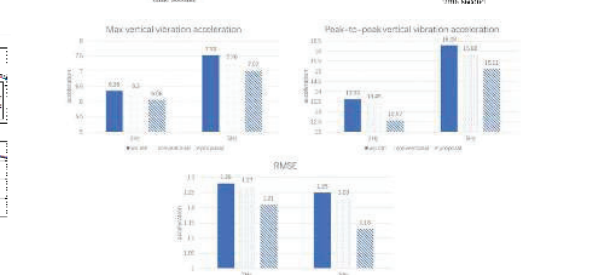
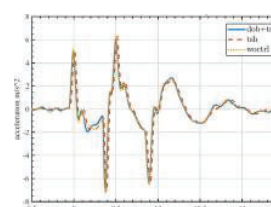


(b) In-wheel motor



(c) Complementary Sensitivity of parameter variation

Simulation result in frequency domain



Experimental results using software disturbance around 2Hz and 5Hz

Fault Diagnosis for Precision Mechatronics

Koen Classens¹, Maurice Heemels¹, Tom Oomen^{1,2}

¹ Control Systems Technology
Section, Dept. of Mechanical
Engineering, Eindhoven
University of Technology
² Delft Center for Systems and
Control, Dept. 3mE, Delft
University of Technology
k.h.classens@tue.nl



BACKGROUND & MOTIVATION

High-tech industry faces:

- ▷ Unexpected downtime
- ▷ Major production loss



Despite:

- ▷ Excellent mechanical design
- ▷ Advanced control strategies

Solution:

- ▷ Online fault diagnosis
- ▷ Predictive maintenance



OPPORTUNITY & CHALLENGE^[1]

Opportunity:

- ▷ Accurate and familiar models
- ▷ Real-time data
- ▷ Control paradigms



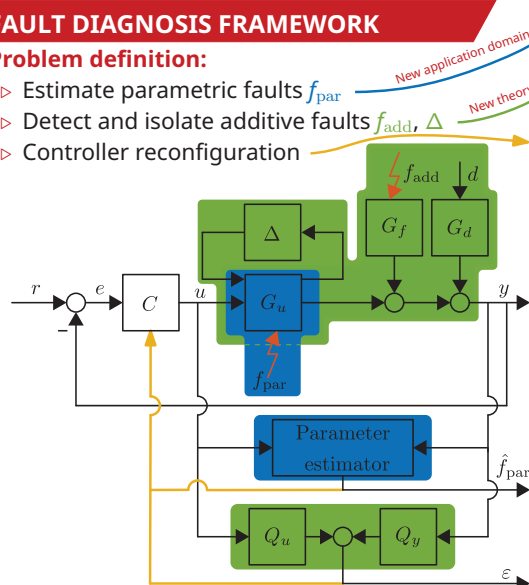
Challenge:

- ▷ Closed-loop aspects
- ▷ Interpretable → Model-based
- ▷ Operational data → No dedicated experiments

FAULT DIAGNOSIS FRAMEWORK

Problem definition:

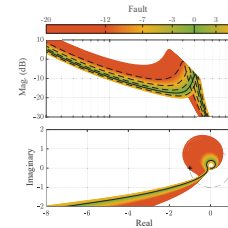
- ▷ Estimate parametric faults f_{par}
- ▷ Detect and isolate additive faults f_{add}, Δ
- ▷ Controller reconfiguration



I. PARAMETRIC FAULT DIAGNOSIS^[2]

Problem:

- ▷ Shifting properties, e.g., resonance dynamics



Affect:

- ▷ Stability margins
- ▷ Performance

Setup:

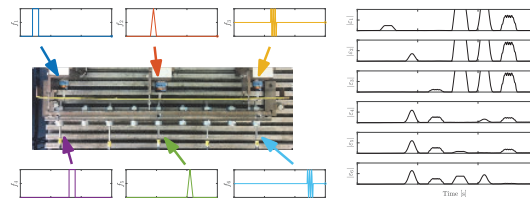
- ▷ Overactuated and oversensed
- ▷ Variable stiffness in design



II. ADDITIVE FAULT DIAGNOSIS^[3,4]

Problem:

- ▷ Additive faults in sensors and actuators



- ▷ Successful fault isolation
- ▷ Robustness guarantees

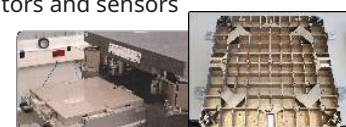
III. CONTROL RECONFIGURATION

Problem:

- ▷ Minimize performance loss due to faults

Approach:

- ▷ Online reconfiguration → Fault-tolerant control
 - ▷ Virtual actuators and sensors
 - ▷ Fault hiding



Setup:

- ▷ Overactuated and oversensed → Opportunity!

REFERENCES & FURTHER READING

Preliminary overview paper!

- [1] K. Classens, W. P. M. H. Heemels and T. Oomen, *Digital Twins in Mechatronics: From Model-based Control to Predictive Maintenance*, 2021 IEEE 1st International Conference on Digital Twins and Parallel Intelligence, 2021.
- [2] K. Classens, W. P. M. H. Heemels and T. Oomen, *Online Fault Detection for Precision Mechatronics: Online Estimation of Mechanical Resonances, 2nd Modeling, Estimation and Control Conference*, 2021.
- [3] A. Varga, *Solving Fault Diagnosis Problems*. Springer, 2017.
- [4] K. Classens, W. P. M. H. Heemels and T. Oomen, *Direct Shaping of Minimum and Maximum Singular Values: An H_{∞}/H_{∞} Synthesis Approach for Fault Detection Filters*, IFAC 22nd Triennial World Congress, 2023.

Time-varying interaction in Gravitational Wave detectors

Mathyn van Dael^{1,2}, Gert Witvoet^{1,3}, Bas Swinkels² and Tom Oomen^{1,4}

¹Eindhoven University of Technology, Eindhoven, the Netherlands

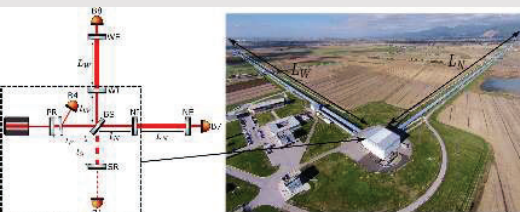
²Nikhef, Amsterdam, the Netherlands ³TNO, Delft, the Netherlands

⁴Delft University of Technology, Delft, the Netherlands



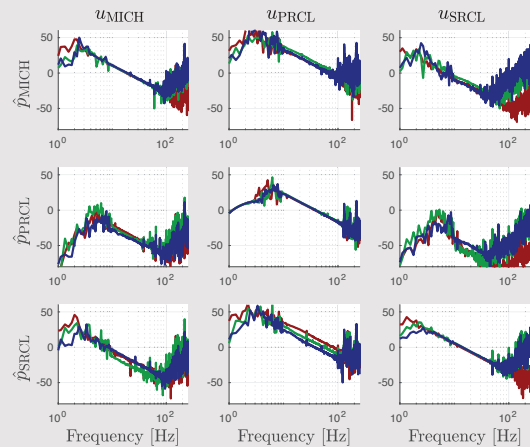
Challenge in detecting Gravitational Waves

- Gravitational Wave detectors Virgo (below) & KAGRA
- Extremely sensitive → spatial fluctuations of 10^{-18} m
- Mirror distances requirements $\sim 10^{-15}$ m RMS
↳ Feedback control essential!



Challenge: time-varying interaction → FRF at t_1 , t_2 and t_3

Problem: Control design for time-varying behaviour



Approach 1: Controller design for stability^[1]

Approximate system by

$$G = \frac{1}{s^2} \cdot g \quad \forall \omega \in 2\pi [10 \ 100] \quad g \in \mathbb{R}^{3 \times 3}$$

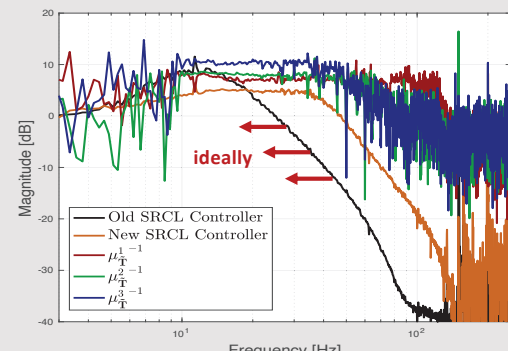
Apply Factorized Nyquist criterion:

$$|\tilde{T}^{ii}(j\omega)| < \mu_{\tilde{T}}^{-1}(E(j\omega)) \quad \forall \omega, i$$

Exploit structure of G :

$$\mu_{\tilde{T}}^{-1}(E(j\omega)) = \alpha \quad \forall \omega \in 2\pi [10 \ 100]$$

Key insight: sufficient SISO stability margins required.



Main performance objective: maximize controller roll-off for a given RMS requirement.

↳ Current approach yields conservative design

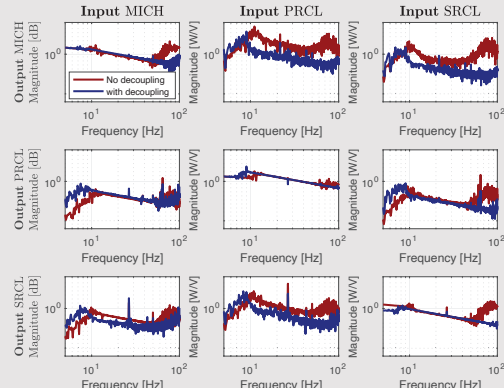
Approach 2: Decoupling for performance

Goal: Decouple system using sensing matrix $T_y \approx g^{-1}$.

Challenge: estimate g in closed loop using excitation

$$\bar{d} = \begin{bmatrix} \sin(2\pi f_1 t) \\ \sin(2\pi f_2 t) \\ \vdots \\ \sin(2\pi f_n t) \end{bmatrix}$$

Next steps: improve algorithm for unbiased estimation of g



References

[1] M. R. van Dael et. al., (2022), Design for interaction: Factorized Nyquist based control design applied to a Gravitational Wave detector, *IFAC-PapersOnLine*, 55(37), 107-112



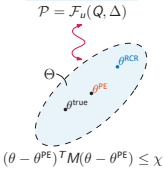
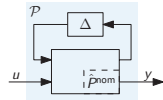
Robust-control-relevant experiment design and system identification applied to a wafer stage

JSPS workshop, Tokyo, Japan, 2023

Introduction

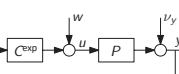
Robust control

- Control goal $C^{RP} = \arg \inf_C \mathcal{J}_{WC}(\mathcal{P}, C)$
- High-performance requires small set \mathcal{P}
- Set must be identified from data



Classical identification

- Delivers ellipsoidal uncertainty region Θ
- Non-standard in robust control
- Central model non-optimal in view of \mathcal{J}_{WC}



Experiment design

- Enables shaping Θ via excitations w
- No straightforward connection to \mathcal{J}_{WC}

Goal: Improve robust control performance by connecting robust control, model set identification, and experiment design:
 $\{C^{RP}, \mathcal{P}^{RCR}, w^{RCR}\} = \arg \inf_{C, \mathcal{P}, w} \mathcal{J}_{WC}(\mathcal{P}(w), C)$

Method

Control-relevant distance measure

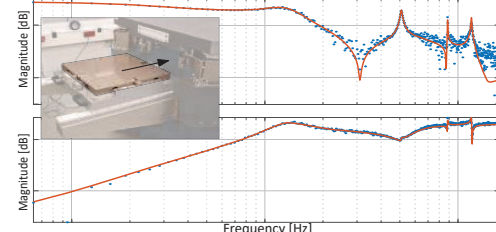
- Control performance is bounded by
- $$\mathcal{J}(P, C) \leq \mathcal{J}(\hat{P}, C) + \underbrace{\|W(T(P, C) - T(\hat{P}, C)V)\|_\infty}_{:=d(P, \hat{P})}$$

d is a control-relevant distance measure

Wafer Stage Results

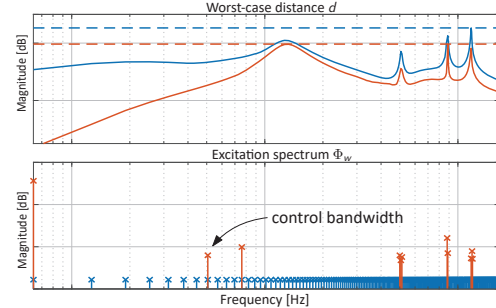
Control-Relevant Coprime Factor Identification

Coprime factors $\{\hat{N}, \hat{D}\}$



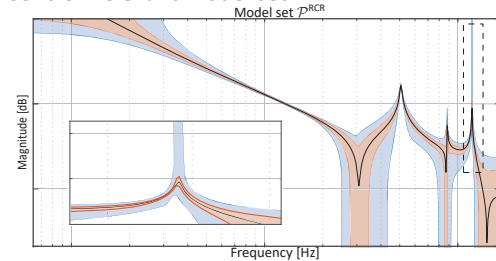
- Frequency Response Function Measurement
- Identified parametric model $\hat{G}(\theta)$

Control-Relevant Experiment Design



- Uniform spectrum design: distance d is large at 3rd resonance
- Control-relevant spectrum design: distance d is reduced 4x by tailored excitations around control bandwidth and resonances

Control-Relevant Model set



- Control-relevance: tight around bandwidth and resonances, loose far below/beyond bandwidth
- Control-relevant spectrum design significantly reduces set size compared to uniform design, especially around 3rd resonance

Conclusions

- Control-relevant coprime factors enable connecting uncertainty size to control, identification, and experiment design criteria
- Improvements demonstrated on wafer stage setup

References

- [1] T. Oomen: "Advanced Motion Control for Next-Generation Precision Mechatronics, Challenges for Control, Identification and Learning", IEEJ Journal of Industry Applications, 7(2), 1-14, 2018
[2] T. Oomen, O. Bosgra: "System identification for achieving robust control", Automatica, 48(9), 1975-1987, 2012

Control-Relevant Coprime Factor Identification

Stage I: Non-parametric Chebicheff center

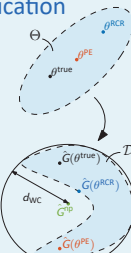
$$\hat{G}^{NP} = \arg \inf_{G \in \mathbb{C}} \sup_{G \in D} d(G, \hat{G})$$

Computed exactly by semi-definite program

Stage II: Parametric model $P(\theta) = B(\theta)A^{-1}(\theta)$

$$\hat{G}(\theta^{RCR}) = \arg \inf_{\hat{G}(\theta) \in D} d(\hat{G}^{NP} - \hat{G}(\theta))$$

Guaranteed coprimeness



Control-Relevant Experiment Design

- Spectrum design Φ_w that connects to identification method:

$$\Phi_w^{RCR} = \arg \inf_{\Phi_w} \inf_{G \in \mathbb{C}} \sup_{G \in D(\Phi_w)} d(G, \hat{G})$$

subject to experimental constraints

Convex design problem

/ department of mechanical engineering

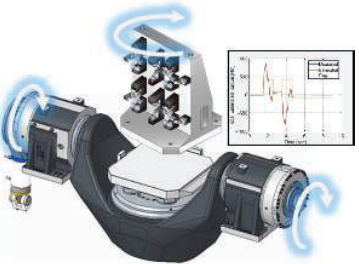
/ control systems technology

 東京大学
THE UNIVERSITY OF TOKYO

A study on Multi-rate Adaptive Control on Five-axis Machine Tools

Chenyu GE, BINH MINH NGUYEN, Hiroshi Fujimoto (The University of Tokyo)

Multi-rate Adaptive Robust Control Theory



Part of 5-axis Machine Tool

Dynamic Model:

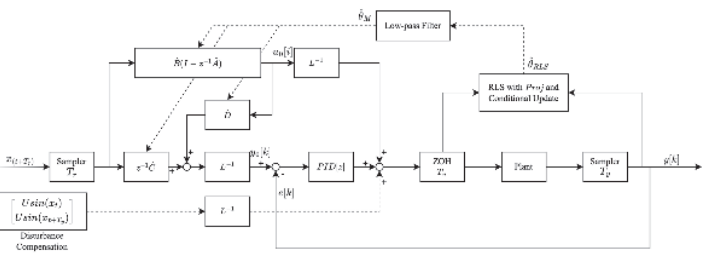
$$T_m = J_M \ddot{\theta} + D_M \dot{\theta} + U_M \sin(\theta) + C \text{sgn}(\dot{\theta})$$


Diagram of Multi-rate Adaptive Robust Control

Online Adaptive Algorithm - RLS

RLS Estimation:

(1) Estimate:

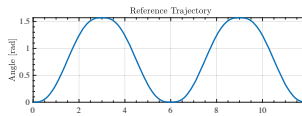
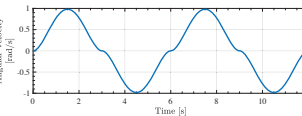
$$\begin{bmatrix} \hat{J}[k] \\ \hat{D}[k] \end{bmatrix} = \begin{bmatrix} \hat{J}[k-1] \\ \hat{D}[k-1] \end{bmatrix} + \text{Proj}_{J,D}\{K[k](u[k] - \varphi^T[k] \begin{bmatrix} \hat{J}[k-1] \\ \hat{D}[k-1] \end{bmatrix})\}$$

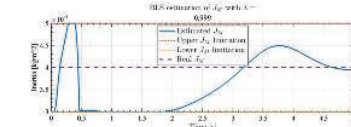
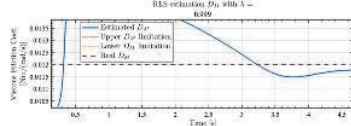
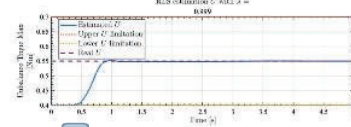
$$\text{Proj}_{\begin{bmatrix} \hat{J}[i] \\ \hat{D}[i] \end{bmatrix}}[H] = \begin{cases} 0, & \text{if } \hat{H}[i] > H_{max} \text{ and } \hat{H}[i] > 0 \\ 0, & \text{if } \hat{H}[i] < H_{min} \text{ and } \hat{H}[i] < 0 \\ \begin{bmatrix} \hat{J}[i] \\ \hat{D}[i] \end{bmatrix}, & \text{otherwise} \end{cases}$$

(2) Update:

$$K[k] = \frac{P[k-1]\varphi[k]}{\lambda + \varphi^T[k]P[k-1]\varphi[k]}$$

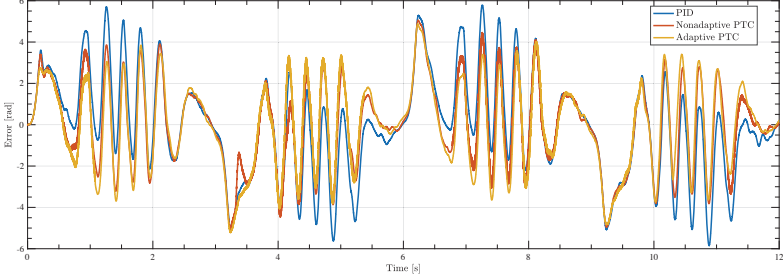
$$P[k] = \frac{(I - K[k]\varphi^T[k])P[k-1]}{\lambda}$$

↑ Sim: RLS Estimation

← Exp: Reference Trajectory



← Exp: Tracking Error

FRF Identification Above the Nyquist Frequency

Max van Haren
Leonid Mirkin
Lennart Blanken
Tom Oomen
m.j.v.haren@tue.nl



Introduction

Goal: Identifying FRFs of slow-sampled systems above the Nyquist frequency, see Figure 1.

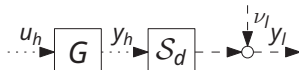


Figure 1: Identification setting, where high-rate FRF G is to be identified, using fast u and slowly-sampled y_l .

Example: Vision-in-the-loop systems.

Main challenge: Aliasing that occurs due to downsampling

The main challenge is described by output

$$Y_l(k) = \frac{1}{F} \sum_{f=0}^{F-1} G(\Omega_{k+Mf}) U(k+Mf).$$

1 data point F unknowns

Figure 2 visually illustrates the main challenge.

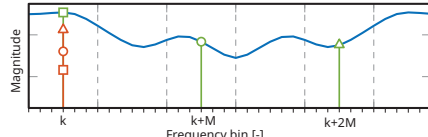


Figure 2: FRF G (-), that is excited (-), resulting in aliasing at output (-), where 3 unknowns appear but only 1 data point.

Method

Method: Exploiting local smoothness of FRF and utilizing neighboring outputs [1].

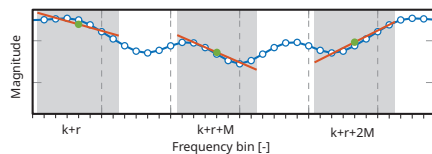


Figure 3: Exploiting smoothness of FRF to identify G (-). Each bin k has $F(R+1) = 6$ unknowns, but $2n+1 = 7$ data points.

Key result: Disentangling aliasing enabled by window

$$[Y_l(k-n) \dots Y_l(k+n)] = \frac{1}{F} \sum_{i=0}^{F-1} G(\Omega_{k+iM}) U(k+iM) + \sum_{j=1}^R g_j(k+iM) K_j$$

2n + 1 data points $F(R+1)$ unknowns

→ Smart input required (e.g. random-phase MS)

Experimental Results

The framework is validated on the experimental setup seen in Figure 4. The identified FRFs using a traditional and the developed approach are shown in Figures 5 and 6.



Property	Variable	Value
Fast sampling rate	$f_{s,h}$	120 Hz
Slow sampling rate	$f_{s,l}$	30 Hz
Downsampling factor	F	4
Measurement time	T_m	120 s
Window size	n_w	150
Polynomial degree	R	2

Figure 4: Experimental (left) setup and (right) settings.

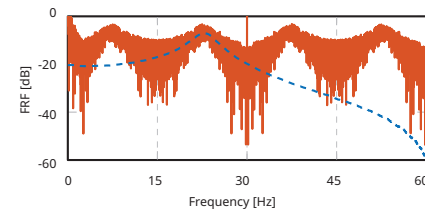


Figure 5: True (-) and identified traditional FRF (-) by ignoring aliasing.

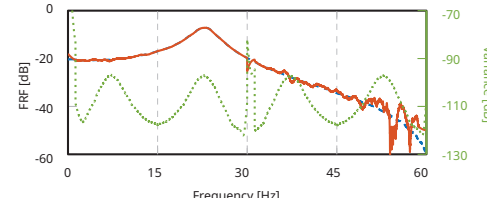


Figure 6: Identified FRF with developed method (-) and associated variance (-).

Observation: Method identifies slow-sampled significantly more accurate compared to traditional approach.

Conclusions

- Output analysis of slow-sampled systems.
- Identification of slow-sampled systems above Nyquist enabled by exploiting smoothness.
- Experimental results give promising results.

References

- [1] M. van Haren, L. Mirkin, L. Blanken and T. Oomen, "Beyond Nyquist in Frequency Response Function Identification: Applied to Slow-Sampled Systems", IEEE L-CSS, 2023

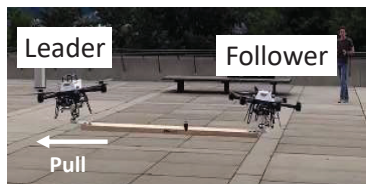
Wind vector estimation considering the difference of propeller characteristics for fully actuated drone

Manto Kamiya, kamiya-manto501@g.ecc.u-tokyo.ac.jp



Force control of drones and problem of wind disturbance

Applications of force control of drones



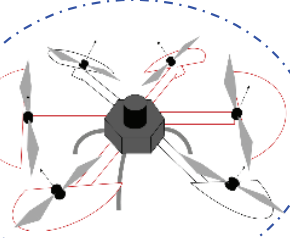
Collaborative transportation
[Andrea Tagliabue, et.al ICRA2017]



Contact inspection
[R. Rashad, et.al IROS 2020]

Fully actuated drone

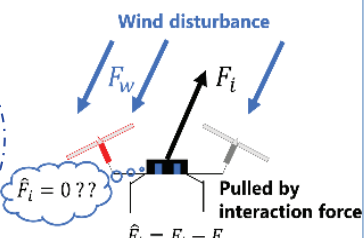
Suitable for high-precision control



- Different propellers direction
- Superiority in mobility performance
- Low energy efficiency

Problem of force control

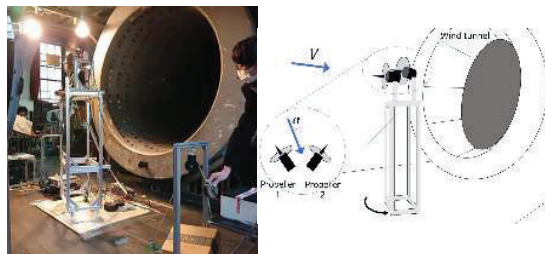
Separation of wind disturbance & other force



$\hat{F}_w = 0 ??$
Fail to admittance & impedance control

- Solution**
- Wind force estimation
→ Wind vector estimation

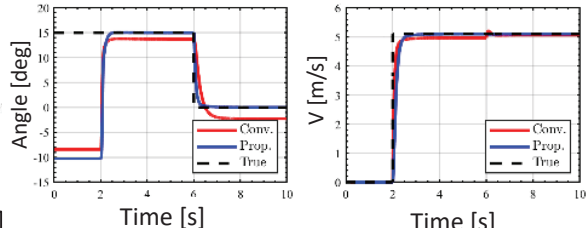
Wind vector estimation using motors & propellers information



Two propellers are used to simplify the situation

Wind vector estimation simulation

- Wind velocity 5.1m/s • Rotational speed(2500rpm)
- Estimate step airflow angle in real time (20 second)



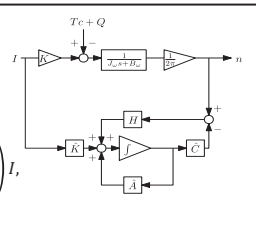
Step 1

Estimate counter torque Q by observer

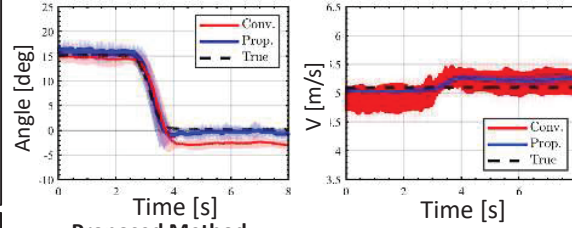
State space eq. ($\dot{Q} \approx 0$)

$$\begin{pmatrix} \dot{\omega} \\ \dot{Q} \end{pmatrix} = \begin{pmatrix} -\frac{B_{\text{on}}}{J_{\text{on}}} & 1 \\ 0 & J_{\text{on}} \end{pmatrix} \begin{pmatrix} \omega \\ Q \end{pmatrix} + \begin{pmatrix} K \\ 0 \end{pmatrix} I_r$$

$$n = \left(\frac{1}{2\pi} \ 0 \right) \begin{pmatrix} \omega \\ Q \end{pmatrix}$$



Wind vector estimation experiment



Proposed Method

- Wind vector estimation without wind sensor
- Only using information of motors & propellers
- Considering the difference of propellers' model characteristics

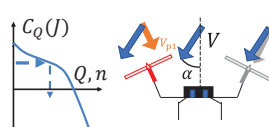
Result

- Succeeded in estimating wind velocity and step airflow angle with test bench
- Improved the accuracy of estimation

Step 2

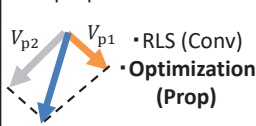
Estimate V_{p1} & V_{p2}

$$V_{p1} = C_Q^{-1}(\hat{Q}_{D1}, n_1) \quad V_{p2} = C_Q^{-1}(\hat{Q}_{D2}, n_2)$$



Step 3

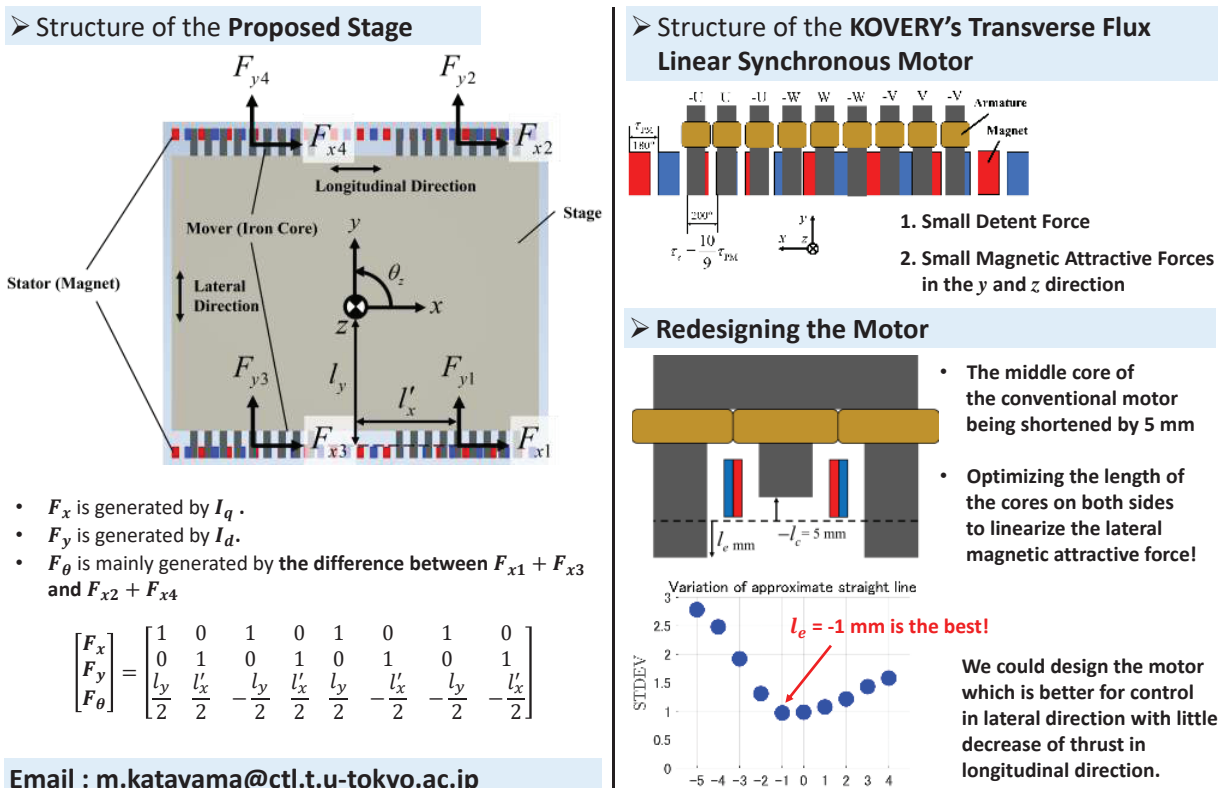
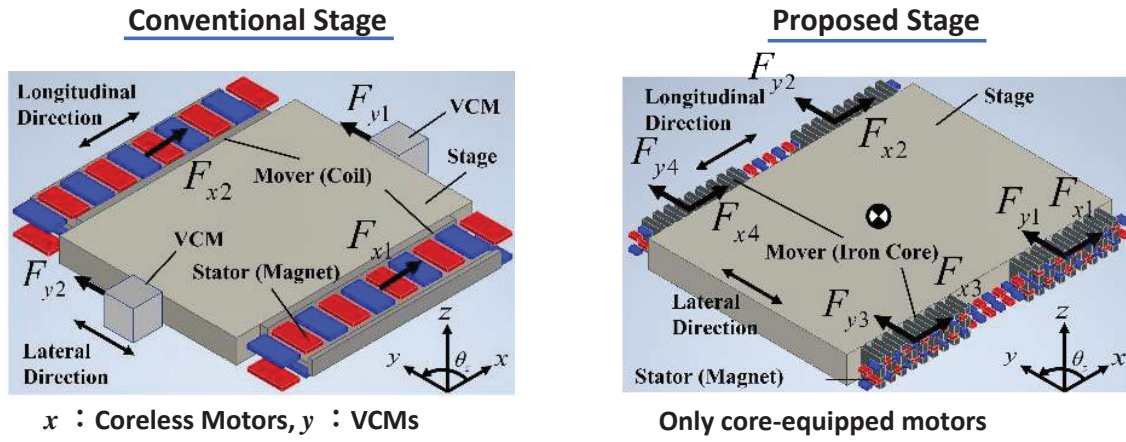
Estimate wind vector Using V_p & difference of propeller direction



Proposal of a high acceleration contactless precision stage with a pair of transverse flux linear synchronous motors

Mamoru Katayama, Wataru Ohnishi, Takafumi Koseki (The University of Tokyo),
Houng-Joong Kim (KOVERY), Koichi Sakata (Nikon)

- Proposal of a new precision positioning stage that eliminates the VCMs and actively uses the attractive force by ***d*-axis current** of the core-equipped linear motors.





Study on Estimation and Adjustment of Lateral Misalignment in Dynamic Wireless Power Transfer with Steering Actuator and Yaw Moment

Tomoaki Koishi, Binh-Minh Nguyen, Osamu Shimizu, Shota Yamada, Hiroshi Fujimoto (The University of Tokyo)

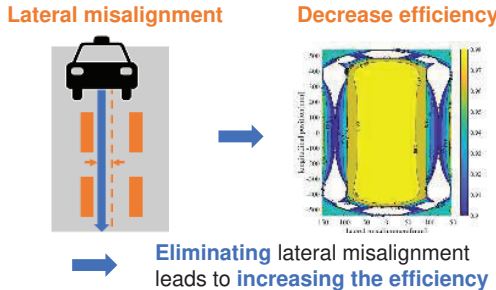
Background

Dynamic Wireless Power Transfer (DWPT)

- Transfer power to running EVs through coils

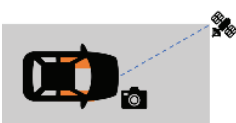


Problem: Lateral misalignment in DWPT



Conventional localization method

GPS, camera, etc.



Estimate position from marker

Good

- Available without DWPT
- Already in practical use

Limitation

- Intolerant to misalignment between marker and Tx coil

DWPT information (voltage, current)



Estimate position from Tx coil

Good

- Directly estimate the position from the Tx coil

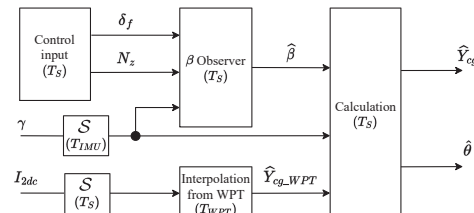
Limitation

- Unavailable with excessive misalignment

DWPT system		Longitudinal	Lateral
Parallel power lines		[9,10]	
Multiple coils	Circular coils	[17]	[8]
	Rectangular coils	[11]	This study

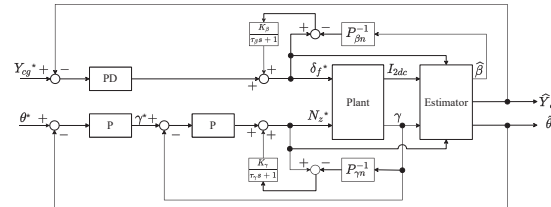
Approach

Estimation: Fusion of DWPT current and IMU



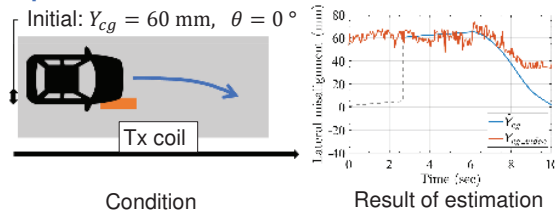
- Observer + calculation of lateral misalignment
- Deal with the different sampling rate

Control: Steering and yaw moment input



- FB control of lateral misalignment and yaw angle

Experimental result of estimation method



Condition

Result of estimation

- Compared to image processing method
- Estimation error increased as time passed
→ multiple coils are expected to reduce the error

Conclusion

Based on the fusion of WPT and IMU, this study proposes a new method for estimating and controlling the lateral misalignment and yaw angle of electric vehicles. The overall control system uses LFO and the PD controller to control the lateral misalignment, and YMO and the P controller of the yaw angle and the yaw rate.

ASML 

NEURAL NETWORKS FOR FEEDFORWARD CONTROL

Johan Kon¹, Dennis Bruijnen², Marcel Heertjes^{1,3}, Tom Oomen¹

¹ Control Systems Technology Section, Dept. of Mechanical Engineering, TU/e
² Philips Engineering Solutions
³ ASML Mechatronics System Design

j.j.kon@tue.nl

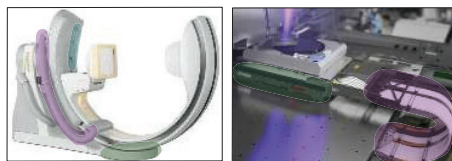

Industrial challenges

Present: feedforward parametrizations based on physical model structures:

- F_1 Mass and snap
 - F_2 Rational transfer functions
 - F_3 Nonlinear multibody
- ↓ Increasing modelling effort

Unmodeled dynamics:

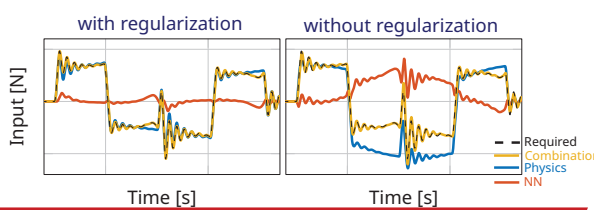
- Complex nonlinear friction
 - Dynamic links/cables
 - Actuator characteristics
- } Limiting for performance

**I: Physics-guided neural networks^{[4],[5]}****Use prior knowledge of physics**

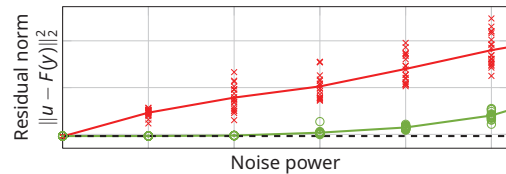
$$f = M_\theta(r) + C_\phi(r)$$

 C_ϕ should be complementary to M_θ

Penalize $C_\phi(r)$ in subspace spanned by $M_\theta(r)$ via orthogonal projection-based regularization

**II: Learning using closed-loop data^[3]****Both u and y contain the same noise**

- Least-squares (LS): biased
- Instrumental variables (IV): consistent
- IV \Rightarrow superior tracking performance

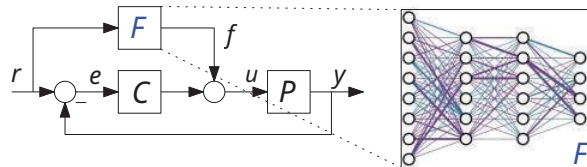
**How to compensate unmodeled dynamics through data-driven learning^[2]:**

- Employ universal approximation structures
 - ⇒ Can capture any unmodelled dynamics
- ↓ This poster

Neural networks as universal approximators^[1]

- Approximate any continuous function
- Parametric

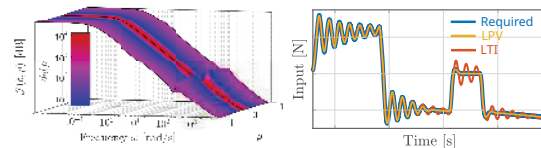
$$f = W_L (W_{L-1} \cdots (W_0 \Psi(r) + b_0) \cdots + b_{L-1}) + b_L$$

**III: LPV feedforward for position-varying zeros^[6]****Position-varying dynamics in mechanical systems**

▷ LTI feedforward too limited

LPV-IO feedforward with NN scheduling

$$u_k = - \sum_{i=1}^{N_\theta-1} b_i(\rho) q^{-i} u_k + \sum_{i=0}^{N_\theta-1} a_i(\rho) q^{-i} r_k$$

Learn position dependent dynamics!**Build in stability guarantees!****REFERENCES & FURTHER READING**

- [1] I. Goodfellow, Y. Bengio, A. Courville, *Deep learning*. MIT Press 2016
- [2] L. Aarnoudse, J. Kon, et al, "Control-Relevant Neural Networks for Feedforward Control with Preview," to appear, 2022.
- [3] J. Kon, M. Heertjes, T. Oomen, "Neural Network Training Using Closed-Loop Data: Hazards and an Instrumental Variable (IVNN) Solution," *IFAC Workshop on Adaptive and Learning Control Systems*, 2022.
- [4] J. Kon, D. Bruijnen, J. van de Wijdeven, M. Heertjes, T. Oomen, "Physics-Guided Neural Networks for Feedforward Control: An Orthogonal Projection-Based Approach," *Proc. Am. Control Conf.*, 2022.
- [5] J. Kon, D. Bruijnen, J. van de Wijdeven, M. Heertjes, T. Oomen, "Unifying model-based and neural network feedforward: Physics-guided neural networks with linear autoregressive dynamics," *61st Conf. Decis. Control*, 2022.
- [6] J. Kon, D. Bruijnen, J. van de Wijdeven, R. Tóth, M. Heertjes, T. Oomen, "Direct learning for parameter-varying feedforward control: A neural network approach," to appear, 2023.

Identification and Robust Control for Motor Commutation

Max van Meer¹, Gert Witvoet^{1,2} and Tom Oomen^{1,3}¹Eindhoven University of Technology, Eindhoven, the Netherlands²TNO, Delft, the Netherlands³Delft University of Technology, Delft, the Netherlands

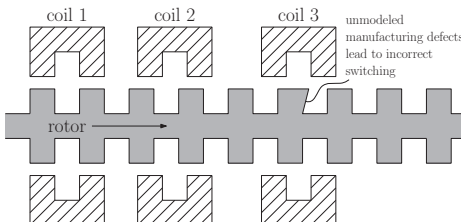
m.v.meer@tue.nl



BACKGROUND

Switched Reluctance Motors (SRMs, Fig. 1) provide

- power-efficient actuation,
- with mechanically simple designs,
- at the expense of increased control complexity.

**Figure 1**

Working principle of SRMs. Sequentially applying currents to the coils attracts rotor teeth, generating torque.

Imperfect switching leads to **torque ripple**. Two solutions:

- **Identification** of the torque-current-angle relation
- **Robust commutation design** for accurate control

NONLINEAR IDENTIFICATION OF SRMs

$$T(\phi, i) = \sum_{c=1}^{n_c} \frac{1}{2} \frac{dL_c(\phi)}{d\phi} i_c^2, \quad (1)$$

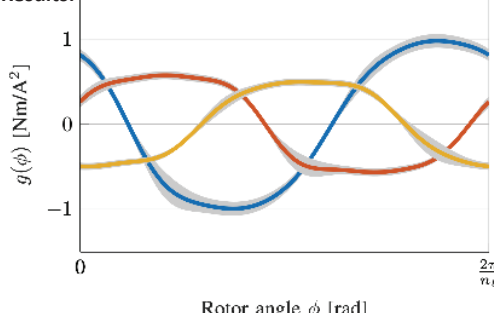
Inductances L_c , angle ϕ , and currents i_c affect the torque T .

Problem: How to identify $g = \frac{1}{2} dL/d\phi$ from only ϕ and i_c , when no torque sensor is available?

Solution: experiment design + Bayesian identification

1. Closed-loop experiments to learn torque
2. **Bayesian identification** to obtain a model g (Fig. 2)

Results:

**Figure 2**

Experimental results. Even without a torque sensor, an accurate model of the SRM is obtained, as well as an expression of the model uncertainty K_θ .

ROBUST COMMUTATION DESIGN FOR CONTROL OF SRMs

Commutation is used to invert SRM dynamics g :

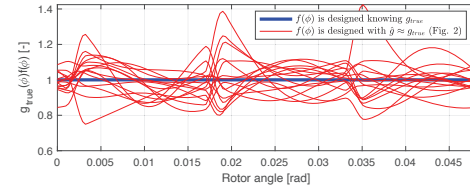
→ Currents $i^{*2}=f(\phi)T^*$ should produce torque $g(\phi)i^{*2}=T=T^*$

→ Design $f(\phi)$ such that $g(\phi)f(\phi) = 1$

Previous work: design $f(\phi)$ based on known $g(\phi)$ ^[1]

Problem: g is uncertain and varies per tooth.

Inverting an uncertain model gives torque ripple! (Fig. 3)

**Figure 3**

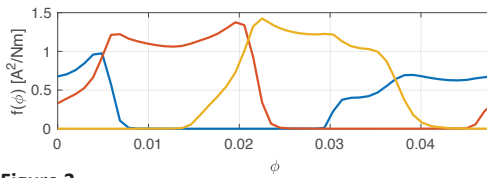
When SRM dynamics are known, perfect inversion is possible (blue). However, a little model uncertainty (Fig. 2) leads to a large torque error when inverted naively (red)!

Solution: design $f(\phi)$ to be **robust to uncertainty in $g(\phi)$!**

$$\begin{aligned} \min_{\alpha} & \mathbb{E} \left[\|g(\phi, \theta)f(\phi, \alpha) - 1\|_2^2 \right] \\ \text{subject to} & f(\phi, \alpha) \geq 0, \\ & g(\phi, \hat{\theta})f(\phi, \alpha) = 1, \\ & \theta \sim \mathcal{N}(\hat{\theta}, K_\theta). \end{aligned} \quad (2)$$

→ solve using convex optimization (Fig. 3)

Results:

**Figure 3**

The solution to (2) leads to current waveforms with large overlap, leading to careful switches that induce limited torque ripple when the switching moments are uncertain.

Simulation results: 50% better tracking performance!

Conclusion: motor commutation is improved by data-driven identification of the nonlinear dynamics and subsequent design of robust commutation functions.

References

- [1] van Meer, M., Witvoet, G., & Oomen, T. (2022). Optimal Commutation for Switched Reluctance Motors using Gaussian Process Regression. *IFAC-PapersOnLine*, 55(37), 302–307.

GAUSSIAN PROCESSES FOR ADVANCED MOTION CONTROL

Maurice Poot^{1,*}, Jim Portegies², Noud Mooren¹, Max van Haren¹, Max van Meer¹, Tom Oomen^{1,3}

¹ Control Systems Technology Section, Dept. of Mechanical Engineering, Eindhoven University of Technology, The Netherlands
² CASA Dept. of Mathematics and Computer Science, Eindhoven University of Technology, The Netherlands
³ Delft Center for Systems and Control, Delft University of Technology, The Netherlands

* Correspondence to: m.m.poot@tue.nl

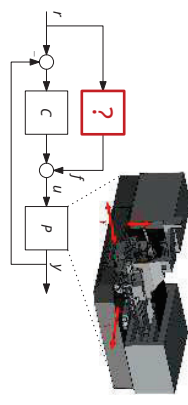
PROBLEM DEFINITION

- Traditional feedforward based on 1st principles structures [1]:
 - Mass
 - Compliance (snap)
 - Rational
 - Parasitic effects:
 - Nonlinear friction
 - Changing configurations
- ↓ Increasing complexity!

↓ Become dominant!

Solution in this poster:

What nonparametric Gaussian Processes have to offer in 4 use cases!



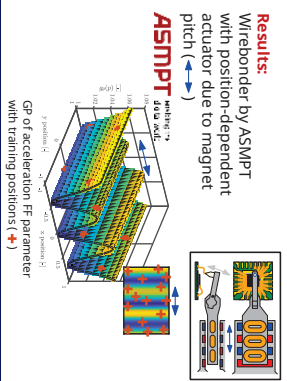
I. POSITION-DEPENDENT FEEDFORWARD

- Problem:**
Position-dependency in actuator or mechanics

- Approach [4]:**
Idea: learn feedforward parameters as continuous function of position using a GP:

$$f(t) = \psi(r(t)) \theta(x_0, y_0)$$

- Learn GP for a few x, y positions:
- Feedforward for entire X, Y range!
- Position-dependency in
- Actuator → Compliance → Snap GP [4]



Results:
Wirebonder by ASMP with position-dependent actuator due to magnet

(\downarrow) → (\uparrow)

GP of acceleration FF parameter with training positions (+)

II. NONLINEAR FEEDFORWARD

- Problem:**
Nonlinear behaviour is unknown

- Approach [3]:**
Idea: model inverse nonlinear system using a GP:

$$f(t) = g^{-1}(y(t))$$

- Based on I/O data: $[y(t), u(t)]_{t=0}^N$
- Requires $y(t)$ close to $r(t)$
- Models unknown nonlinearities



Results:
Desktop A3 printer with friction

ASMP

(\downarrow) → (\uparrow)

Traditional (—), Nonlinear GP FF (—)

III. KERNEL-BASED LEARNING CONTROL

- Problem:**
Complexity of feedforward structure unknown

- Approach [6]:**
Idea: essentially very high-order feedforward:

$$f(t) = \sum_{\tau=\tau_0, \tau_0}^{n-1} \theta_\tau r(t-\tau)$$

where θ_τ is noncausal impulse response

- New perspective on order selection with kernel-based regularization:
- Smoothness & decay rate
- Learn in closed-loop using ILC
- Flexible to varying motion tasks



Results:
Desktop A3 printer with friction

ASMP

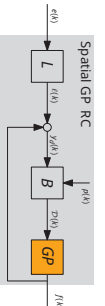
(\downarrow) → (\uparrow)

Traditional (—), Kernelbased ILC (—)

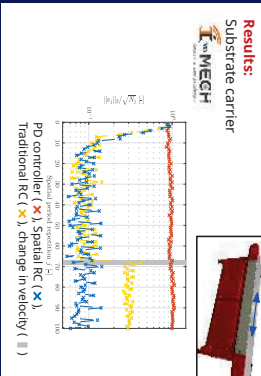
IV. SPATIAL REPETITIVE CONTROL

- Problem:**
Repeating disturbances in position domain

- Approach [7]:**
Idea: GP-based disturbance model:



- Uses non-equidistantly distributed position-domain data
- Specify periodicity of disturbance
- Invariant under velocity changes



Results:
Substrate carrier

ASMP

(\downarrow) → (\uparrow)

Traditional RC (—), GP RC (—)

TU/e



Last 2 decades successful in ML [2,3]:
² Powerful mathematical framework
 Interpolation of continuous functions
³ Nonparametric
 Incorporate prior knowledge in kernel
 Provides uncertainty estimates

M

J

N

T

M

G

H



/Department of Mechanical Engineering

/Control Systems Technology Section

TU/e

- REFERENCES:** (available on www.tueopen.eu)
- [1] T. Oomen, Advanced Motion Control for Precision Mechatronics: Control, Identification, and Learning of Complex Systems, *IEEE Journal of Industry Applications*, 2018, Vol. 77, No. 2, pages 127-140.
 - [2] C. Rasmussen and C. Williams, *Gaussian processes for Machine Learning*, Massachusetts Institute of Technology, 2006.
 - [3] M. Poot, J. Portegies, N. Mooren, M. van Haren, M. van Meer, and T. Oomen, Gaussian Processes for Advanced Motion Control, *IEEE/ASME Transactions on Mechatronics (TMM)*, 2021, pages 1052-1057.
 - [4] M. van Haren, M. Poot, J. Portegies, and T. Oomen, Gaussian process repetitive control for suppressing spatial disturbances, *IFAC-PapersOnLine*, 2020, 53(2), pages 1487-1492.

Learning Uncertainty For Advanced Motion Control

Paul Tacx, Tom Oomen

Background

Next-generation motion systems:

TNO Deformable Mirror
57-217-2000 ActuatorsASML Reticle Stage (FFR)
14 × 14

- ▷ Interaction \Rightarrow Inherently multivariable
- ▷ Active control \Rightarrow many inputs and outputs
- \Rightarrow **Model-based control**

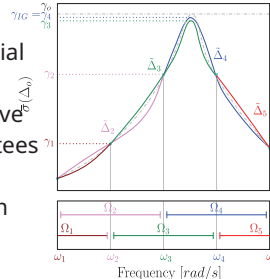
This poster: From data to Robust Performance (RP)

$$\text{FRF} \rightarrow \mathcal{P} \text{ s.t. } P_0 \in \mathcal{P} \rightarrow C^{RP}$$

I. Data-based \mathcal{H}_∞ -norm estimation [1]

Problem:

Uncertainty bound γ crucial for RP



- ▷ $\|\Delta\|_\infty \ll \gamma$: Conservative
- ▷ $\|\Delta\|_\infty > \gamma$: No guarantees
- ▷ $\|\Delta\|_\infty \leq \gamma$: RP
- $\Rightarrow \mathcal{H}_\infty$ -norm estimation is crucial

Approach:

Exploit local smoothness through local modeling techniques

$$\Delta_o(\xi_{k+r}) \approx D_k^{-1}(r)N_k(r) \quad (\text{LMFD})$$

$$T_\Delta(\xi_{k+r}) \approx D_k^{-1}(r)M_k(r) \quad (\text{LMFD})$$

Global \mathcal{H}_∞ -norm through local finite-frequency \mathcal{L}_∞ -norms (gKYP)

Result: Accurate \mathcal{H}_∞ -norm estimation

II. Visualizing & Comparing \mathcal{P} [2]

Problem:

Uncertainty structure is crucial for RP

- ▷ $\mathcal{P}^{ADD} = \hat{P} + \Delta$
- ▷ $\mathcal{P}^{dy} = (\hat{N} + D_c\Delta)(\hat{D} + N_c\Delta)^{-1}$

Increasing complexity!

Key issue: Design, comparison, insight?

→ Visualize \mathcal{P} !

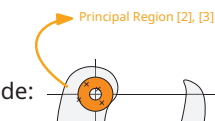
/ department of mechanical engineering

Approach:

(Multivariable) Bode of \mathcal{P}

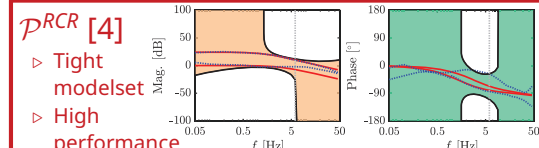
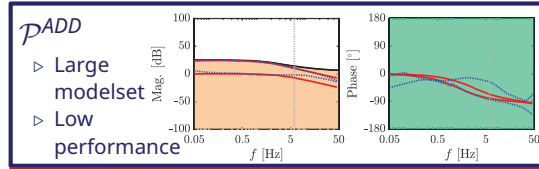
- ▷ Multivariable magnitude: \Rightarrow Singular Values
- ▷ Multivariable phase? \Rightarrow Numerical range!

LMI-based approach



Result:

Industrial CVT (2×2)



III. One-step Centralized Overactuation

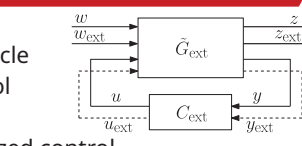
Problem:

Overactuated reticle stage (FFR) control

Approach:

One-step centralized control

$$\text{FRF} \rightarrow \mathcal{P}_{ext} \rightarrow \text{RP}$$



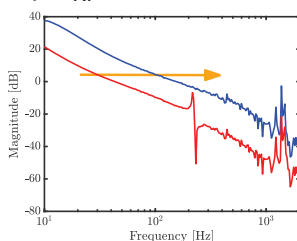
Result:

- ▷ Traditional:

$$f_{BW} = 60 \text{ Hz}$$

- ▷ This poster:

$$f_{BW} = 160 \text{ Hz}$$



References & Further Reading

[1] P. Tacx, and T. Oomen. Accurate \mathcal{H}_∞ -norm estimation via Finite-Frequency Norms of Local Parametric Models. In Proc. 2021 Americ. Contr. Conf., New Orleans, LA, USA, 2021.

[2] P. Tacx, and T. Oomen. Comparing Multivariable Uncertain Model Structures for Data-driven Robust Control: Visualization and Application to a Continuously Variable Transmission. Int. J. of Robust and Nonlin. Contr., 2023.

[3] I. Postlethwaite et al., Principal Gains and Principal Phases in the Analysis of Linear Multivariable Feedback systems. IEEE T. on Autom. Contr., 1981, Vol 26(1), Pages 32-46.

[4] T. Oomen et al., Connecting System Identification and Robust Control for Next-generation Motion Control of a Wafer Stage, IEEE T. on Contr. Sys. Tech., 2014, Vol. 22(1), Pages 102-118.

Control Systems Technology

A Proposal for a Simulated Running Environment for Railway Vehicle Control Engineering Tests Using a Scaled Roller Rig that Simulates High-Speed Friction Fluctuations

So Ueno, Wataru Ohnishi, Takafumi Koseki (The University of Tokyo)

s.ueno@ctl.t.u-tokyo.ac.jp

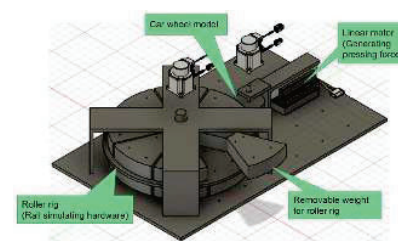
Demand for automatic train operation

- Low birth rate is social issue in Japan and the Netherlands (The World Bank 2023)
- Low birth rate causes decline of railroad worker number
- Existence of platform door limits acceptable stopping position
→ Precise automatic control technology for railroad vehicle is required



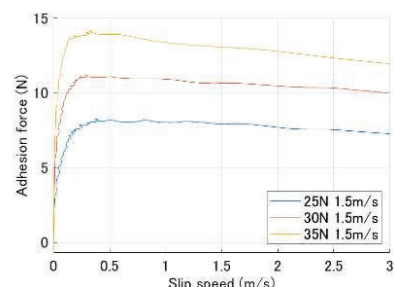
Proposal for roller rig system simulating high-speed friction fluctuations (Ueno January 2023)

- Roller rig system simulates adhesion between wheel and rail
 - Full scale (Yamanaga 2018) and scaled system (Matsudaira 1953) are used in previous research
- Features of proposed system
 - 1/10 scale
 - Pressing wheel and roller rig using linear motor thrust
 - Simulate the variation of maximum adhesion force between the wheel and the roller rig quickly by controlling linear motor thrust



Roller Rig System Adhesion Characteristics Measurement (Ueno May 2023)

- Adhesion force is measured by disturbance observer using car wheel rotation angle information
- Three adhesion characteristics of actual train below is simulated by scaled roller rig system
 - Adhesion force increases with slip speed in low slip speed area
 - Adhesion force takes maximum value at certain slip speed (static friction force)
 - Adhesion force decreases under high slip speed condition (sliding friction force)

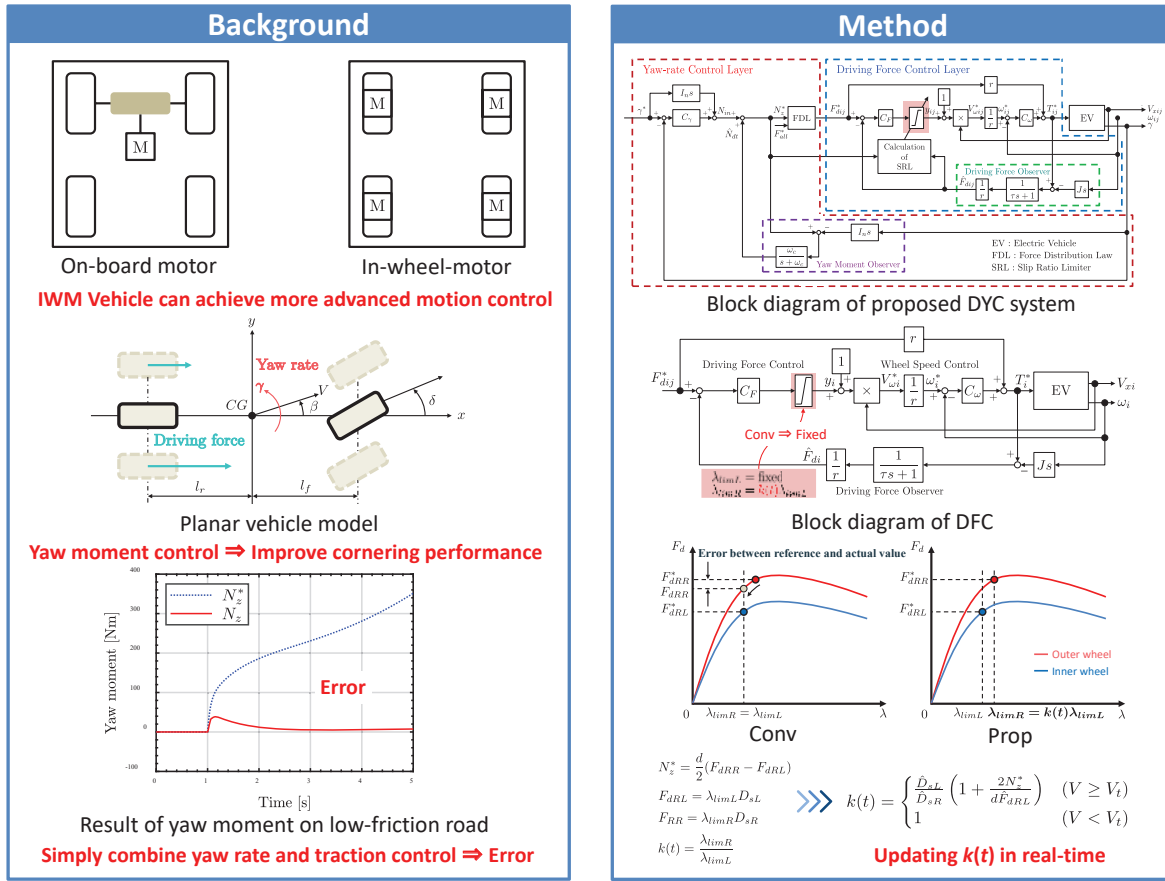


References

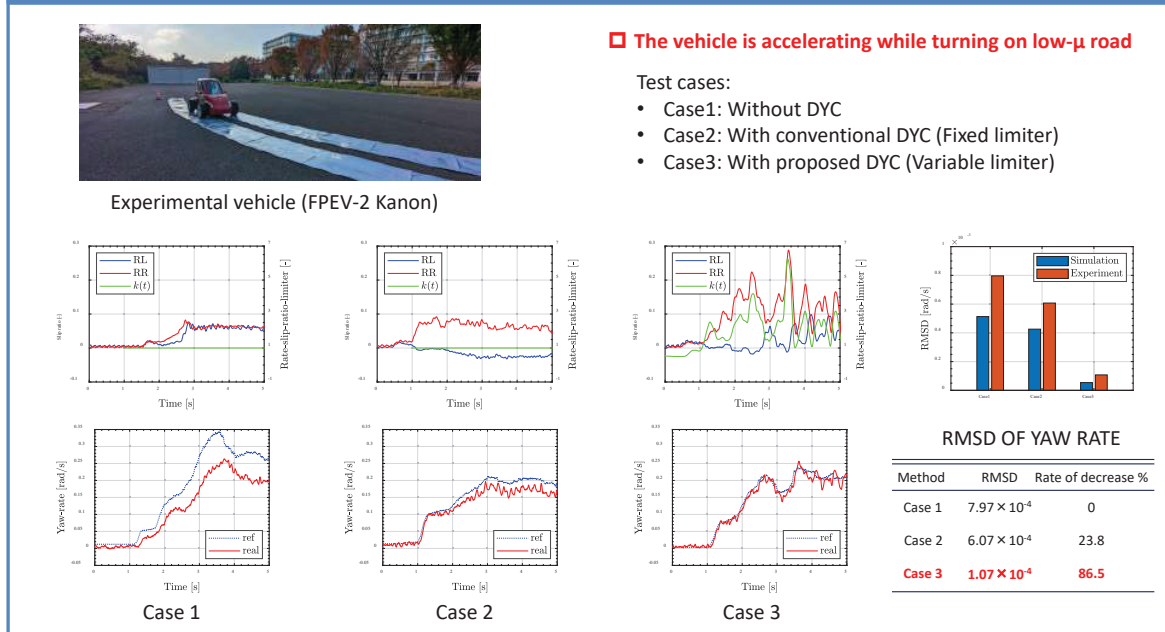
- The World Bank, "Fertility rate, total (births per woman) - Japan, Netherlands," <https://data.worldbank.org/indicator/SP.DYN.TFR.TIN?end=2021&locations=JP-NL&start=1960&view=chart>.
- Y. Yamanaga, "蛇行動限界速度評価の精度向上に向けた研究," JSME Transportation & Logistics Newsletter, no. 56, 2018.
- T. Matsudaira, "Nosing of 2-axle Railway Cars and its Prevention : 2nd Report, Model Experiment," Transactions of the Japan Society of Mechanical Engineers, vol. 19, no. 87, pp. 146-153, 1953.
- S. Ueno, W. Ohnishi, and T. Koseki, "A proposal for a simulated running environment for railway vehicle control engineering tests using a scaled roller rig that simulates high-speed friction fluctuations," Joint Technical Meeting on Transportation and Electric Railway/Linear Drives, January 2023, TER-23-011 LD-23-011.
- S. Ueno, W. Ohnishi, and T. Koseki, "Measurement of adhesion by a scaled roller rig device to emulate fast change of it for evaluating performance of railway traction control technology," Joint Technical Meeting on Transportation and Electric Railway/Linear Drives, May 2023, TER-23-049.

Yaw Moment Control for Electric Vehicles on Low Friction Road

Takumi Ueno, ueno.takumi22@ae.k.u-tokyo.ac.jp



Results



Survey on Robust Perfect Tracking Controller Design for Stage Positioning with Ball Screw Feed Drive System

Shogo Yamada, yamada.shogo23@ae.k.u-tokyo.ac.jp

Perfect Tracking Control(PTC)

Plant definition

$$\dot{x}(t) = A_x x(t) + b_x u(t), \quad y(t) = c_x x(t)$$

$$x[k+1] = A_x x[k] + b_x u[k], \quad y[k] = c_x x[k]$$

Multirate feedforward [Fujimoto, Hori, Kawamura, 2001]

- Stable inversion for discretization zeros

Singlare system $x[k+1] = A_x x[k] + b_x u[k], \quad y[k] = c_x x[k]$

Multirate sytem $x[i+1] = Ax[i] + Bu[i], \quad y[i] = cx[i]$

$$A = A_x^n, \quad B = [A_x^{n-1}b_x \quad A_x^{n-2}b_x \cdots A_x b_x \quad b_x], \quad c = c_x$$

$$u_o[i] = B^{-1}(I - z^{-1}A)x_d[i+1]$$

- Perfect tracking at every reference period time(T_r) is guaranteed for nominal plant.

Simulation

Two plots for PTC for nominal plant:

- Top plot: Track [rad] vs Time [s]. Reference (blue) and output (red) are identical, showing a smooth transition from 0 to 1 rad.
- Bottom plot: Error [rad] vs Time [s]. The error oscillates between -0.5 and 0.5 rad.

Previous Research

Adaptive Vibration Suppression PTC

- During the cutting process, the dominant axial resonance mode of the system varies with the position and mass of the workpiece.

- A higher-order multirate feedforward controller to suppress the excitation of the resonance modes
- Online robust adaptation for system using the recursive least squares(RLS)

[T. Beauduin, and H. Fujimoto, AMC2016]

Previous Research Experiment

Experimental Result

- Higher-order tracking control can reduce the axial oscillation.
- Without estimation scheme, the vibration suppression capacity is degraded.
- Better suppression of the stage oscillation is shown with estimation scheme.

My research

- Robust PTC
- A study on how to obtain robust feedforward control inputs without using adaptive law

High-precision motion control of 6-DOF magnetic levitation Transverse Flux Permanent Magnet Linear Motor

Yueying Yang, Wataru Ohnishi, Takafumi Koseki (The University of Tokyo)

Attractive Maglev Transverse Flux Permanent Magnet Linear Synchronous Motor

Structure of the motor

Maglev system

- Attractive EMS technology
- Five DOF unstable system
- Two E-type electromagnets
- Four levitation coils (Inputs of the plant)

Propulsion system

- Iron-core permanent magnet linear synchronous motor
- Two independent movers
- Three C-type armature coils in each phase

Dynamic model of the maglev system

Dynamic equations :

$$\begin{cases} M\ddot{z} = f_z - Mg + f_{pz} \\ I_{yy}\ddot{\theta}_y = \tau_{\theta_y} + x_dMg + \tau_{py} \\ I_{xx}\ddot{\theta}_x = \tau_{\theta_x} - y_dMg + \tau_{px} \end{cases}$$

Coordinate conversion
Linearization

$$\begin{bmatrix} M\Delta\ddot{z} \\ I_{yy}\Delta\ddot{\theta}_y \\ I_{xx}\Delta\ddot{\theta}_x \end{bmatrix} = \begin{bmatrix} k_{izz} & k_{izy} & k_{izx} \\ k_{iyz} & k_{yyy} & k_{iyx} \\ k_{ixz} & k_{ixy} & k_{ixx} \end{bmatrix} \begin{bmatrix} \Delta z \\ \Delta\theta_y \\ \Delta\theta_x \end{bmatrix} + \begin{bmatrix} [k_{zz} & k_{zy} & k_{zx}] \\ [k_{yz} & k_{yy} & k_{yx}] \\ [k_{xz} & k_{xy} & k_{xx}] \end{bmatrix} \begin{bmatrix} k_{pz} & 0 & 0 \\ 0 & k_{py} & 0 \\ 0 & 0 & k_{px} \end{bmatrix} \begin{bmatrix} \Delta z \\ \Delta\theta_y \\ \Delta\theta_x \end{bmatrix}$$

- Unstable system
- MIMO system
- Coupled system

Identification and Decentralized Control for the Maglev System

Target: To obtain more accurate mathematical models and more robust control performance of the maglev system

I-PD decentralized feedback control system

- For an unstable system, the stable operation is the basis for the system identification experiments.

- Simplifying complex MIMO systems into SISO systems
- Diagonal control of each DOF using independent controllers

Frequency domain system identification

- Fix the system model parameters by system identification experiments for each degree of freedom.

Sample time: 62.5 [μs]
Excitation signal: Chirp Sine
Frequency range: 0.1 ~ 120 [Hz]
Period time: 15 [s]

Estimation method:

$$\hat{g}_{avg}[k] = \frac{GS}{S} = \frac{(ZR)_{avg}[k]}{(IR)_{avg}[k]}$$

Diagonal models

Coupled models

[Y. Yang et al., IEEJ J. Ind. Appl., 2023]

Decoupling Control between the Pitch and Thrust - DOFs

Target: To eliminate the coupling effect from Thrust (x) degree of freedom to Pitch (θ_y) degree of freedom

Estimation of the vertical center of gravity

Dynamic equations:

$$\begin{cases} I_{yy}\ddot{\theta}_y = \tau_{\theta_y} + \tau_{fx} + \tau_{mg} + \tau_{py} \\ m\ddot{x} = f_x \\ \tau_{\theta_y} = (f_b - f_a)l_x \\ \tau_{fx} = f_xz_g \\ \tau_{mg} = mgx_g \end{cases}$$

$$z_g = \frac{I_{yy}\ddot{\theta}_y - \tau_{\theta_y} - \tau_{mg} - \tau_{py}}{f_x}$$

Recursive least squares estimator:

- Realize the online estimation
- With forgetting factors to weigh the data with time

Estimation of the vertical center of gravity

Pre-compensator

- Simple structure implement
- Requiring estimated value of z_g

Simulation Verifications of numerical case study:

Cases with and without pre-compensator Cases with different Forgetting factors

[Y. Yang et al., International conf. on LDIA, 2023]

Locations

The locations of the workshop, in addition to some useful locations, can be found at <https://goo.gl/maps/Uc4Bu3S8YQXUXaW37>, or scan the left QR-code in Figure 1.

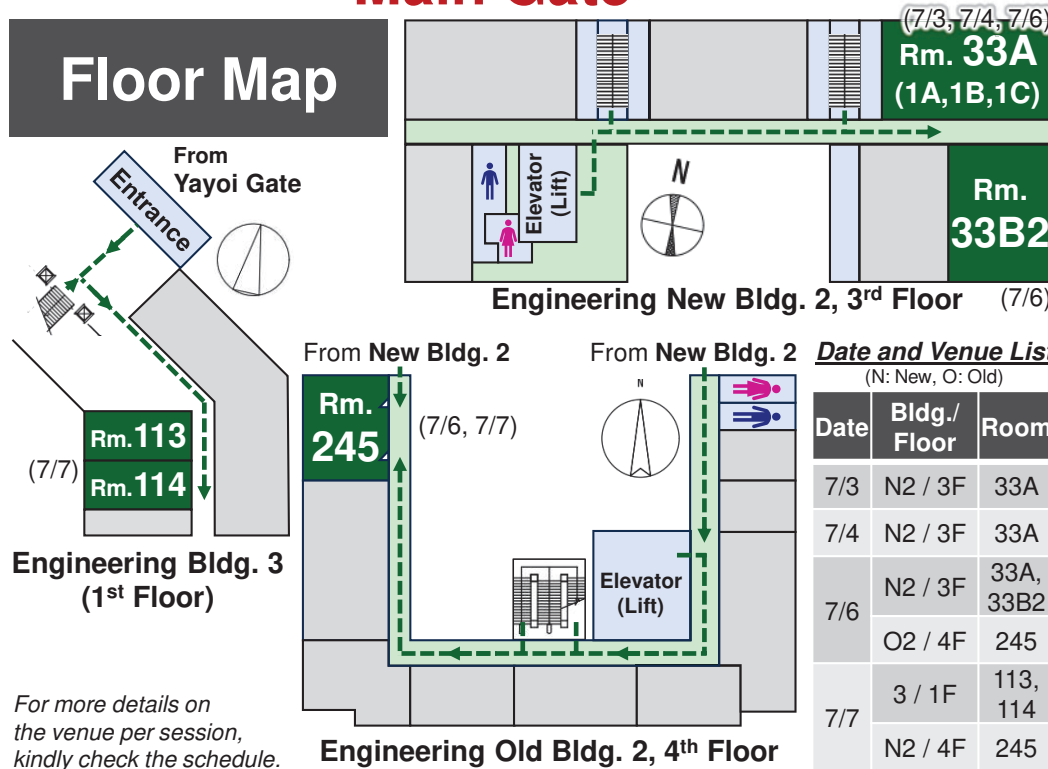
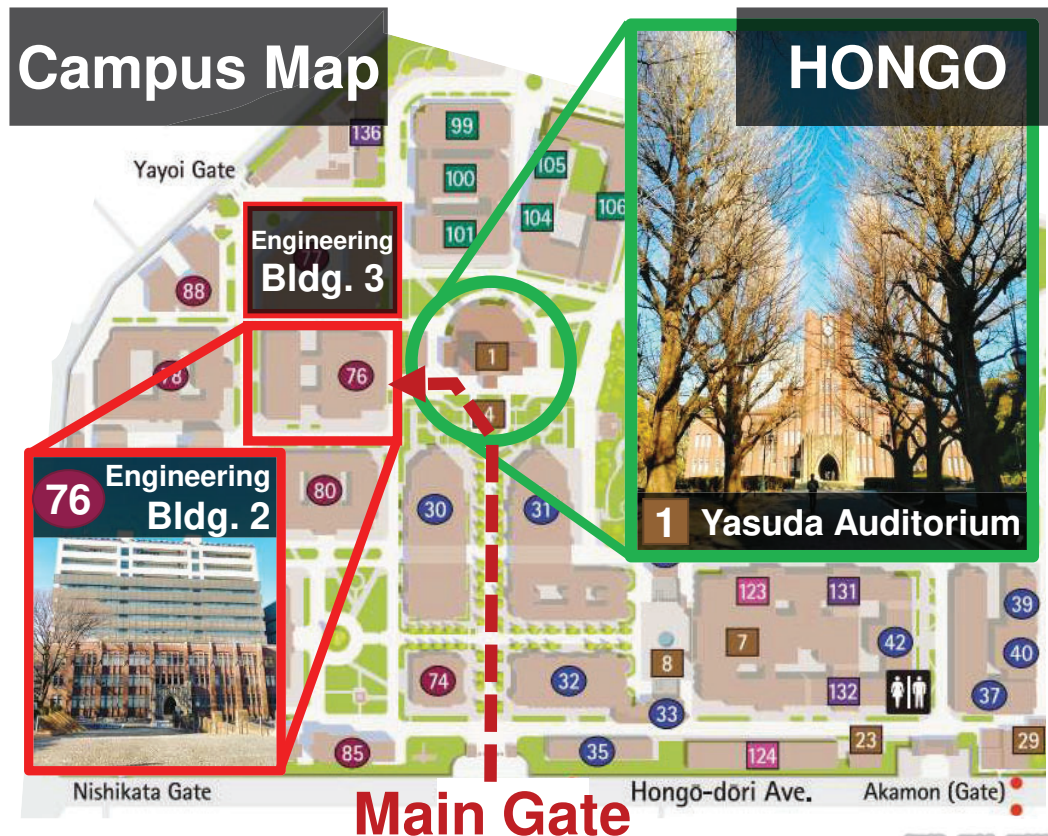
Additionally, some recommended food options for dinner and the free lunches can be found at https://docs.google.com/document/d/1x2zua9fcitals_FhCpR7obdFQG-S9Bmy3ztPcJ-uj6e4/edit?usp=sharing, or be found by scanning the right QR-code in Figure 1.

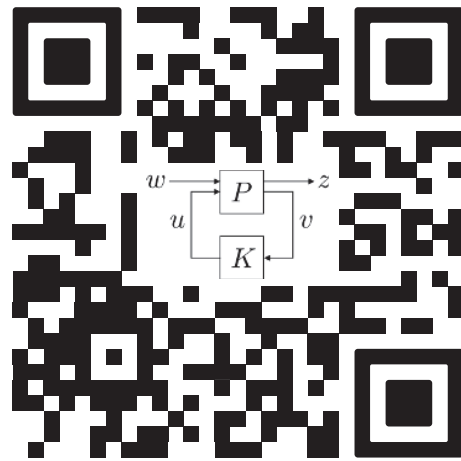


Figure 1: Left: QR-code for the map containing locations of the seminar. Right: QR-code for recommended lunch and dinner options.

For the closing ceremony, it is essential that you arrive at the Yakatabune Amikou Ryogoku Pier no later than 17:45. The location can also be found using <https://goo.gl/maps/HgdVpvCeAE5T6iFJ6> and is walking distance from Ryogoku Station.

On the following pages, a detailed map containing walking routes and the precise locations of the rooms where the presentations will be held is presented.





Program

Monday 3rd of July: Opening @Hongo campus

Time	Session (chair)	Presenter	Room
10:20-10:30	Opening	Ohnishi and Oomen	Bldg. 2, Rm. 33A (3rd floor)
10:30-11:00	Coffee		Bldg. 2, Rm. 33A (3rd floor)
11:00-12:00	MoB (Kon)	Kentaro Tsuromoto Max van Haren	Bldg. 2, Rm. 33A (3rd floor)
12:00-13:30	Lunch		Free (see recommendation)
13:30-14:30	MoC (Tsuromoto)	Johan Kon Masahiro Mae	Bldg. 2, Rm. 33A (3rd floor)
14:30-15:30	Poster Session A		Bldg. 2, Rm. 33A (3rd floor)
15:30-16:30	Lab tour	Koseki and Ohnishi	
Evening	Welcome reception		Matsumotoro (Bldg. 2 2nd floor)

Tuesday 4th of July: Hongo campus and TEL

Time	Session (chair)	Presenter	Room
09:30-10:30	TuA (Classens)	Reon Sasaki Leontine Aarnoudse	Bldg. 2, Rm. 33A (3rd floor)
10:30-11:00	Coffee		Bldg. 2, Rm. 33A (3rd floor)
11:00-12:00	TuB (Sasaki)	Max van Meer Paul Tacx	Bldg. 2, Rm. 33A (3rd floor)
12:00-13:00	Lunch		Lunch box
13:00-14:00	Train to TEL		
14:00-14:30	TEL walk-in		
14:30-15:35	TEL presentations	Yamaguchi and Budiono	Bldg. A, 901 (9th floor)
15:35-17:00	TEL lab tour		Bldg. B (1st floor)
17:10-18:00	TEL Presentation	Hirata	Bldg. A, 901 (9th floor)
Evening	Social program		

Wednesday 5th of July: Kashiwa Campus

Time	Session (chair)	Presenter	Room
09:30-10:30	Free discussion time		
11:00-12:00	Train to Kashiwa		
12:00-13:15	Lunch		Trans. Bldg. 1C3 (1st floor)
13:15-14:45	SS WeC (Oomen)	Koen Tiels Ohnishi, Mae and Fujimoto	Kashiwa campus media hall
14:45-15:00	Lab introduction	Fujimoto	Kashiwa campus media hall
15:00-15:30	Coffee		Community salon
15:30-17:30	Lab tour		
18:00-20:00	Social dinner at Kashiwa		FARMERS TABLE (near station)

Program

Thursday 6th of July: Hongo campus			
Time	Session (chair)	Presenter	Room
09:30-10:30	ThA (Atsumi)	Yuto Naoki Nic Dirkx	Bldg. 2, Rm. 245 (4th floor)
10:30-11:00	Coffee		Bldg. 2, Rm. 33B2 (3rd floor)
11:00-12:00	ThB (Poot)	Takenori Atsumi Maurice Poot	Bldg 2, Rm. 245 (4th floor)
12:00-13:30	Lunch		Lunch box
13:30-14:30	ThC (Mae)	Shota Yabui Koen Classens	Bldg. 2, Rm. 245 (4th floor)
14:30-15:30	Poster Session B		Bldg. 2, Rm. 33A (3rd floor)
15:30-16:00	Coffee		Bldg. 2, Rm. 33A (3rd floor)
16:00-18:00	IEEJ talk	Tom Oomen	Bldg. 2, Rm. 245 (4th floor)
Evening	Social program		

Friday 7th of July: Hongo campus			
Time	Session (chair)	Presenter	Room
09:30-10:30	Free discussion time		Bldg. 3, Rm 113, 114 (1st floor)
10:30-12:00	SS FrB (Ohnishi)	Gert Witvoet Lennart Blanken	Bldg. 3, Rm 113, 114 (1st floor)
12:00-13:30	Lunch		Free (see recommendation)
13:30-14:30	FrC (Budiono)	Mathyn van Dael Koichi Sakata	Bldg. 3, Rm 113, 114 (1st floor)
14:30-15:00	Coffee		Bldg. 3, Rm 113, 114 (1st floor)
15:00-17:00	UTokyo lecture	Tom Oomen	Bldg. 2, Rm. 245 (4th floor)
Evening (17:45!)	Closing ceremony		Yakatabune Amikou Ryogoku Pier

Poster session A	Poster session B
Mo 14:30-15:30	Th 14:30-15:30
Mamoru Katayama	Shogo Yamada
Chenyu Ge	Takumi Ueno
Yueying Yang	Kaiki Akizuki
So Ueno	Tomoaki Koishi
Maurice Poot	Manto Kamiya
Koen Classens	Qi Chen
Paul Tacx	Johan Kon
Max van Haren	Leontine Aarnoudse
Max van Meer	Mathyn van Dael
	Nic Dirkx

